

**THE SEISMIC STRUCTURE OF TOFINO BASIN AND
UNDERLYING ACCRETED TERRANES**

by
STEWART GORDON LANGTON
B.Sc., University of Victoria, 1981

A Thesis Submitted in Partial Fulfilment of the
Requirements for the Degree of

MASTER OF SCIENCE

in
the Department of Physics and Astronomy

We accept this thesis as conforming
to the required standard



Dr. G.D. Spence, Supervisor (School of Earth and Ocean Research, Department of
Physics and Astronomy)



Dr. H.W. Dosso, Departmental Member (Department of Physics and Astronomy)



Dr. R.D. Hyndman, Outside Member (Pacific Geoscience Centre, Geological Survey
of Canada)



Dr. C.J. Yorath, Outside Member (Pacific Geoscience Centre, Geological Survey of
Canada)



Dr. E.E. Davis, External Examiner (Pacific Geoscience Centre, Geological Survey of
Canada)

© STEWART LANGTON, 1995. University of Victoria
All rights reserved. This thesis may be reproduced in whole or in part,
by mechanical or other means, without the permission of the author.

Supervisor: Dr. G.D. Spence

ABSTRACT

Tofino Basin, located west of Vancouver Island, is a sedimentary basin overlying the Cascadia subduction zone. Convergence of the Juan de Fuca plate with the North American plate has resulted in an accretionary prism formed from sediments scraped from the subducting Juan de Fuca plate. The sediments have been trapped against a backstop of two allochthonous terranes, the Eocene Crescent Terrane and the Mesozoic Pacific Rim Terrane. Multichannel seismic reflection data, traversing Tofino Basin and extending into Cascadia Basin beyond the continental shelf, were acquired in 1985 and 1989 by the Geological Survey of Canada. Six of these seismic profiles, along with previously collected geological and magnetic field data, were used to study the 3-D structure and development of Tofino Basin in relation to the accretionary prism and accreted terranes.

According to critical wedge theory, vertical growth of an accretionary prism occurs if the dip of the subducting oceanic plate is less than a critical angle of 11° . The seismic data indicate that the dip of the oceanic crust increases landward from 3° near the shelf edge, to 15° at the eastern limit of Tofino Basin, near Vancouver Island. The critical angle of 11° is reached at the western limit of Tofino Basin near the shelf-slope transition. West of this point, growth and uplift of the accretionary wedge continues, with associated entrapment of overlying sediments and increase in lateral size of Tofino Basin.

The lower boundary of the Crescent Terrane was clearly imaged on many seismic sections. The Crescent Terrane was observed to terminate against the subducting oceanic plate, indicating that little or no sediments are being eroded from the accretionary prism. The thickness of Crescent Terrane to the west of Vancouver Island is at least 6-9 km. This supports a model whereby a sliver of oceanic crust was detached from the top of

the subducting oceanic plate. However, the very thick Crescent Terrane on the Olympic Peninsula supports a second model in which the complete lithosphere was faulted and underthrusting of the oceanic plate stepped seaward.

In the southeast portion of Tofino Basin, a linear trench parallel to Vancouver Island contains up to 3500 m of sediments, the thickest accumulation of sediments in the basin. This feature is interpreted as a fossil trench, a relic of past subduction of the Crescent Terrane beneath the Pacific Rim Terrane. The northern limit of the fossil trench occurs near the Zeus Structure, where the thickness of Tofino Basin sediments overlying the Crescent Terrane is less than 500 m. This suggests that after the time of emplacement, the Crescent Terrane was an exposed island, with water depths increasing to the south into the fossil trench. Growth of the accretionary prism and uplift of the Zeus Structure have resulted in variable motion and erosion of the Crescent Terrane which constrained the thickness of Tofino Basin sediments.

Deformation of Tofino Basin sediments is minimal over the Crescent Terrane which acts as a stable buttress, restricting deformation. Deformation increases toward the outer shelf, over the accretionary prism. Over the fossil trench, possible motion along the Tofino Fault that separates the Crescent and Pacific Rim terranes may have influenced the greater amount of deformation of Tofino Basin sediments observed in the seismic profiles.

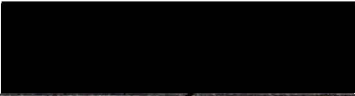
Examiners:



Dr. G.D. Spence, Supervisor (School of Earth and Ocean Research, Department of Physics and Astronomy)



Dr. H.W. Dosso, Departmental Member (Department of Physics and Astronomy)



Dr. R.D. Hyndman, Outside Member (Pacific Geoscience Centre, Geological Survey of Canada)



Dr. C.J. Yorath, Outside Member (Pacific Geoscience Centre, Geological Survey of Canada)



Dr. E.E. Davis, External Examiner (Pacific Geoscience Centre, Geological Survey of Canada)

TABLE OF CONTENTS

ABSTRACT	ii
TABLE OF CONTENTS	v
LIST OF FIGURES	vii
LIST OF TABLES	x
ACKNOWLEDGEMENTS	xi
CHAPTER 1 INTRODUCTION	1
1.1 Geographical Setting and History of Previous Work	1
1.2 Regional Tectonics	4
1.3 Regional Geology	8
1.4 Stratigraphy of Tofino Basin	10
1.5 Geophysical studies	11
1.6 Objectives	13
CHAPTER 2 DATA BASE	14
2.1 Seismic Reflection Data	14
2.1.1 Acquisition and Processing of 1989 Reflection Data	18
2.2 Magnetic And Gravity Data	19
2.3 Well Data	22
CHAPTER 3 DATA PROCESSING	24
3.1 Well Velocity Logs and Synthetic Seismograms	24
3.2 Reprocessing Seismic Line 89-02	24
3.2.1 Velocity Analysis	35
3.2.2 Comparison of Velocities from well and seismic data	37
3.3 Analysis of Velocity Data - Line 89-02	38
CHAPTER 4 INTERPRETATION OF DATA	39
4.1 Seismic Data	40
4.1.1 Oceanic Plate	49
4.1.2 Pacific Rim Terrane	53
4.1.3 Crescent Terrane	55
4.1.4 Accretionary Prism	60
4.1.5 Tofino Basin Sediments	61
4.2 Mapping	64
4.2.1 Tofino Basin Sediment Thickness	65
4.2.2 Structure Map - Tofino Basin	69
CHAPTER 5 DISCUSSION	72
CHAPTER 6 CONCLUSIONS	78

REFERENCES	80
APPENDIXES	
1. Processing Parameters - 1989 Seismic Data	85
2. Well Sonic Logs	87

LIST OF FIGURES

Figure 1.	Continental margin of Canada and northwest United States with tectonic plates.	3
Figure 2.	Plate interactions at the western North America boundary for the last 100 million years.	5
Figure 3.	Cross sections through Tofino Basin and Olympic Peninsula showing dip of the oceanic crust and size of the accretionary wedge.	7
Figure 4.	Regional tectonic elements of Vancouver Island and Olympic Peninsula.	9
Figure 5.	Cross section through Tofino Basin wells.	11
Figure 6.	Coverage of 1985 and 1989 reflection seismic data in Tofino Basin and Cascadia Margin.	15
Figure 7.	Data set of 1985, 1989, and CSP seismic data within Tofino Basin.	16
Figure 8a.	Contour magnetic-anomaly map.	20
Figure 8b.	Contour gravity-anomaly map	21
Figure 9.	CDP 1941-1944 - gather from tape.	26
Figure 10.	CDP 1941-1944 - gather with 5/10 Hz - 25/50 Hz filter and mute.	27
Figure 11.	CDP 1941-1944 - Semblance and super gather.	28
Figure 12.	CDP 1961 Gather with NMO applied - original & reprocessed.	31
Figure 13.	Stacking velocity curves from reprocessing and interpolated stacking velocity from Geophoto processing.	32
Figure 14.	Line 2 Stack CDP 1801-2604 - Original and reprocessed data.	34
Figure 15a.	Line 2 Stack CDP 1801-2604 - Reprocessed data	36

Figure 15b.	Constant stacking velocity cross-section	36
Figure 15c.	Constant interval velocity cross-section	36
Figure 16.	Interval velocity profiles - well and seismic data (CDP 1941-44)	37
Figure 17.	Line 89-01 migrated seismic data and interpretation.	41
Figure 18.	Line 89-02 migrated seismic data and interpretation.	42
Figure 19.	Line 85-01 migrated seismic data and interpretation.	43
Figure 20.	Line 89-06 migrated seismic data and interpretation.	44
Figure 21.	Line 85-02 migrated seismic data and interpretation.	45
Figure 22.	Line 89-09 migrated seismic data and interpretation.	46
Figure 23.	Line 85-05 migrated seismic data and interpretation.	47
Figure 24.	Interpretation of Crescent Terrane and Oceanic Plate.	48
Figure 25.	Contour map - depth to top of oceanic plate.	53
Figure 26.	Contour map - depth to top of Crescent Terrane.	59
Figure 27.	Contour map - thickness of Crescent Terrane.	59
Figure 28.	Contour map - time to base of Tofino Basin sediments.	66
Figure 29.	Contour map - interpolated stacking velocity to base of Tofino Basin sediments.	67
Figure 30.	Contour map - Tofino Basin sediment thickness.	68
Figure 31.	Contour map - structural features within Tofino Basin sediments	70
Figure 32.	CSP Line 68-B-10	71
Figure 33.	Shell Anglo Apollo J-14. Log and reflectivity in depth.	87
Figure 34.	Shell Anglo Apollo J-14. Log, reflectivity and synthetic seismogram in time.	88

Figure 35.	Shell Anglo Zeus D-14. Log and reflectivity in depth.	89
Figure 36.	Shell Anglo Zeus D-14. Log, reflectivity and synthetic seismogram in time.	90
Figure 37.	Shell Anglo Zeus I-65. Log and reflectivity in depth.	91
Figure 38.	Shell Anglo Zeus I-65. Log, reflectivity and synthetic seismogram in time.	92
Figure 39.	Shell Anglo Pluto I-87. Log and reflectivity in depth.	93
Figure 40.	Shell Anglo Pluto I-87. Log, reflectivity and synthetic seismogram in time.	94
Figure 41.	Shell Anglo Prometheus H-68. Log and reflectivity in depth.	95
Figure 42.	Shell Anglo Prometheus H-68. Log, reflectivity and synthetic seismogram in time.	96
Figure 43.	Shell Anglo Cygnet J-100. Log and reflectivity in depth.	97
Figure 44.	Shell Anglo Cygnet J-100. Log, reflectivity and synthetic seismogram in time.	98

LIST OF TABLES

Table 1.	Summary of Tofino Basin Wells	23
Table 2.	Dip of the top of oceanic crust beneath the continental shelf.	50
Table 3.	Dip of the base of Crescent Terrane	56

ACKNOWLEDGEMENTS

I would like to thank my supervisor Dr. G.D. Spence for his support throughout this research project. His suggestions and advice during the preparation of this thesis are appreciated. I would also like to thank the other members of my committee, Drs. Hyndman and Yorath of the Pacific Geoscience Centre, and Dr. Dosso of the Physics Department, for their comments which improved the quality of this study.

I am grateful to the members of the Physics Department for the opportunity to have studied in the department, and to Dr. Dosso for the use of space in his lab.

CHAPTER 1

INTRODUCTION

1.1 Geographical Setting and History of Previous Work

Tofino Basin underlies the continental shelf of western North America, offshore from Vancouver Island, Canada (Fig. 1). It is centred on latitude 49°N - longitude 126°W and underlies an area greater than 10,000 square kilometres. The basin overlies sediments that have been scraped from the top of the Juan de Fuca plate as it subducts beneath the North American plate. Two allochthonous terranes form a backstop for this accretionary prism of sediments which, at the seaward edge of the continental shelf, is over 6000 m thick (Hyndman *et al.* 1990; Dehler *et al.* 1992; Davis and Hyndman 1989). Tofino Basin is bounded by Vancouver Island to the northeast and the continental shelf edge to the southwest. The Olympic Peninsula and Juan de Fuca Strait limit the basin to the east. In its southern portion the basin contains sediments with local thicknesses of over 3500 m. To the northwest, the basin decreases in thickness as Tofino Basin sediments unconformably onlap older sediments of the accretionary prism.

Petroleum exploration of Tofino Basin was initiated by Shell Canada Ltd. in the late 1960's, with a regional seismic survey and a program of 7 wells (Shouldice 1971). More recently, the Geological Survey of Canada acquired multichannel seismic data in 1985 (Yorath *et al.* 1987) and in 1989 (Spence *et al.* 1991). Systematic regional gravity and magnetic data are available in the area from the Geological Survey of Canada. The earlier data interpretation by Shell was mainly concerned with determining the location and post drilling evaluation of the petroleum exploration wells. Stratigraphic correlations were based on outcrops on Vancouver Island and the Olympic Peninsula, and on limited palynology and micropalaeontology from the wells (Shouldice, 1971; 1973).

During the 1970's and 80's a regional structural model was developed which included the effects of plate tectonics. This model included an accretionary prism to the west of Vancouver Island which formed from sediments transported by the Juan de Fuca plate and scraped from the plate when it subducted beneath the North American plate to the east of Tofino Basin.

The seismic data presented in Shouldice (1971) allowed only limited shallow structural interpretation. The 1985 and 1989 seismic data were of higher CDP (Common Depth Point) fold and quality and a detailed description and explanation of structure and development of Tofino Basin is possible from the interpretation of these data sets.

This thesis presents reprocessing of seismic data over Tofino Basin and integration of the results with other geological and geophysical data to provide new constraints on the basin structure and tectonic history.

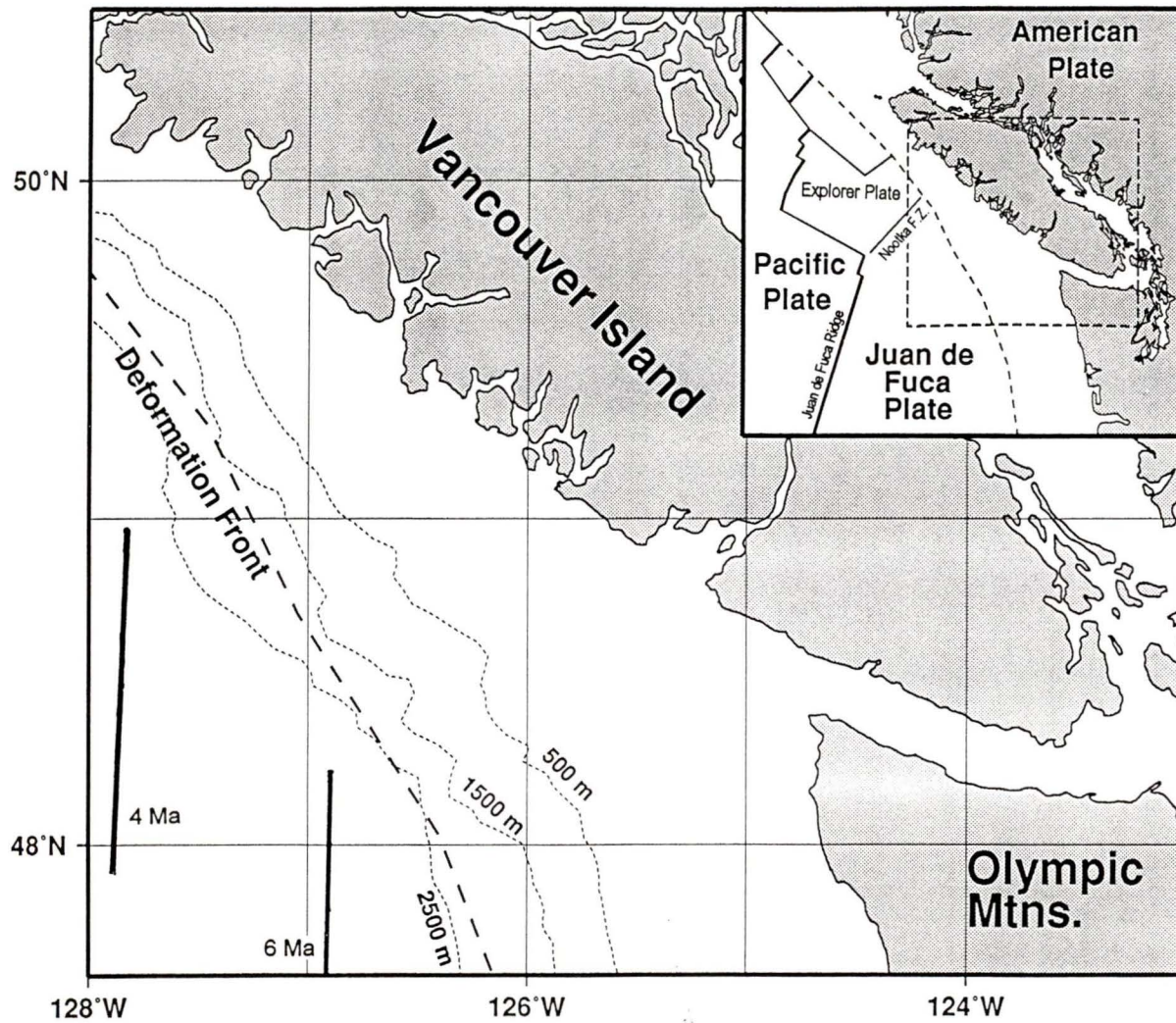


Figure 1: Continental Margin of Canada and northwest United States with tectonic plates. Solid lines indicate oceanic plate, of age shown, entering subduction zone (after Davis and Hyndman 1989).

1.2 Regional Tectonics

For at least the last 100 Ma (since Mid-Cretaceous time) the west coast of North America has been the convergent boundary between the North American plate and the Farallon plate to the west (Riddihough 1982). Relative motion of the Farallon plate with respect to the North American plate has been predominantly to the north or northwest, resulting in strike-slip or oblique convergence at the continental margin (Riddihough 1982; Hyndman and Hamilton 1993). Several allochthonous terranes riding on the Farallon plate have been accreted to the North American plate during periods of convergence and transported northward during episodic periods of margin-parallel transform motion.

The Juan de Fuca plate (Fig. 1) is the residual portion of the formerly much larger Farallon plate, of which the major segment has been subducted beneath North America. Evidence for the Farallon plate and the former Kula plate in the northern Pacific is based on sea floor magnetic anomalies of the Pacific Ocean that extend to at least 75 Ma in the mid-Pacific (Grow and Atwater 1970), and on hot spot traces and palaeomagnetism (Atwater 1970; Atwater 1989; Engebretson 1985; Riddihough 1982; Stock and Molner 1988).

Figure 2 is a postulated plate reconstruction for the last 100 Ma (Riddihough 1982). At 100 Ma North America was bounded by the Farallon plate (and the Pacific Ocean) to the west. Between 100 Ma and 40 Ma the accretion of extensive oceanic terranes occurred along the edge of the North American plate. Since the direction of convergence of the Farallon plate with respect to the present position of the North American plate has been generally northward, the location of these terranes may, at the time of accretion, have been far south of their present location. It has been estimated that the total northward translation may be as much as 2000 km (Irving and Wynne 1991).

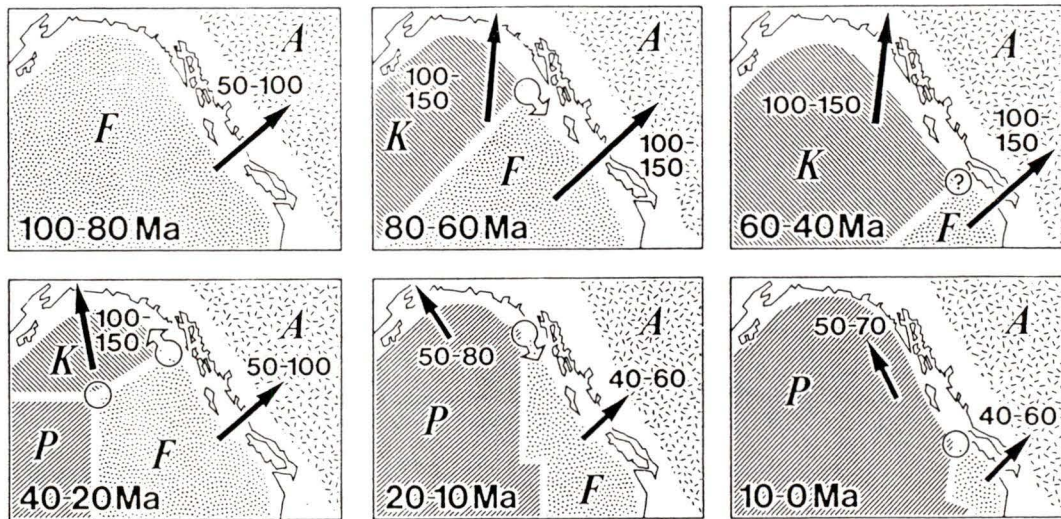


Figure 2: Plate interactions at the western North American continental margin for the last 100 million years. (after Riddihough, 1982) - Arrows and numbers represent motion relative to North America plate in mm/yr. Open circles are triple junctions with motion where shown.

The Juan de Fuca plate formed from the northern portion of the Farallon plate which split into two pieces when the Farallon/Pacific spreading ridge intersected the Cascadia subduction zone. A new triple junction, since transported northward and subducted beneath North America, was created between the Pacific, Juan de Fuca and North American plates. Triple junctions presently exist in the Tuzo Wilson-Dellwood area south of the Queen Charlotte Islands and at Cape Mendocino, offshore California, where the Mendocino Fault meets the San Andreas Fault. In the last 10 Ma the Explorer plate has broken off the Juan de Fuca plate to the north (Fig.1).

The relative rates of convergence of the Farallon (Juan de Fuca) plate with North America have been calculated by Engebretson *et al.* (1985) from hot spot data, on the assumption that hot spots in the Pacific Ocean have remained fixed with respect to hot spots in the Atlantic Ocean. From 80 to 43 Ma the velocity (of the Juan de Fuca plate) was 120-170 mm/year in a northeast direction. At 42 Ma a major reorganization of plate geometries resulted in a reduction in rates of motion and a change in relative direction

(Riddihough 1982) as well as the initiation of the present phase of subduction of the Juan de Fuca plate (Davis and Hyndman 1989). Currently the Juan de Fuca plate is converging with the North American plate at 40-50 mm/year (at N56°E), and the Explorer plate is converging with North America at approximately 21 mm/year, with the difference in rates of convergence between the Juan de Fuca and Explorer plates being taken up along the Nootka Fault Zone (Hyndman *et al.* 1979) (Fig. 1). Recent interpretation of geophysical data indicates vertical differential motion across the Nootka fault zone, such that the top of the Explorer plate may be 2 km shallower than the top of the Juan de Fuca plate offshore and as much as 6 km higher beneath Vancouver Island (Dehler and Clowes 1995).

Tofino Basin overlies the Cascadia subduction zone west of Vancouver Island. Since 42 Ma the plate velocities have remained relatively constant, and the age of the oceanic crust entering the subduction zone has been less than 10 Ma during this period (Riddihough 1979). The present age of oceanic crust is 6 Ma near the southern limits of Tofino Basin (Fig. 1), decreasing to about 2 Ma near the Nootka Fault Zone. The size of the accretionary prism underlying Tofino Basin is a consequence of this young age and high buoyancy of the crust. As well, it appears that most sediments have been scraped from the Juan de Fuca plate, accumulating in the accretionary prism (Davis and Hyndman 1989).

The difference between the Tofino Basin, where approximately 3 km of sediments overlie the submarine accretionary wedge, and the Olympic Peninsula, where accretionary rocks have been lifted above sea level to elevations over 2000 m, can be described by models of critically tapered wedges (Davis *et al.* 1983). The angle of dip of the oceanic crust controls the size of the accretionary prism since growth of the wedge stops if dip of the oceanic crust is greater than 11°. Hyndman *et al.* (1990) estimate the dip of the oceanic crust to be about 14° beneath Vancouver Island (150 km from the deformation front), while under the Olympic Peninsula the dips are less than 10° as far as 300 km from the deformation front (Fig. 3) (Davis and Hyndman 1989). Another factor which

has influenced the relative size of the accretionary wedge beneath Tofino Basin is the sediment supply. The age of oceanic crust entering the subduction zone is less than 6 Ma and therefore overlain by a thin section of sediments which contribute to the accretionary prism. The geometry of the accretionary prism backstop also differs between Tofino Basin and the Olympic Peninsula. An embayment and oblique convergence of the oceanic plate resulting in entrapment of comparatively large volumes of sediments occurs in the Olympic Peninsula, compared to normal convergence and longshore distribution of accreted sediments beneath Tofino Basin.

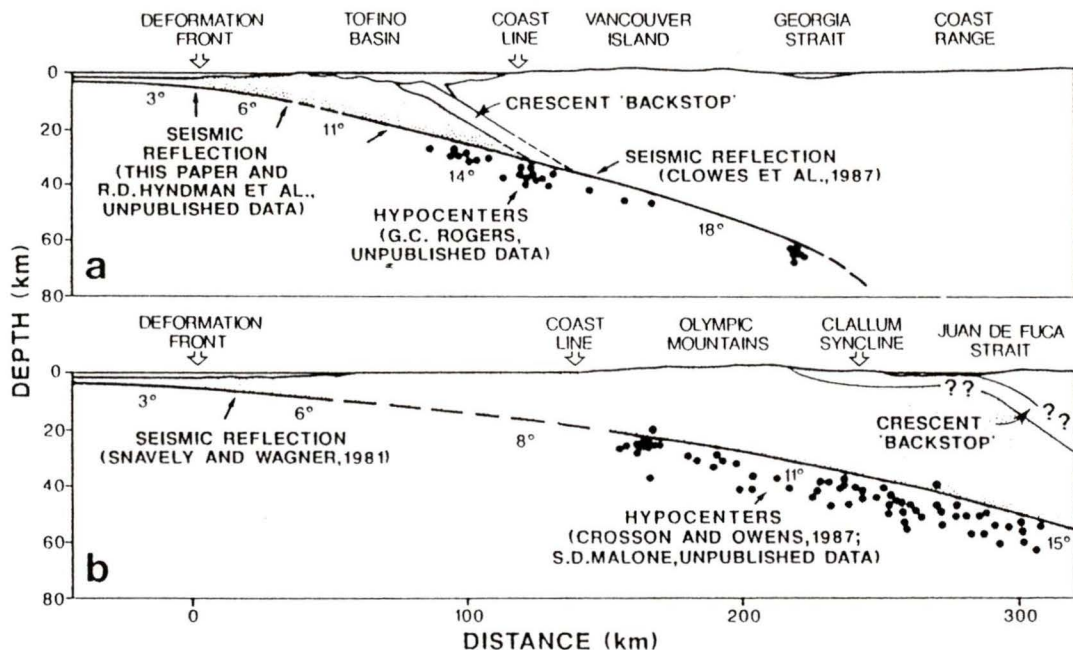
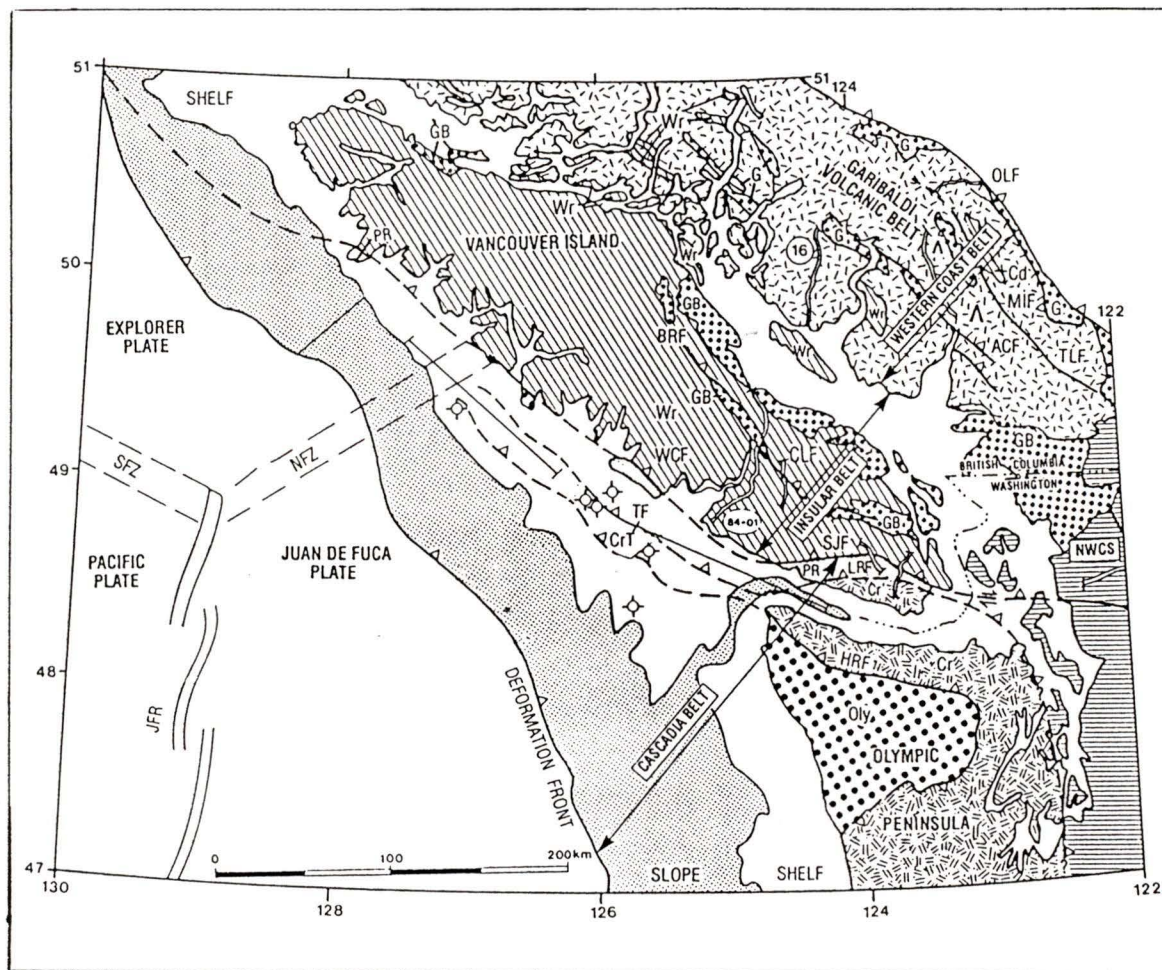


Figure 3: Cross sections through Tofino Basin and Olympic Peninsula showing dip of the oceanic crust and size of the accretionary wedge. (after Davis and Hyndman 1989)

1.3 Regional Geology

Figure 4 illustrates a generalized tectonic element map of Vancouver Island, Tofino Basin, and the Olympic Peninsula of Washington. The rocks of Vancouver Island are assigned to Wrangellia, a tectonic stratigraphic terrane consisting of Devonian, upper Triassic, and lower Jurassic marine and non-marine volcanic submarine arc complexes separated by late Paleozoic and late Triassic sedimentary rocks (Yorath, 1995). Adjacent to the west coast of Vancouver Island, Tofino Basin overlies the Pacific Rim and Crescent terranes. To the west the basin overlies the prism of accreted sediments associated with the Cascadia subduction zone. The Pacific Rim rocks are exposed along the west coast of Vancouver Island as Jurassic-Cretaceous sediments and volcanics which formed in a continental margin setting and which may have then been displaced, sometime in the interval 67 Ma to 52 Ma, along the Westcoast Fault to their present position (Johnson 1984; Wells *et al.* 1984; Hyndman *et al.* 1990, Brandon 1989, Yorath 1995). The Crescent Terrane outcrops as the Metchosin Igneous Complex on southern Vancouver Island and the Crescent Formation on the Olympic Peninsula (Muller *et al.* 1983; Massey 1986). This formation consists of Lower Eocene igneous rocks which recent studies indicate formed in a marginal basin dominated by transform motion, similar to the present situation in the Andaman Sea (Massey 1986; Snavely 1987). Within Tofino Basin the Zeus D-14 and Prometheus H-68 wells terminated in rocks interpreted as the Crescent volcanics. On the Olympic Peninsula the Crescent Formation is a horseshoe shaped outcrop open to the west and generally dipping to the east (Fig. 4). It consists of submarine pillow basalt and associated sedimentary rocks which, on the north flank of the peninsula, dip steeply to the north with thicknesses ranging from a few hundred meters at Cape Flattery to an overall thickness (which may include increased section due to folding and faulting) of over 16 km (Babcock *et al.* 1992). In northern Oregon and southwestern Washington the Crescent Terrane is equivalent to the Siletz Terrane which outcrops in the Coast Range and has been modelled most recently by Trehu *et al.* (1994). On the Olympic Peninsula the Crescent Formation (Fig. 4) is underlain by the Eocene to Miocene marine siltstones, sandstones and conglomerates collectively called the core

rocks (MacLeod 1977). The Crescent Terrane is separated from the core rocks by the landward dipping Crescent Fault.



Legend:	NFZ	Nootka Fault Zone	TF	Tofino Fault
	JFR	Juan de Fuca Ridge	WCF	West Coast Fault
	CrT	Crescent Terrane	SYF	San Juan Fault
	PR	Pacific Rim Terrane	LRF	Leech River Fault
	Oly	Core Rocks of Olympic Mountains		
	HRF	Hurricane Ridge Fault (Equiv. to Crescent Thrust)		

Figure 4: Regional tectonic elements of Vancouver Island and Olympic Peninsula. (After Varsec and Cook, unpublished)

1.4 Stratigraphy of Tofino Basin

At several locations on Vancouver Island - west of Sooke and on the Hesquiat Peninsula - a narrow band of marine (Tofino Basin) sediments outcrop as the Mid-Eocene to Oligocene Carmanah Group (Cameron 1980). The Carmanah Group consists of the Hesquiat, Escalante and Sooke Formations.

The Escalante Formation is predominantly calcareous sandstone with minor conglomerate and argillaceous sandstone which unconformably overlies the Westcoast Crystalline Complex and Bonanza Volcanics. The age of the Escalante sediments have been estimated to be late Eocene (Cameron 1980). The Escalante Formation grades conformably upward into the Hesquiat Formation. The Hesquiat type section consists of interbedded sandy shales, shales and pebbly mudstones. Cameron (1980) interprets the depositional environment of the Escalante Formation as neritic to upper bathyal which grades into the proximal Hesquiat Formation. The distal Hesquiat facies are interpreted as representing deposition in bathyal fan complexes.

Offshore, the exploration wells on the continental shelf (Fig. 1) penetrated sediments of Eocene through Recent age (Shouldice 1971) (Fig. 5). The Palaeogene volcanics encountered at the base of several wells are, as previously discussed, thought to be equivalent to the Crescent Formation of the Olympic Peninsula and the Metchosin Igneous Complex of Vancouver Island. The Palaeogene sediments in Zeus I-65 and Pluto I-87 have been considered as partially equivalent to the Carmanah Group (Yorath 1980). All of the sedimentary rocks encountered in the wells were monotonous sequences of fine grained sandstones, silts and shales, with numerous local unconformities (Yorath 1980; Shouldice 1971; Shell Canada Ltd. 1968-1971).

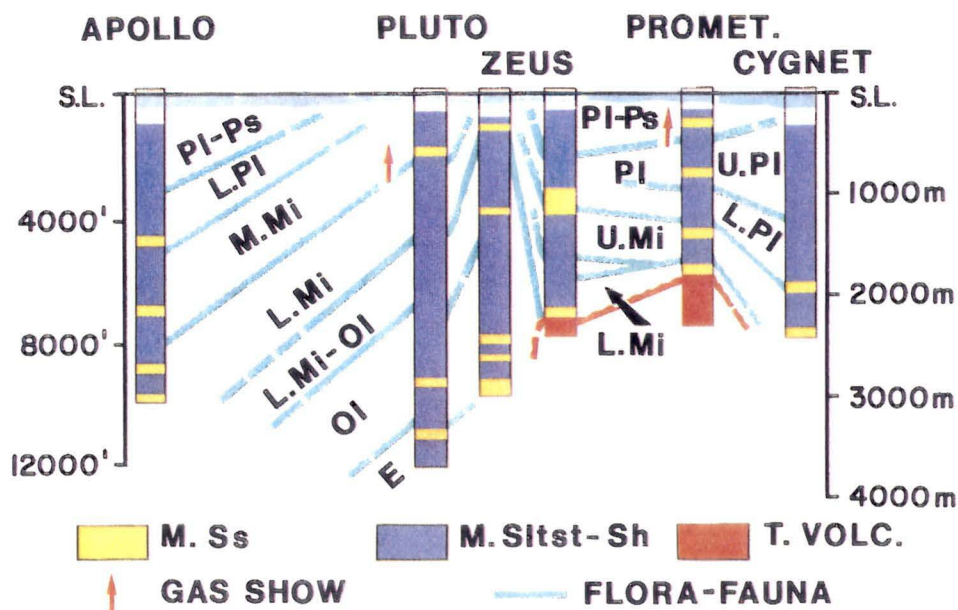


Figure 5: Cross section through Tofino Basin wells (after Shouldice 1971).

1.5 Geophysical studies

Tofino Basin and adjacent Cascadia Basin have been studied by numerous authors since the recent phase of land and marine seismic acquisition started in 1984 (summarized in Hyndman *et al.* (1990) and Hyndman 1994). More recently Davis and Hyndman (1989), Hyndman *et al.* (1990) and Spence *et al.* (1991) presented interpretations of the 1985 and 1989 seismic data sets which focused on the tectonic mechanisms and structural development of the accretionary prism and Crescent and Pacific Rim terranes underlying Tofino Basin, as well as the structural style of the deformation front of the accretionary wedge. Calvert (1995) interpreted two profiles of the 1989 data set to delineate internal structure of the accretionary prism. To date, interpretations of seismic data have not focused on analysis of Tofino Basin strata.

The interpretations of Hyndman *et al.* (1990), Dehler (1992) and Dehler and Clowes (1992) provide constraints on the boundaries of the Crescent and Pacific Rim

terrane. The position and structure of the Crescent Terrane are identified from seismic, magnetic and well data. A narrow sediment filled trough of Eocene age which separates the Crescent and Pacific Rim terranes at shallow depths was first observed on Line 85-01 (Hyndman *et al.* 1990). This may be a "fossil trench" which formed as the Crescent Terrane underthrust the Pacific Terrane before the time of accretion (Hyndman *et al.* 1990; Hyndman 1994) The Tofino Fault separates the Pacific Rim and Crescent terranes and approximately limits Tofino Basin to the east. The Tofino Fault is identified on seismic data beneath the fossil trench at the base of Tofino basin and is correlated to outcrop data on Vancouver Island and to geophysical data beneath Juan de Fuca Strait (Hyndman *et al.* 1990).

In studies of the magnetic field data in southern Vancouver Island and on the Olympic Peninsula (MacLeod *et al.*, 1977) the Crescent Terrane is correlated to magnetic highs on the south end of Vancouver Island and on the continental shelf. Dehler (1992) developed structural models of the continental margin from density and magnetic susceptibility data, constrained by seismic refraction and reflection data. The location of the Crescent and Pacific Rim terranes was estimated on profiles normal to the margin extending from the Cascadia Basin to the mainland of British Columbia, crossing Tofino Basin.

Deep earthquake data (Rogers, unpublished data, *qtd.* in Davis and Hyndman, 1989) constrain the depth of the oceanic crust to the east of Tofino Basin under Vancouver Island, from which dips on the crust can be calculated (see Fig. 3). Models which include oceanic crust are consistent with seismic refraction data across Vancouver Island (Spence *et al.*, 1985; Taber *et al.*, 1984).

1.6 Objectives

In this thesis the structural development of Tofino Basin is examined in relation to the underlying accretionary wedge and adjacent accreted terranes. The 3-D geometry of the accreted Crescent and Pacific Rim terranes is determined from interpretation of recent seismic data collected across Tofino Basin, including four lines from the 1989 data set and portions of two lines from the 1985 data set. The magnetic field data are used as constraints on the location of the Crescent Terrane. Data from wells in the basin and velocity-depth information of Tofino Basin sediments from reprocessing of a portion of Line 89-02 are used for comparison with the interpreted geological structure.

Reprocessing of a section of Line 89-02 was undertaken to improve the seismic image of the eastern limits of Tofino Basin where identification of the boundaries of the Crescent and Pacific Rim terranes was not possible from earlier seismic sections.

CHAPTER 2

DATA BASE

2.1 Seismic Reflection Data

Three sets of reflection data beneath Tofino Basin were used in this study. For this thesis Tofino Basin is considered as limited to the west by the shelf break rather than by the limit of slope and shelf sediments overlying the accretionary prism. The continental slope is not steep seaward of the shelf break and sedimentary deposition occurs in numerous small pondings in fold depressions on the slope in many locations.

1) The 1985 multichannel data (Fig. 6) were acquired as part of the Frontier Geoscience Program of the Geological Survey of Canada. Three lines crossed Tofino Basin: LP-85-01 and LP-85-02, which cross the continental shelf to deep water of the Cascadia Basin, and LP-85-05 which parallels Vancouver Island in the nearshore region and extends southeast into the Strait of Juan de Fuca. An additional line, 85-06 parallel to the coast of Vancouver Island, was acquired but until recently not processed. Dehler and Clowes (1995) have presented this data which is generally of poorer quality than the other lines of the 1985 data set.

2) The 1989 multichannel reflection seismic program (Fig. 6) was carried out as part of the site survey prior to drilling off Vancouver Island in September/October 1992 by the Ocean Drilling Program. This seismic program complemented the 1985 data set and provided improved 3-D resolution of structure along the Vancouver Island subduction zone (Spence *et al.* 1991). Lines 89-01 and 89-02 are completely over Tofino Basin. Lines 89-06 and 89-09 start near Vancouver Island and extend over the continental shelf into the deep water of Cascadia Basin. The remaining lines of the 1989 survey were further seaward and traverse the continental slope and the deformation front of the accreted sedimentary wedge.

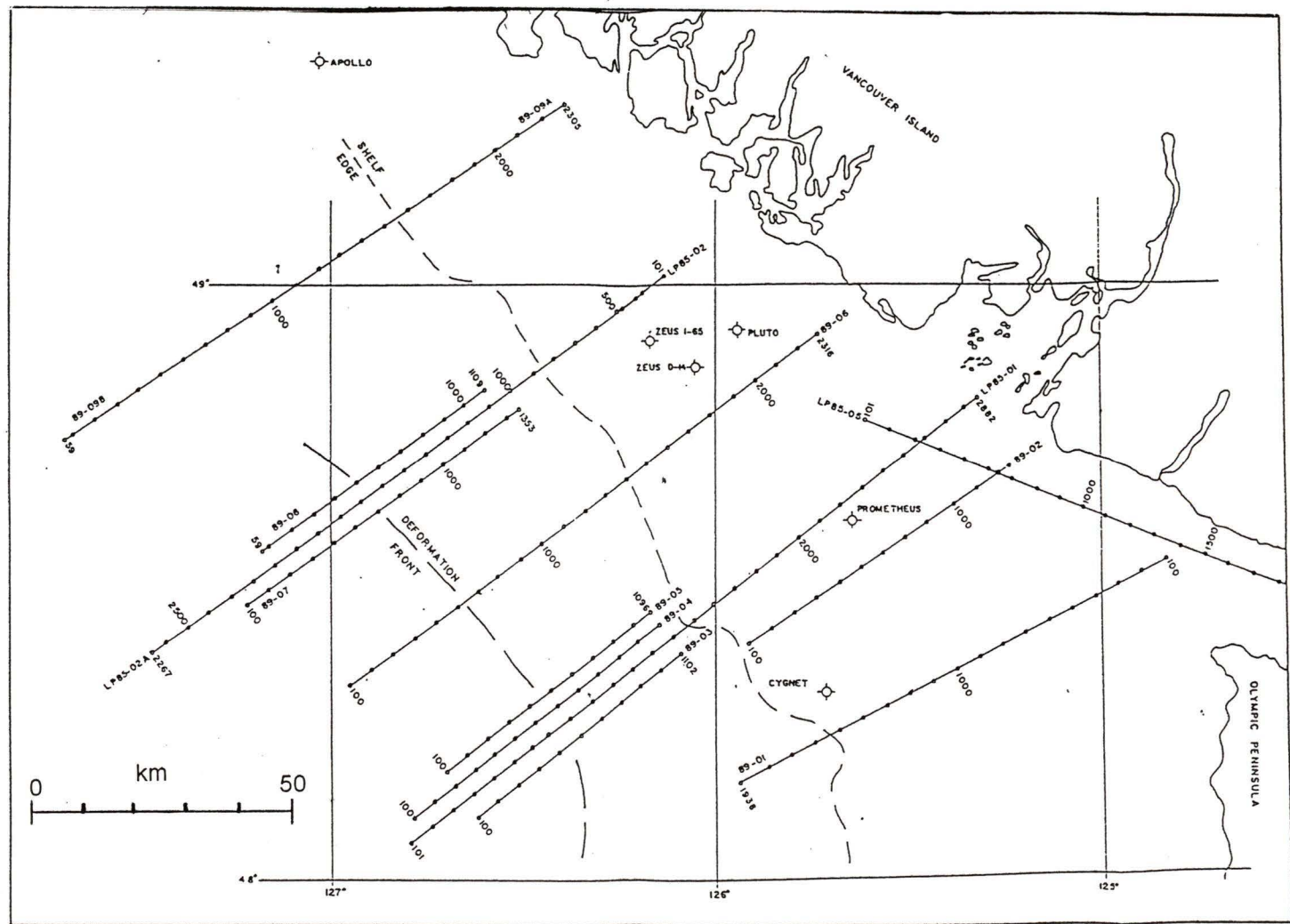


Figure 6: Coverage of 1985 and 1989 reflection seismic data in Tofino Basin and Cascadia Margin. (Shot Points are marked along each line at 100 SP intervals)

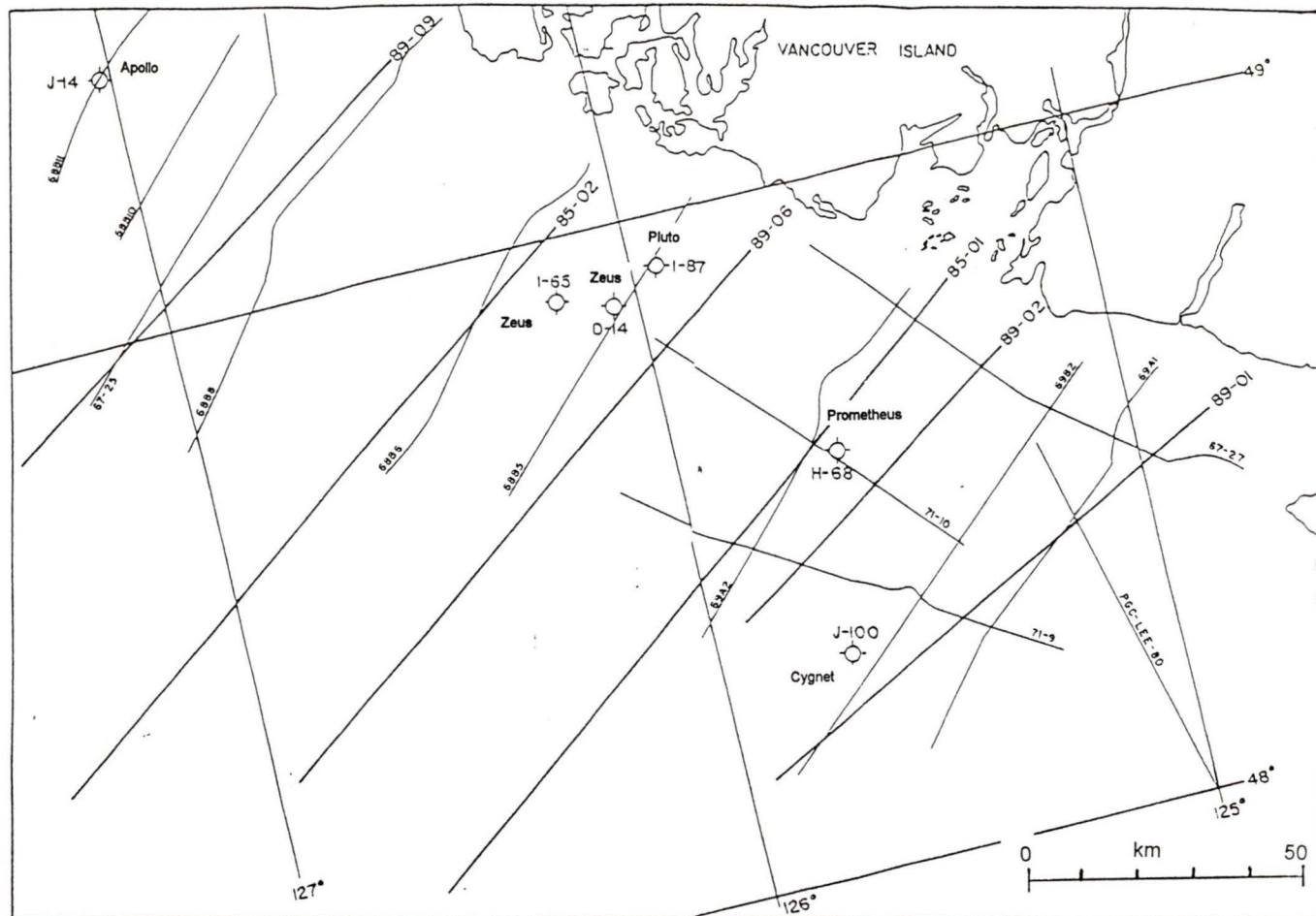


Figure 7: Location of CSP lines within Tofino Basin and location of 1985 and 1989 reflection seismic lines.

3) Extensive single channel Continuous Seismic Profiling (CSP) data were obtained in conjunction with early geophysical and oceanographic cruises by the Pacific Geoscience Centre and the Institute of Ocean Sciences (Fig. 7). The data set includes more than 30,000 km of single fold, analogue, paper record profiles along the west coast of Canada. These profiles provide information of regional features, but a variety of seismic systems were used to acquire these data and some profiles image only a few tens of metres of section. Across Tofino Basin, 14 of these profiles (approximately 1000 km) of better quality and greater penetration were used in this study.

A multichannel seismic line, USGS WO76-19, was previously recorded across Tofino Basin, but not used in this thesis. This line, located southeast of the Cygnet well, is near to Line 89-01, which is better quality.

Line 89-01, the most southerly profile across Tofino Basin, is 92 km long and traverses the continental shelf from the shelf break to a point about 10 km west of Vancouver Island, near the mouth of the Strait of Juan de Fuca (Figure 6). At the nearest location (SP 1500), this line is approximately 8.5 km southeast of the Shell-Anglo Cygnet exploration well. Line 89-02 is parallel to and 25 km to the northwest of line 89-01. Line 89-02 is 60 km long and extends from the shelf break to a point 8 km offshore Vancouver Island. Line 89-02 is 8 km southeast of Shell-Anglo Prometheus H-68 at SP 670. Line 85-01 is 11 km northwest of line 89-02. It is 137 km long and extends from near Vancouver Island, over the continental slope and into deep water of the Cascadia Basin. This line extends offshore from the Lithoprobe land reflection line 84-01 on Vancouver Island (see Hyndman et al. 1990). Line 85-01 lies 3.5 km to the northwest of Prometheus H-68 at SP 2200. Line 89-06 extends 110 km from near the shoreline of Vancouver Island and continues across the continental slope. It is 10 km southeast of the Pluto I-87 well at SP 2050, 20 km southeast of the Zeus D-14 well at SP 2080 and 18 km southeast of the Zeus I-65 well at SP 1780. Line 85-02 is 125 km long and extends from 20 km offshore Vancouver Island, over the shelf slope and into the Cascadia Basin. The line is 8 km northeast from Zeus I-65 at SP 250 and 15 km northwest from Zeus D-14

at SP 150. Line 89-09 is the northernmost line of this study. It starts 10 km from Vancouver Island and extends 112 km over the shelf slope. It is 33 km to the southeast of the Apollo J-14 well at SP 1600.

The analogue CSP data (1969 to 1972) are limited in image depth to the upper few 100 m of Tofino Basin sediments. The data were recorded using analogue techniques on paper records and consequently no processing has been attempted to remove strong water bottom multiples which obscure deeper reflections. These data were used to delineate and map near surface structure within Tofino Basin.

2.1.1 Acquisition and processing of 1989 reflection data

The 1989 data were acquired through the Frontier Geoscience Program of the Geological Survey of Canada. The acquisition of data was by Digicon (Canada) Ltd. and initial processing by Geophoto Ltd. (Haliburton Geophysical Services Ltd.). The shot point interval was 50 m, group interval 25 m and CDP spacing 12.5 m, resulting in 36 fold data. The complete acquisition and processing parameters of the 1989 data are listed in Appendix 1. Shot domain F-K filtering was applied as a dip filter to attenuate low velocity back-scatter (Spence 1991), using velocities at handpicked locations for multiple attenuation. The distance between velocity functions used for normal move-out (NMO) varied from approximately 2 km to 5 km. Stacking velocity values were chosen from semblance analysis in areas of better data quality. In areas of poor data quality and at greater depth a velocity profile from refraction models was used (Spence 1991). All velocity functions include 16 time-velocity picks from water bottom to 12.0 s. These data were time migrated (F-K migration) using migration velocities equal to 90% of stacking velocities.

2.2 Magnetic and Gravity Data

A magnetic field intensity map obtained from the Pacific Geoscience Centre (from Geological Survey of Canada, National Geophysical Data Centre) is shown in Figure 8a. Magnetic field profiles at the same locations as the seismic data are plotted above the seismic sections (Fig. 17-23). All magnetic data are computed from marine and aeromagnetic total-intensity values from which the value for the Definitive Geomagnetic Reference Field (DGRF) was subtracted. The DGRF is calculated from the observed magnetic field over a large area (Currie *et al.* 1983). The International Geomagnetic Reference Field which had previously been used by Hyndman *et al.* (1990), Spence *et al.* (1991) and Dehler (1992) is an advance prediction of the global magnetic field for the time of the survey. The DGRF now available provides a better fit to marine magnetic data off Vancouver Island (R.G. Currie, pers. comm., 1992). The feature of interest for this study is the high amplitude anomaly (shaded in Figure 8a) parallel to Vancouver Island in the southeastern portion of the basin. The high anomaly is due to the underlying Crescent Terrane and the adjacent low closer to Vancouver Island is situated over the Pacific Rim Terrane.

A contour map of gravity data is available over the area of Tofino Basin from the Geological Survey of Canada (Geophysical Map Series) as shown in Figure 8b. Over the area of Tofino Basin the main feature of interest is the gravity low (-60 mGal closure) overlying the location of the sediment filled trough between the Crescent and Pacific Rim terranes (Hyndman *et al.* 1990). The gravity high (+30 mGal closure) over the southwestern tip of Vancouver Island approximately outlines the surface outcrop of the Metchosin volcanics (Crescent Terrane) (Dehler 1992).

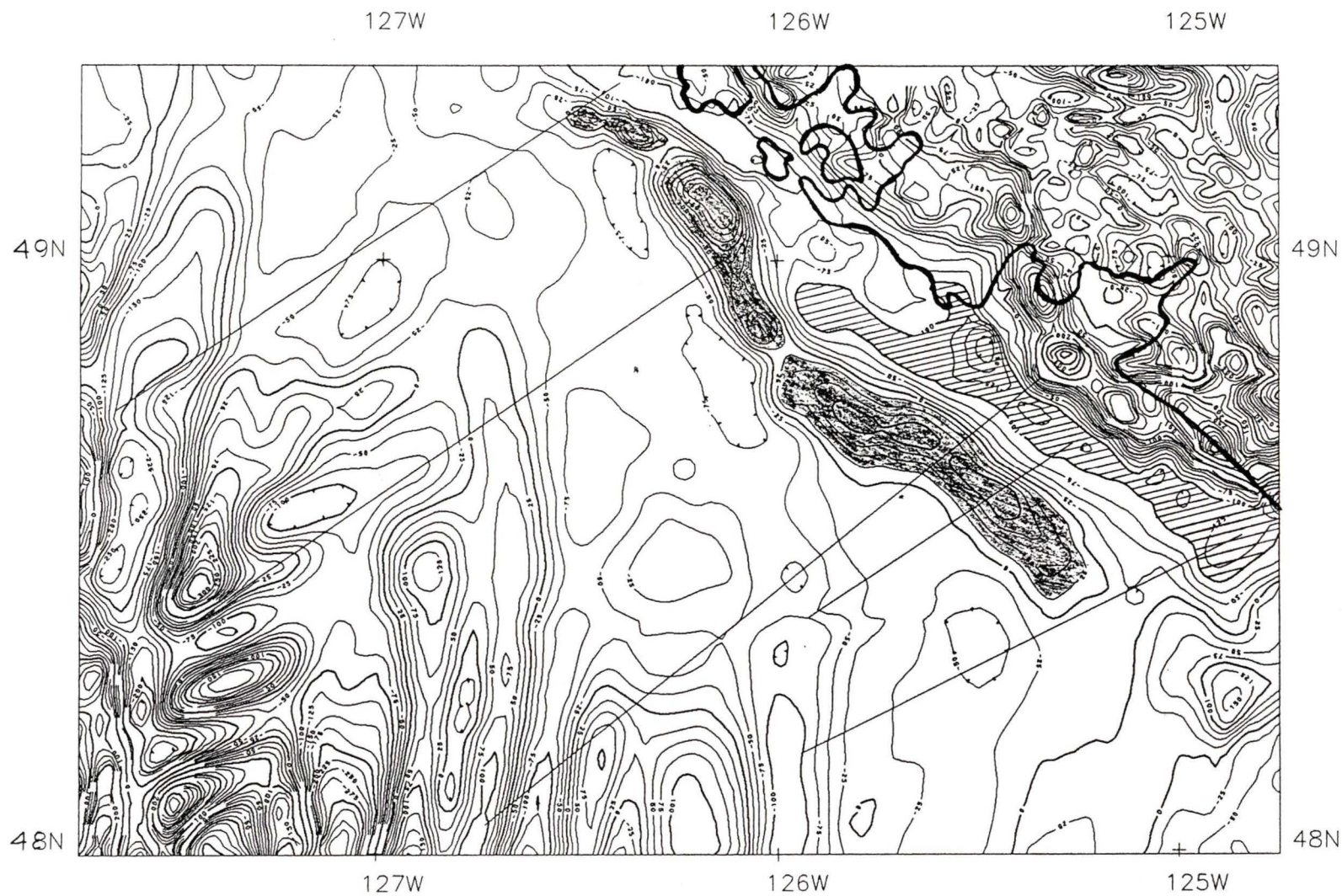


Figure 8a: Contour magnetic-anomaly map. Contour interval is 25γ (1γ=1nT)

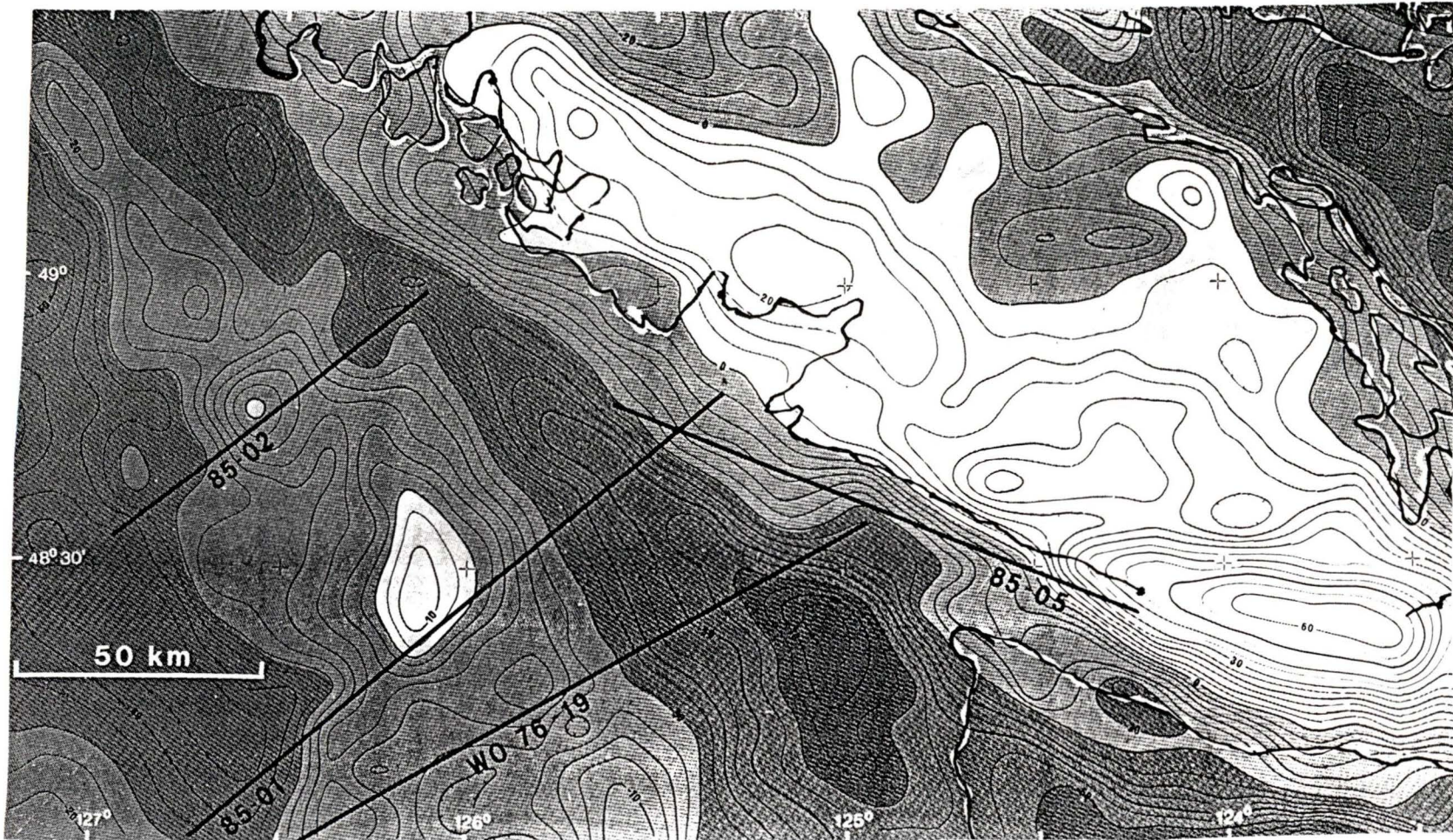


Figure 8b: Contour gravity-anomaly map; Bouguer onshore and Free Air offshore.
Contour interval is 5 mGal (1 mGal = 10^{-5} m/s²)

2.3 Well data

The locations of the six wells drilled in Tofino Basin by Shell Canada Ltd. from 1967 to 1969 are shown in Figures 1, 7 and 8. All wells were designated New Field Wildcat prior to drilling and the post drilling status for all wells was Dry and Abandoned. All of the wells had similar drilling and testing parameters. Cuttings from well fluids were obtained at 3.0 ft (0.91m) intervals, from below the first casing string to total depth of drilling. No conventional full diameter cores were cut. Sidewall cores were obtained from which sediment descriptions and faunal tops are available (Shell Canada Ltd. 1968 - 1971). These cores are in general taken at locations in the well where potential production reservoirs exist, and would therefore not be representative of the total well section. The majority of samples were mudstone, silts and fine grained sandstone. Induction Electric Spontaneous Potential logs (IES), Borehole Compensated Sonic (with Gamma Ray and Calliper) (BHCSGR-C), and Continuous Dipmeter (CDM) logs were run. Details of the six wells are summarized below (Table 1). The sidewall core descriptions available in the Well History Reports (Shell Canada Ltd. 1968-1971). All of the wells were drilled on structures of interest for petroleum exploration, and thus the drilled sections, especially horizon thicknesses, are somewhat atypical of Tofino Basin as a whole.

Well	Location	Objective	TD (RT)	Reservoir
Cygnets J-100	48° 19.67' N 125° 43.96' W	Anticline	8070'	none
Pluto I-87	48° 56.61' N 125° 57.02' W	Anticline	12225'	Thin gas bearing sand @ 1890'
Prometheus H-68	48° 37.33' N 125° 39.11' W	Anticline	7662' volcanics	none
Zeus I-65	48° 54.57' N 126° 9.00' W	Anticline	9981'	none
Zeus D-14	48° 53.02' N 126° 2.99' W	Anticline Flank	7984' volcanics	none
Apollo J-14	49° 23.58' N 127° 2.08' W	Anticline	10152'	none

Table 1: Summary of Tofino Basin wells

TD - Total Depth RT - Rotary Table

CHAPTER 3

DATA PROCESSING

3.1 Well Velocity Logs and Synthetic Seismograms

Borehole compensated sonic logs were run for all 6 wells of the Shell exploration programme. These have been used to calculate synthetic seismograms. The sonic logs were first edited for noisy sections in the data. Most edited sections occurred at cave-ins in the well bore or at casing joints. The original analogue data logs were recorded with transit time in microseconds and depth in feet. These data were digitized with a maximum of 5 ft (1.5 m) spacing between digitized points. The digitized data were resampled to 5 m which retains higher resolution than the seismic data. Since the frequency band limit of the seismic data is below 100 Hz, the maximum resolution is about 15 m for a velocity of 1500 m/s. The OUTFRIDER programme (from Microseis Technology Ltd. and Seismic Image Software Ltd.) was used to convert the digitized log to velocity-depth values. Reflection coefficients were calculated from the velocity depth profiles and convolved with a 35 Hz Ricker wavelet to determine the synthetic traces. The six synthetic sonograms are shown in Appendix 2 with the velocity depth curves, velocity time curves, reflection coefficients, and the synthetic traces. The velocity data from the wells are compared to velocities derived from seismic data later in this chapter.

3.2 Reprocessing seismic line 89-02

A portion of Line 89-02 (CDP 1801-2675) which crossed the boundary between Pacific Rim and Crescent terranes, over the location of the sedimentary "fossil trench", was selected for detailed velocity analysis at closely spaced intervals. It was hoped that a change in velocity might delineate the boundary. Improved section quality was also expected using more accurate stacking velocities. The selected data set varied in quality, with significantly fewer good reflectors east of the Crescent Terrane.

A PC-386 with VISTA processing software from Seismic Image Software Ltd. was used for data analysis. Analysis began with CDP gathers, uncorrected for NMO, as supplied by Geophoto Inc. (described in Appendix 1). Filters were applied to test gathers to reduce low and high frequency noise. The filter points were chosen qualitatively by observing continuity of wavelets across the gathers within the band pass points. The filter chosen was trapezoidal in shape, with low pass transition from 5 Hz to 10 Hz, constant gain from 10 Hz to 25 Hz and decreasing gain from 25 Hz to 50 Hz. A pre-NMO mute had been applied to the data for far trace noise attenuation. A more severe far trace mute (Fig 9 - solid line) was applied to eliminate any data on each trace with arrival time less than that from the water bottom reflection. During velocity analysis inside trace muting was applied to allow discrimination of primary and multiple reflections. At near traces multiple and primary reflections have nearly equal moveout and therefore cannot be separated, so the mute process set the amplitude value to zero at near offsets. High amplitude wavelets, likely due to "ground roll", were observed on most gathers at far offsets. This can be observed in Figure 9 on CDP 1941 below 4.0 sec on the last 10 traces. For the purposes of velocity analysis only, a far trace mute was applied from the fourth trace of each gather at water bottom to 6.0 sec at the far trace to eliminate these arrivals (Fig. 10). Four consecutive gathers were combined, which resulted in a super-gather of 144 traces containing all possible offsets (Fig. 11b). Velocity analysis was performed at locations separated by 40 CDP's (500 m or 10 SP).

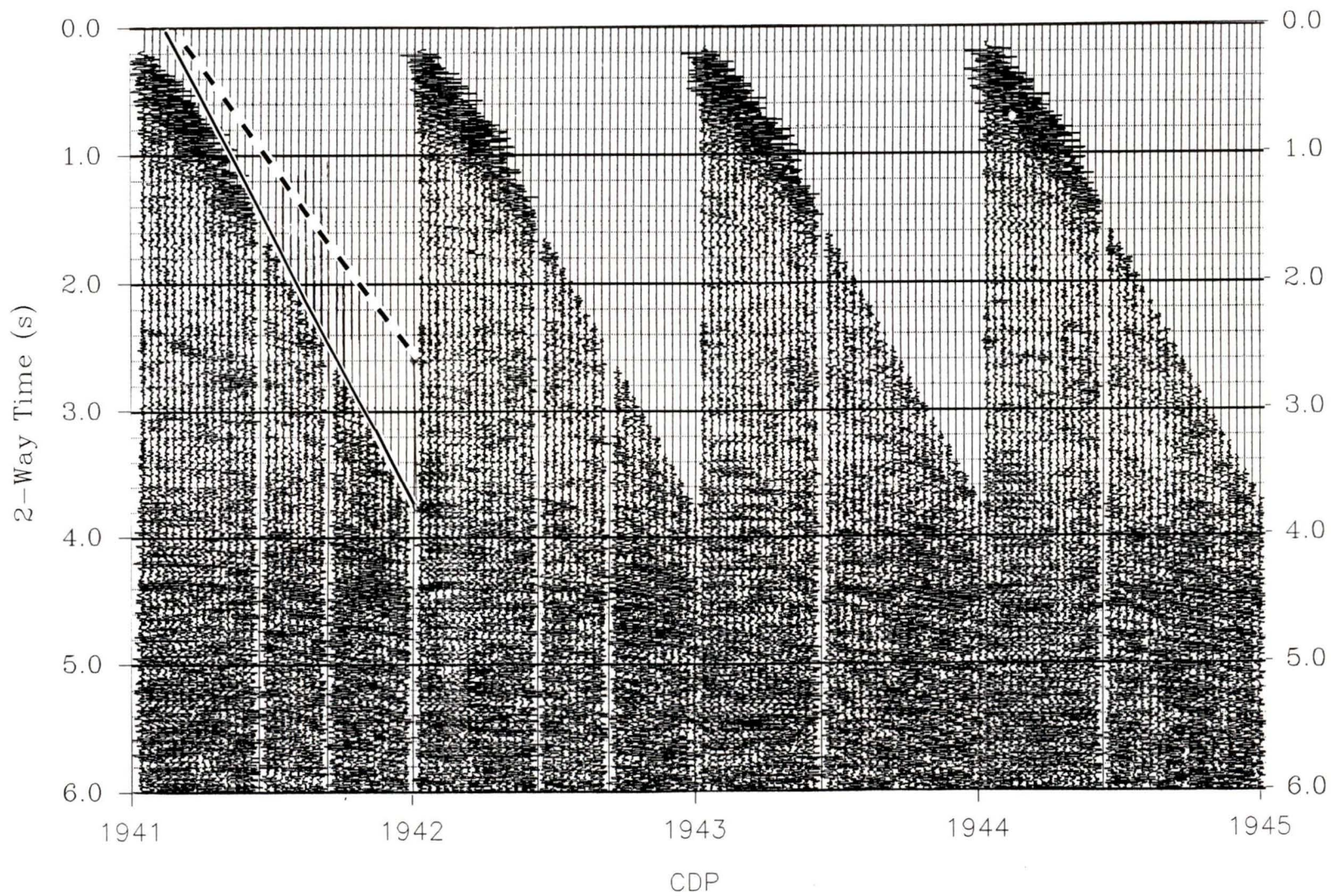


Figure 9: CDP 1941-1944 - gather from tape. Dashed line - mute pattern applied by Geophoto.
 Solid line - mute pattern for first arrivals.

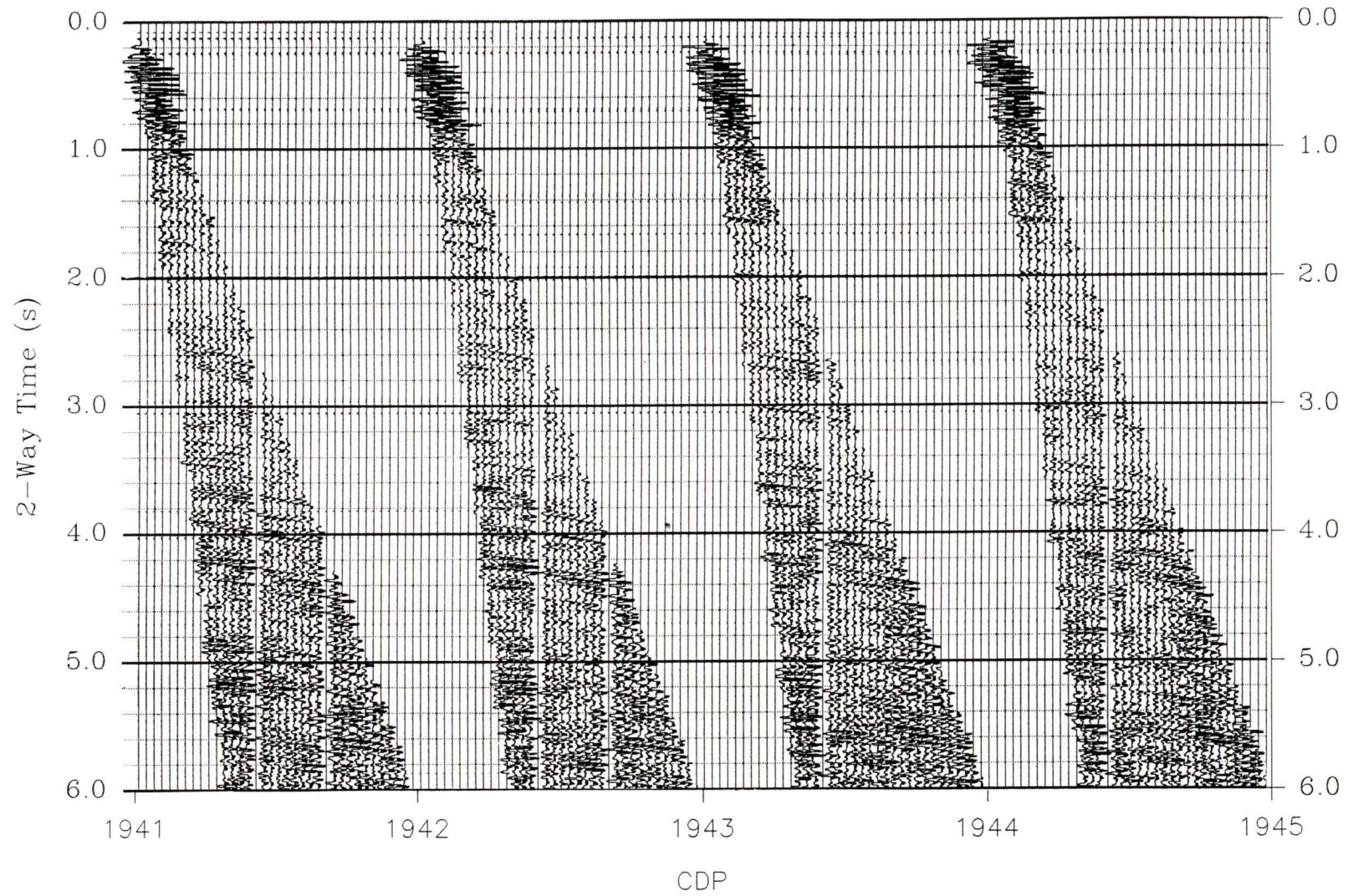


Figure 10: CDP 1941-1944 - gather with 5/10 Hz - 25/50 Hz filter and mute.

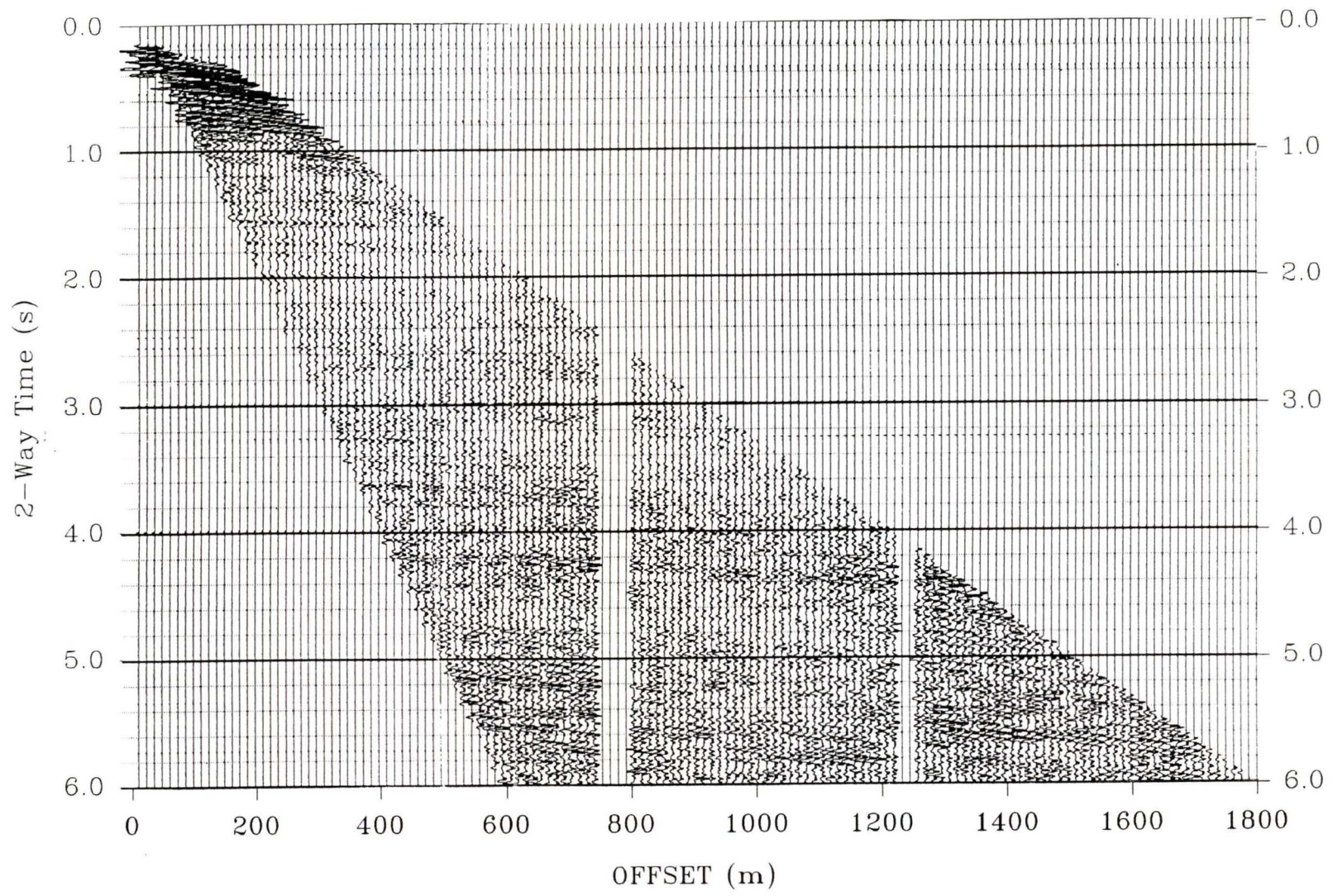


Figure 11: CDP 1961-1964

Super-gather.

Velocity analysis was performed using the VISTA system. Semblances were calculated, as defined below:

$$\text{SEMBLANCE } S = \frac{\sum_t S_t^2}{M \sum_t \sum_{i=1}^M (f_{i,t(i)})^2}$$

S_t = the Stack over M Receivers

$f_{i,t(i)}$ = data sample at trace i and time $t(i)$

M is the number of traces in the CDP gather.

Two-way time $t(i)$ lies along the trial stacking hyperbola.

$$S_t = \sum_{i=1}^M f_{i,t(i)}$$

Semblance is the normalized output to input energy ratio for a specific stacking hyperbola (Yilmaz, 1987). Prior to display and velocity picking a 2/4 Hz - 10/20 Hz filter was applied to the semblance panels to reduce the number of closed contours on the semblance plots. The input gather from Line 89-02, CDP 1641-1644 (SP 850) is shown in Figure 11. Velocities were chosen from the semblance plot by selecting a time velocity point at a closed contour. The hyperbolic moveout curve for that time-velocity pair was displayed (overlayed) on the gather. The validity of the pick could then be confirmed by visually comparing the correlation between the curve and the data. Due to the sparsity of closed contours on the semblance display as well as the wide range of velocities covered by most of the closed contours, the semblance plot was of limited value and most

time-velocity values were determined by comparing the moveout curve to the gathered data.

It was not possible to flatten all reflections across a gather using a single velocity. The velocity function from the original processing had flattened reflections at near offsets (Fig 12a at 1.58 s and 2.17 s), but this resulted in undercorrection for most reflections of lesser amplitude at middle offsets. In the new analysis the velocities were lower, with better correction of more reflections in the section (Fig. 12b 1.7 s, 2.2 s, 2.6 s). Since the near traces had been muted before velocity analysis, the larger amplitude reflections at near traces were slightly overcorrected (by approximately 1/2 wavelength from near to far trace on some of the gathers). Very high velocities were discounted in the velocity analysis by observing cycle skipping on the gather.

The stacking velocity functions from the reprocessing and the original Geophoto velocity function (linearly interpolated to CDP 1961 from the section header) are shown in Figure 13. The lower velocities produce larger moveout corrections and subsequently change the stacked trace (Fig. 12 - trace #36). Improvement in data quality can be observed in the stacked section, as described below. On the lower to middle slope region of the accretionary prism RMS velocities have been calculated from detailed velocity analysis of the 1989 reflection seismic data (Yuan *et al.* 1994). The curve of RMS velocity for that slope region is shown in Figure 13, but a direct comparison with the shelf region is not made since large variations in velocities occur across and near the deformation front due to changes in sediment porosities and pore pressures.

Reflections due to primary multiples can be reduced by F-K filtering which applies a filter dependent on velocity. Since multiples will have significantly lower velocity than direct reflections, the multiples will be attenuated. This process was included in the Geophoto processing. However, interbed multiples may still be present, since their velocities are closer to that of the direct reflections due to the smaller difference in path length. A possible method of improving the data quality and velocity picks from the

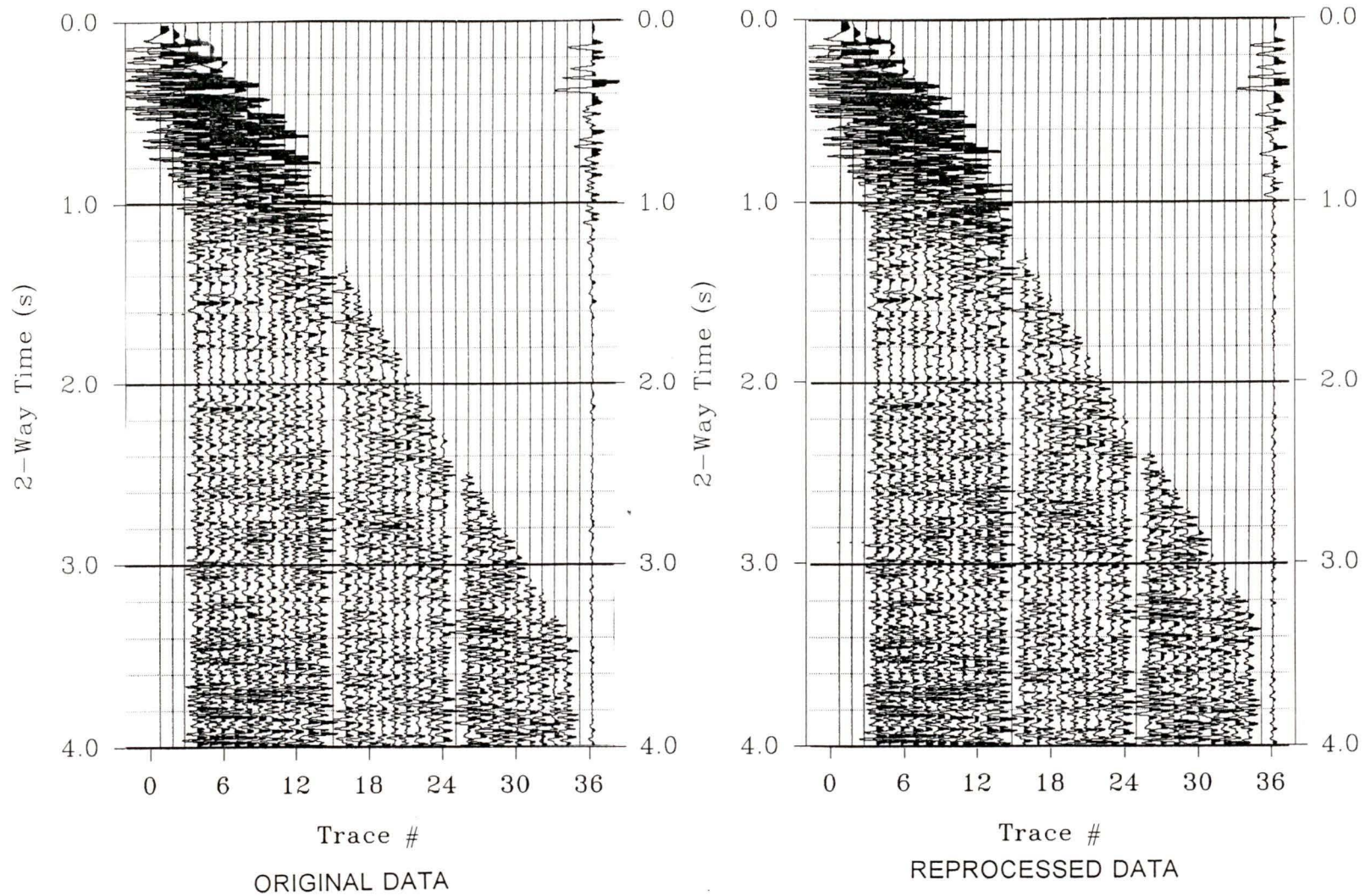


Figure 12: CDP 1961 - Gathers with NMO applied. a) Data with Geophoto velocity function and 5/10 - 40/60 Hz filter.
 b) Data with new velocity function and 5/10 - 40/60 Hz filter. Trace 36 is stacked data from each gather.

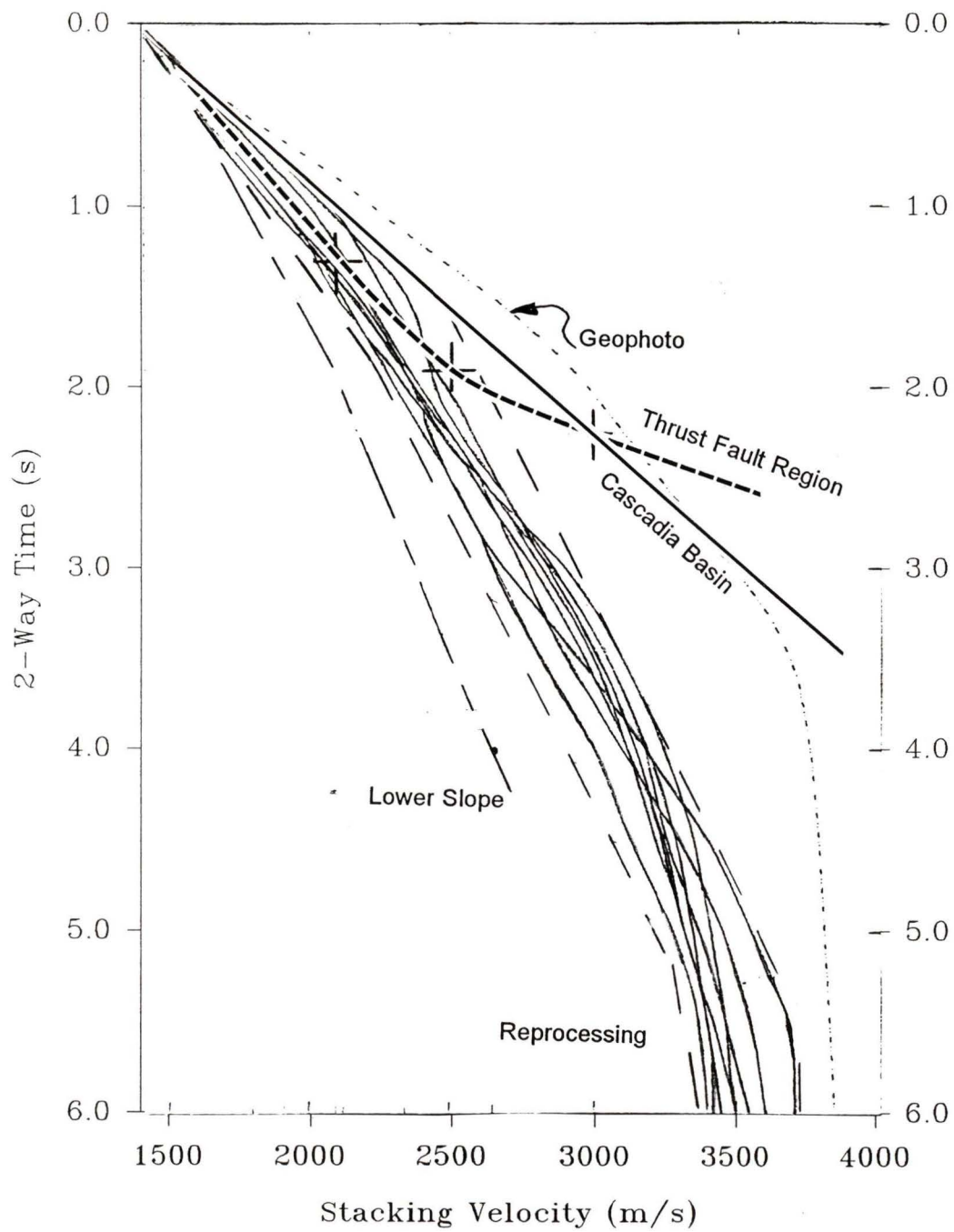


Figure 13: a) Stacking velocity curves from reprocessing, b) stacking velocity from Geophoto processing c) lower slope velocities d) thrust faulted region velocities e) Cascadia Basin velocities. (Curves c,d and e from Yuan *et al.* 1994).

semblance plots would be to apply time varying F-K multiple attenuation using the velocity picks chosen from this reprocessing and applying F-K dip filters below 90% of the velocity within short (possibly 1 s) windows.

After the velocity analysis, processing on the CDP gathers included:

- 1) Filtered gathers - 5/10 Hz - 40/60 Hz
- 2) NMO using velocity picks
- 3) Post NMO Mute
- 4) CDP Sort and Stack (36 fold)
- 5) Decon (VISTA DECON)- predictive decon for further attenuation of multiples
- 6) Filter 5/10 Hz - 40/60 Hz
- 7) Plot

The filters and mute patterns used on the data were the same as for the Geophoto processing for better comparison between the two final stacked sections. Post-stack migration of the data was not performed, due to the limited processing capability of the VISTA PC system.

A comparison of the original (Geophoto) processing and the reprocessed section from CDP 1800-2600 is shown in Figure 14. The original data were read from the stack data tape, with the original post-stack deconvolution and filter applied (Appendix 1) using VISTA routines. A 1000 ms AGC (automatic gain control) was applied to provide trace balancing. The reprocessed data had the same post-stack processes applied. The following difference can be observed between the two sections:

- (1) The reprocessed data have higher amplitude reflections and improved continuity in the top .5 sec below the water bottom.
- (2) Greater amplitude and higher continuity exists on the reprocessed data for the west dipping events from CDP 2500 -2100 at .5 to 2.5 s.
- (3) Improved continuity and greater variation in dip of the band of reflectors from

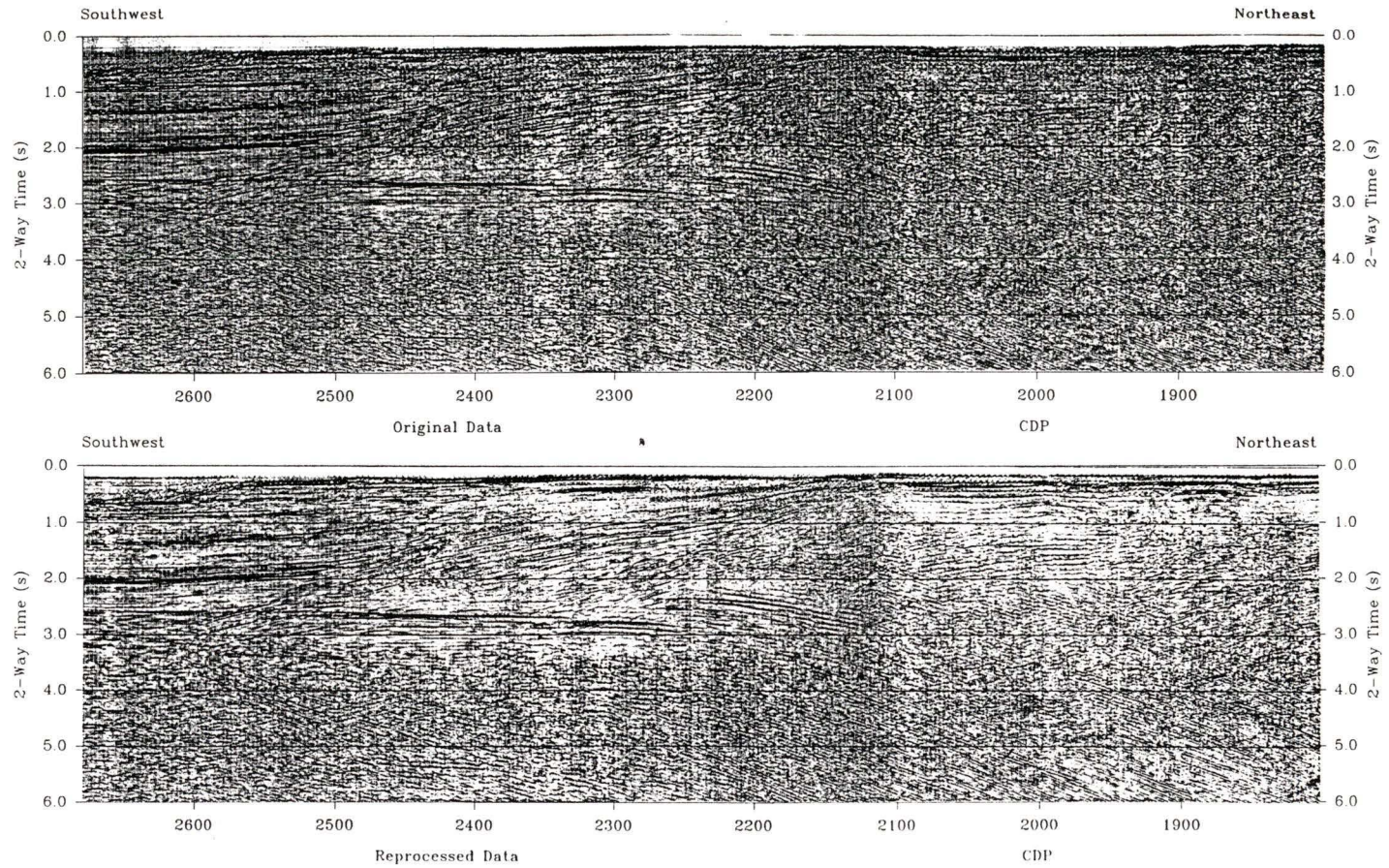


Figure 14: Line 2 Stack - CDP 1801-2604 a) Original data b) Reprocessed data

CDP 2300-2150 centred at 2.5 s.

- (4) From CDP 2100-1800 the improvement is marginal, but a change in the relative amplitudes between the horizontal and steeply dipping reflections can be seen which might result in changes to the migrated data.

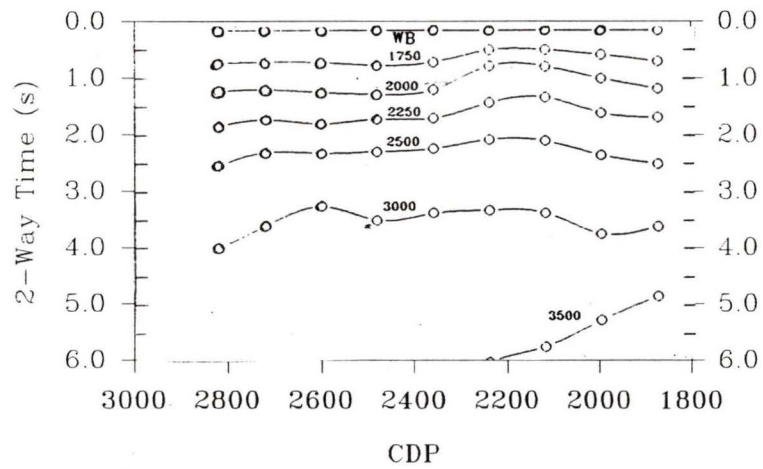
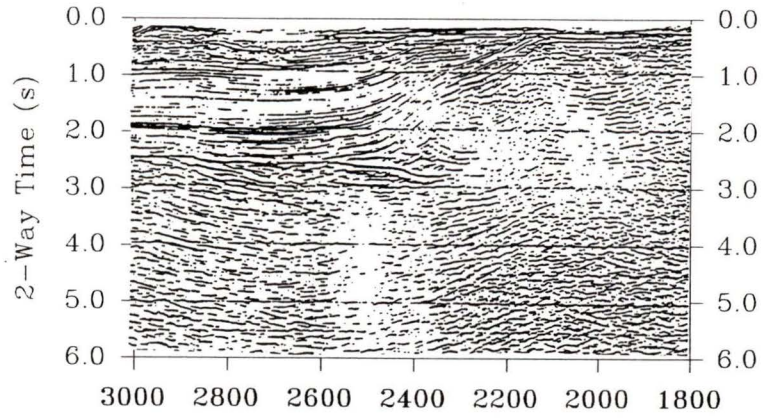
3.2.1 Velocity Contouring

To observe the variation in velocity across the reprocessed section (Fig. 15a), stacking velocities (Fig. 15b) and interval velocities (Fig. 15c) were contoured. The velocity picks from the reprocessed data were linearly interpolated to allow sampling at 500 ms intervals from water bottom to 6.0 s. Five adjacent velocity profiles (spanning 160 CDP's) were then plotted and a smooth curve drawn by hand through the values to obtain a velocity estimate at the location of the central CDP. This procedure was repeated at every third velocity analysis point (120 CDP's), overlapping the previous average by 2 velocity points (80 CDP's). Velocity contours were then plotted from these average time-velocity curves.

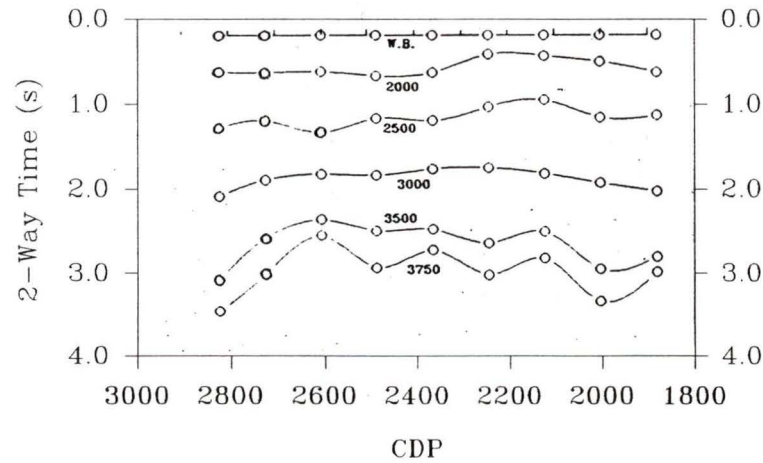
The smoothed stacking velocity curves, sampled at 500 ms, were then used to calculate the interval velocities using the DIX equation (Hajnal and Sereda 1981):

$$V_{INT}^2 = \frac{(V_{S_{i+1}})^2 t_{i+1} - (V_{S_i})^2 t_i}{t_{i+1} - t_i}$$

These interval velocities were then contoured and plotted.



Constant Stacking Velocities



Constant Interval Velocities

Figure 15: a) Line 2 reprocessed seismic data CDP 1801- 2880. b) Constant stacking velocity cross section. c) Constant interval velocity cross section .

3.2.2 Comparison of Velocities from Well Data and Seismic Data

The interval velocity-time profiles for the six exploration wells (discussed in section 3.1) were plotted together with an interval velocity-time curve for the reprocessed data in Figure 16. The curve for the reprocessed data is a least squares fit of the ten velocity profiles in Figure 13. The velocity curve from the original processing is also shown.

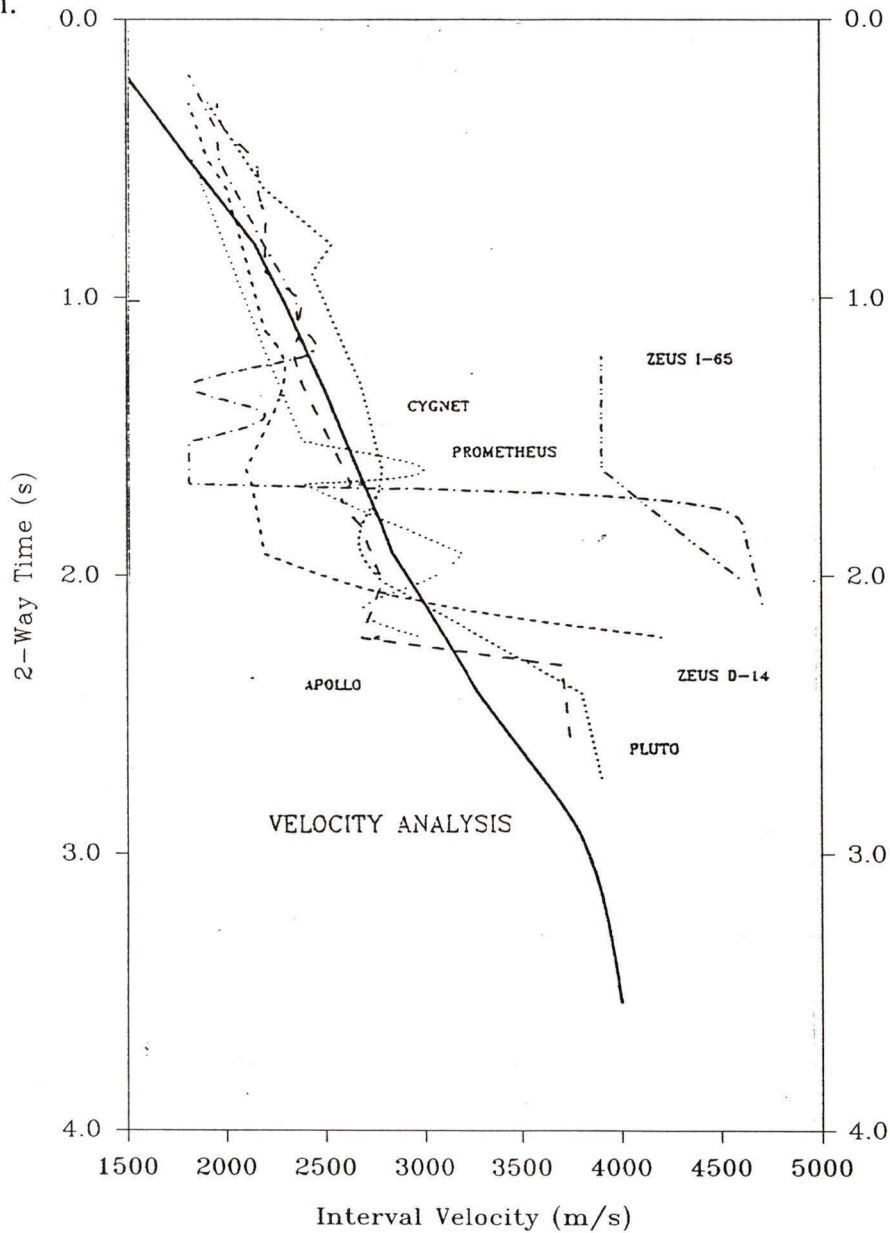


Figure 16: Interval velocity profiles - wells and seismic data (CDP 1941-44)

3.3 Analysis of Velocity data - Line 89-02

Stacking velocities from analysis of the seismic data on Line 89-02 (Fig. 13) are uniformly lower than the original values from the Geophoto processing. Although there is significant variation in the interval velocity values from the wells, the curve of interval velocity from the reprocessing (Fig. 16) follows the trend of most of the well data. The velocities from deep sections of the wells which encountered volcanics (Prometheus and Zeus D-14) should not match velocities from the seismic section, since the seismic data at the eastern end of Line 89-02 have been interpreted as sedimentary (Tofino Basin sediments or perhaps Pacific Rim Terrane). The improved velocities also resulted in an improved stack section (Fig. 14). Lateral variation in the stacking velocity functions of the reprocessed data is most significant above 1.5 s (Fig. 13). Since the corresponding section of the Geophoto data was processed with only one velocity function, some of the improvement may be due to the higher density of velocity analyses.

The interval velocity functions for the reprocessed data (Fig. 15) show an increase in velocity above 2.0 s to the east of CDP 2400. This corresponds to the region where Tofino Basin sediments are thinning against the basement structure. The increased velocity represents either 1) material uplifted in the section due to diapirism or folding, or 2) rocks of the Pacific Rim Terrane. Migration of the reprocessed data and replotting with a higher quality plotter is needed to confirm the improvement in the stacked data.

CHAPTER 4

INTERPRETATION

The structure beneath the continental shelf has been interpreted from the 1985 and 1989 multichannel seismic data over Tofino Basin, with additional constraints from magnetic field, well and CSP data. Multichannel seismic reflections were interpreted from the subducting oceanic crust, the Pacific Rim and Crescent terranes, and within the overlying Tofino Basin sediments.

Refinements to the location of the Crescent Terrane were determined from the data in the region of the Prometheus Magnetic High. Only limited information on the location of the Pacific Rim Terrane can be interpreted from the seismic data. The location of the Crescent and Pacific Rim terranes is best constrained by magnetic field data (Fig. 8a). The striped pattern at the western limits of the magnetic field map is associated with the seafloor spreading anomalies, which originate within the oceanic crust and are parallel to the Juan de Fuca Ridge. As the crust is overlain by increasing thickness of sediments of the accretionary wedge, this pattern decreases in amplitude partly because of increasing depth to the oceanic crust and partly due to thermal effects on magnetization (eg. Dehler 1992). The large closed magnetic high (> 200 nT) parallel to Vancouver Island from Cape Flattery to west of Clayoquot Sound has been named the Prometheus Magnetic High (PMH) by MacLeod *et al.* (1977). Measurements of susceptibility of outcrop from Vancouver Island and the Olympic Peninsula indicate that a large contrast exists between the Metchosin Volcanics (Crescent Formation) and any other rocks of the area so that the probable source of the Prometheus Magnetic High is the Crescent Terrane (MacLeod *et al.* 1977). The region of relative low magnetic field values between the PMH and Vancouver Island is due to low susceptibility values of the Pacific Rim Terrane (Arkani-Hamed and Strangway 1988; Hyndman *et al.* 1990; Dehler 1992).

The oceanic plate is clearly imaged by seismic data over much of the region to the west of Tofino Basin, beneath the continental slope, and can be interpreted in many areas beneath the basin. It is imaged as a smooth surface with increasing dip landward on all of the profiles (Hyndman *et al.* 1990). An example of this is Line 85-01 (Fig. 19) between SP 101 at 5.0 s and SP 700 at 5.6 s.

4.1 Tofino Basin Seismic Data Interpretation

Stratigraphic and structural details were interpreted from the 1989 and 1985 seismic data within sediments of Tofino Basin, integrated with information from the six wells in the basin. The CSP data were used to provide structural information for the upper section of the basin. Seismic data from the 1985 and 1989 data sets image sediments of Tofino Basin and, with less resolution, the underlying accretionary prism, the Crescent and Pacific Rim terranes and the subducting oceanic plate. The migrated seismic lines from the 1985 and 1989 data sets (Fig. 6) with associated geological interpretations are shown in Figures 17 to 23.

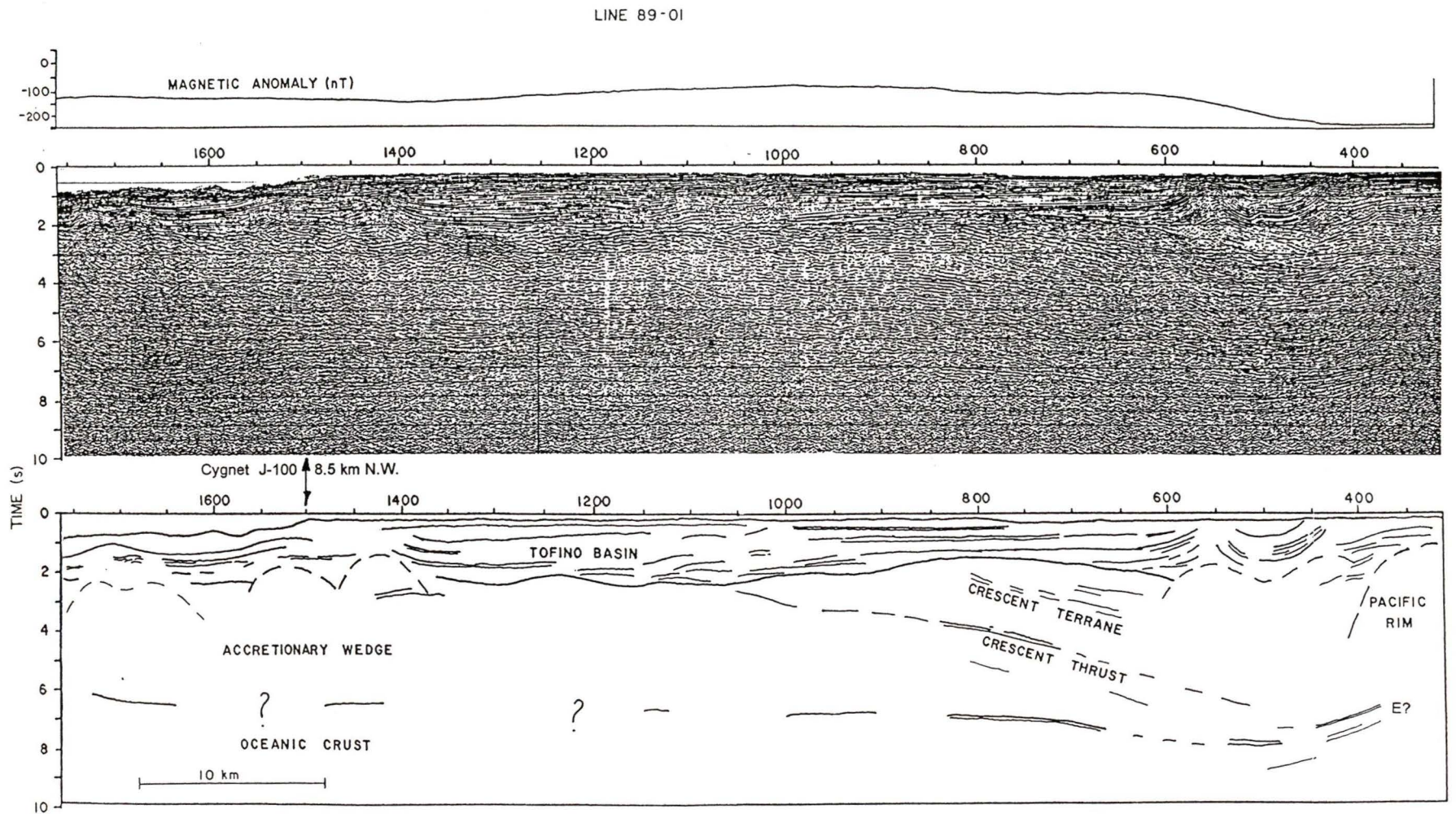


Figure 17: Multichannel seismic reflection data (migrated) and interpretation - Line 89-01

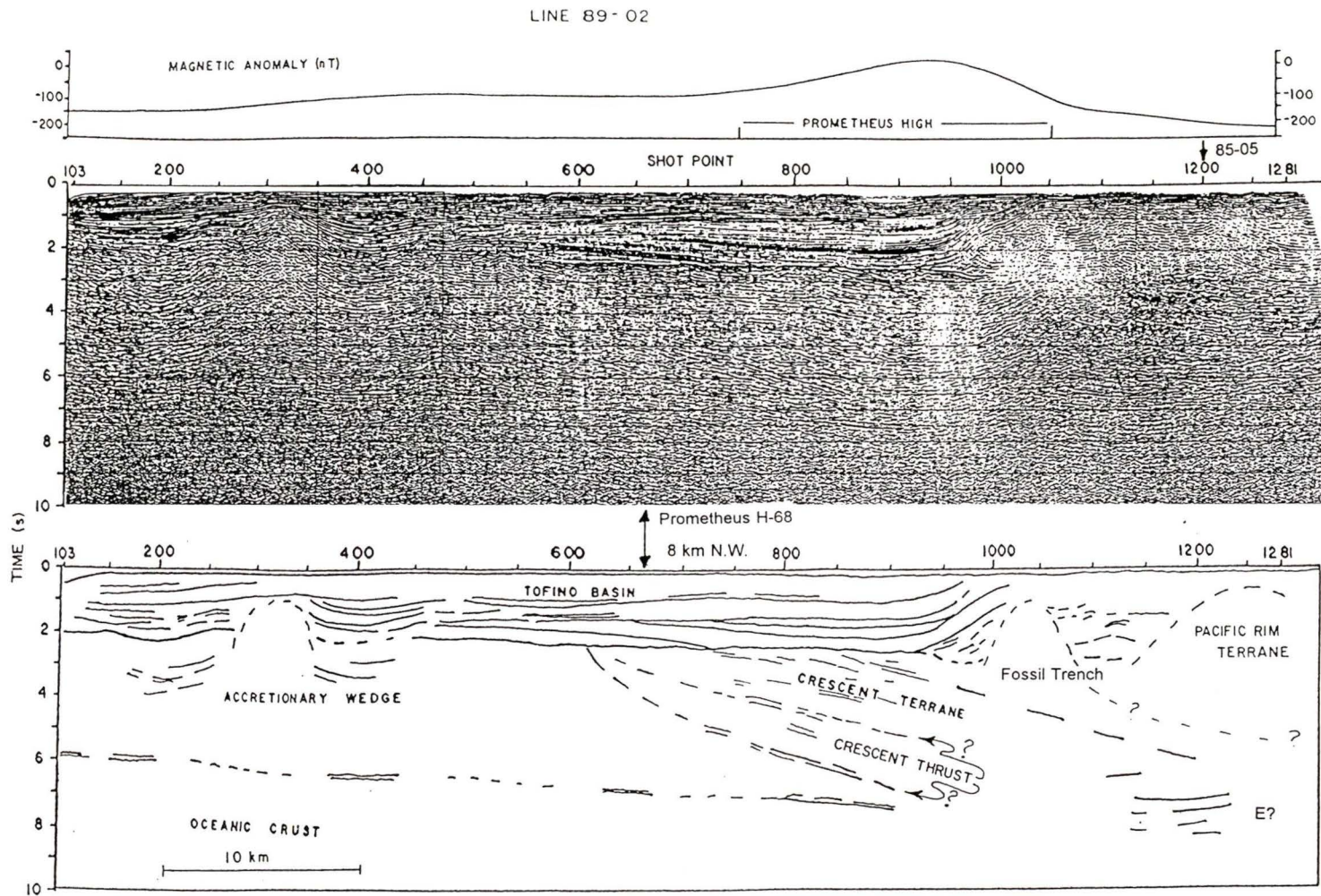


Figure 18: Multichannel seismic reflection data (migrated) and interpretation - Line 89-02

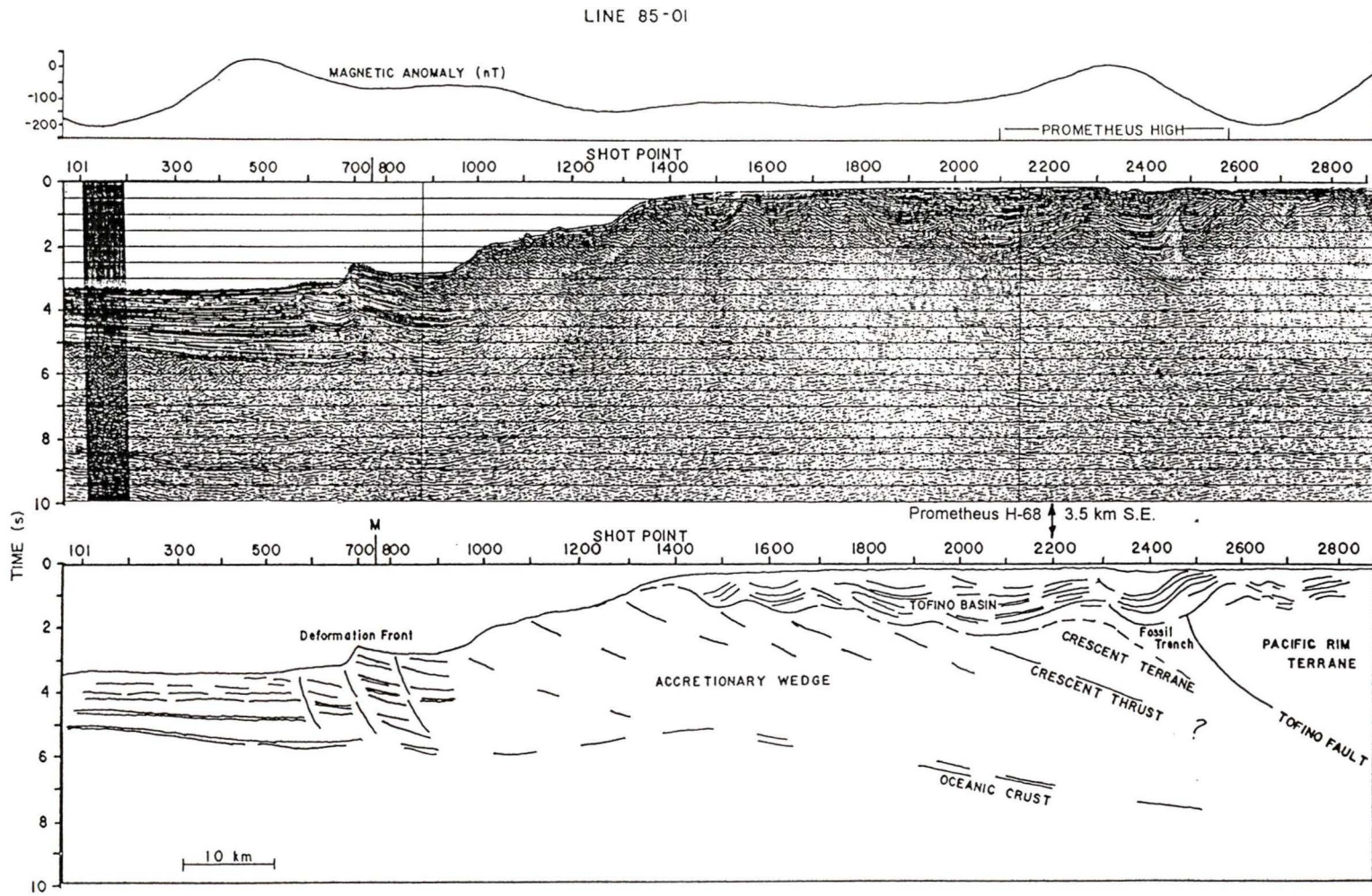


Figure 19: Multichannel seismic reflection data (migrated) and interpretation - Line 85-01

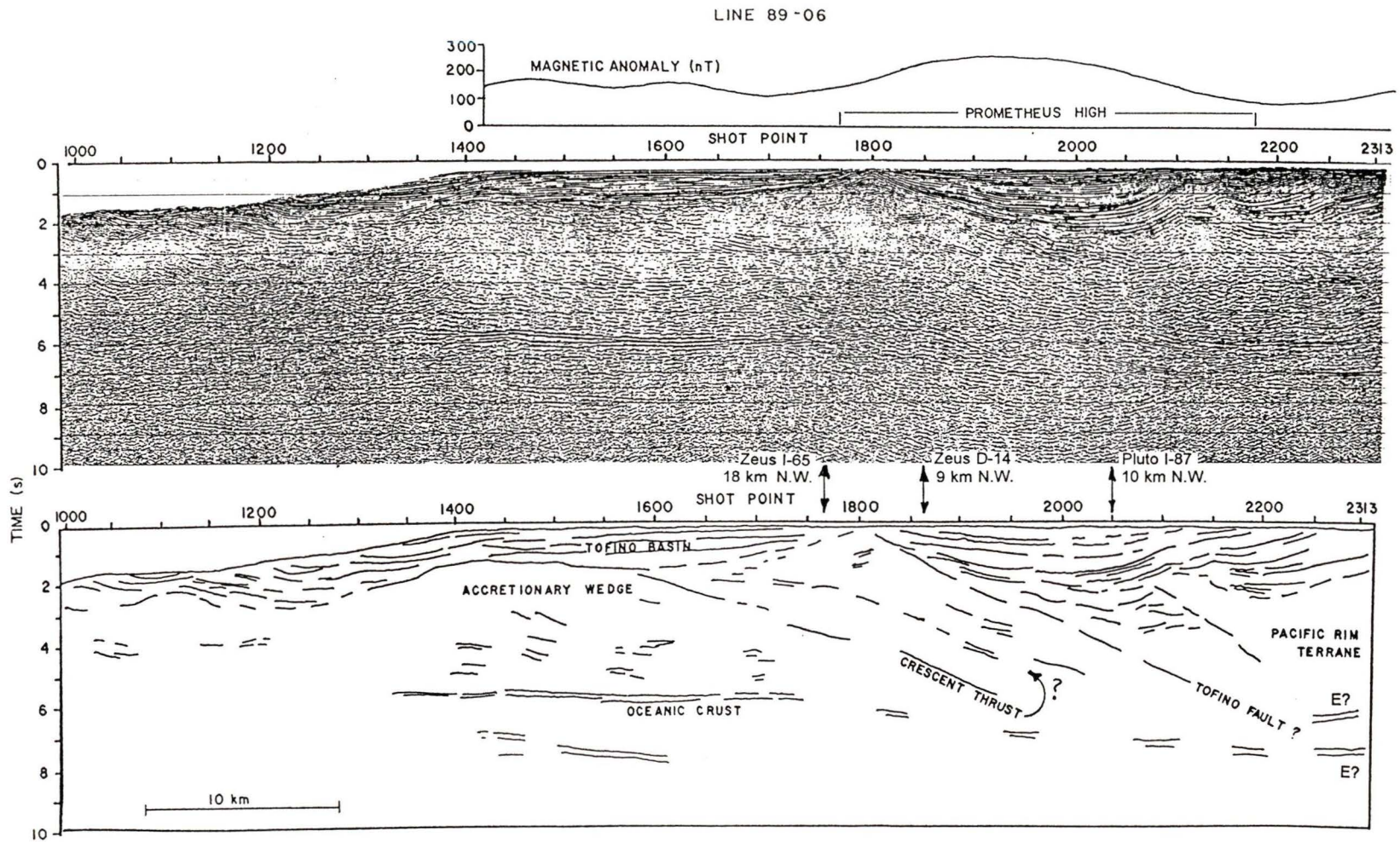


Figure 20: Multichannel seismic reflection data (migrated) and interpretation - Line 89-06

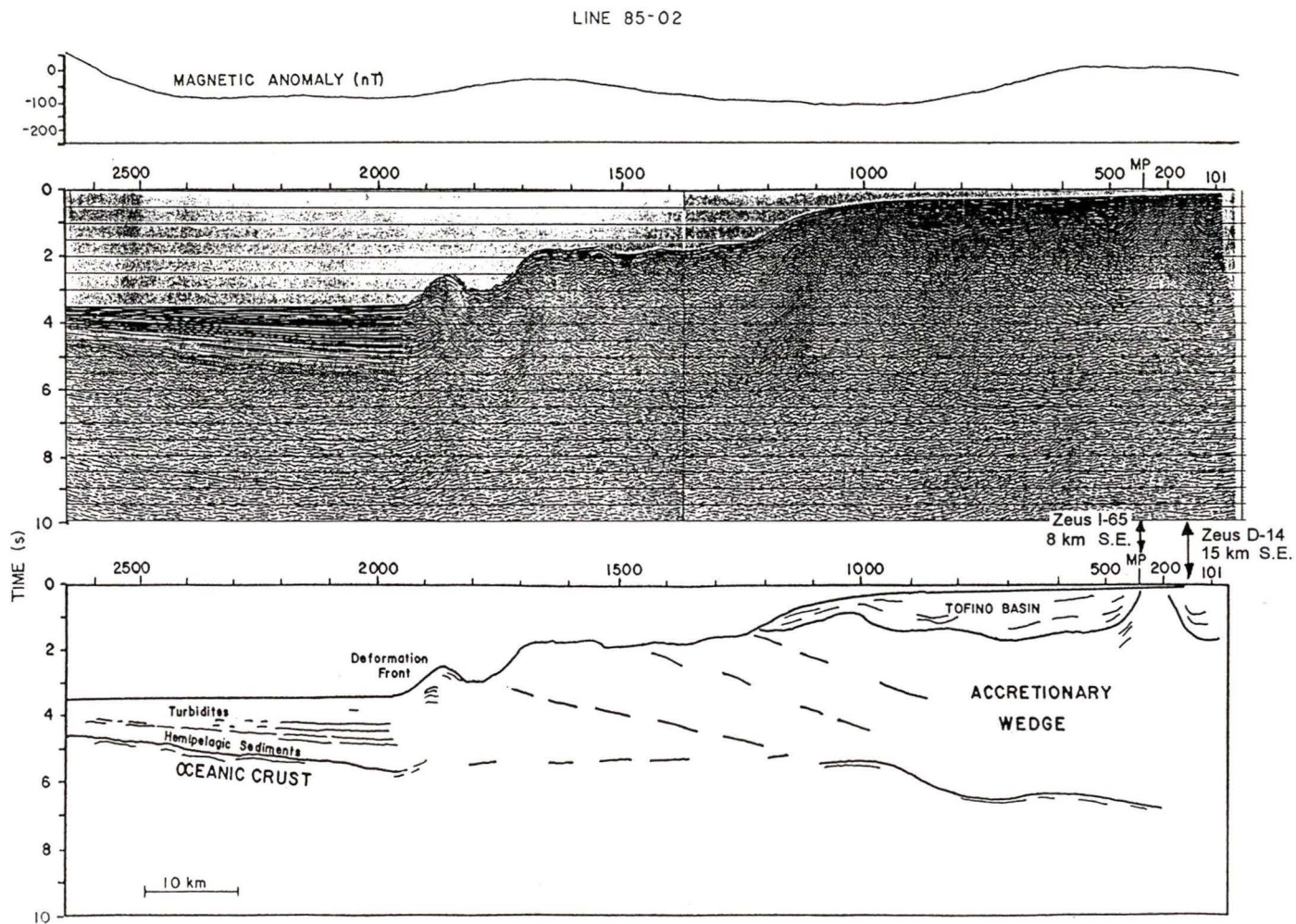


Figure 21: Multichannel seismic reflection data (migrated) and interpretation - Line 85-02

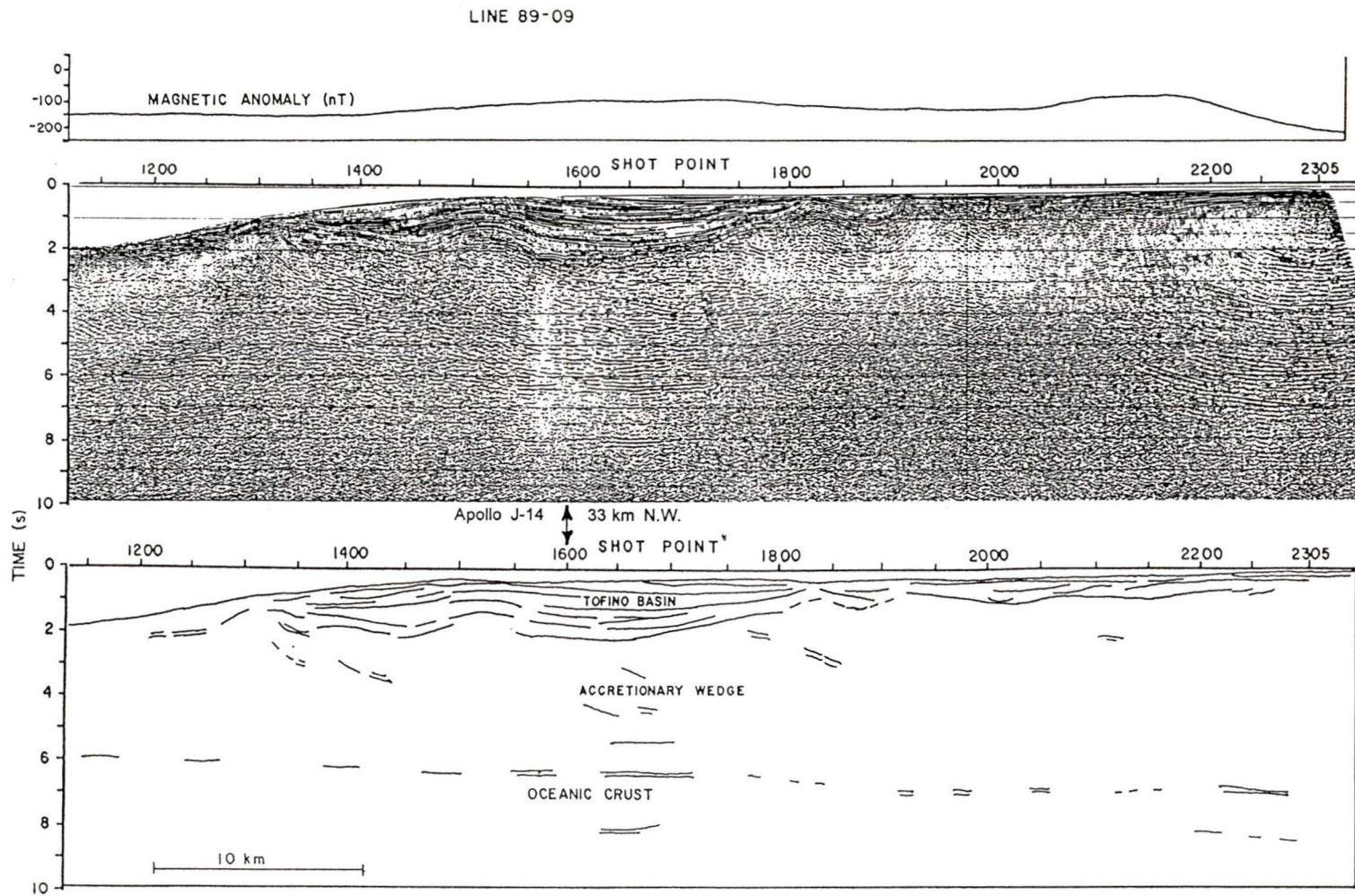


Figure 22: Multichannel seismic reflection data (migrated) and interpretation - Line 89-09

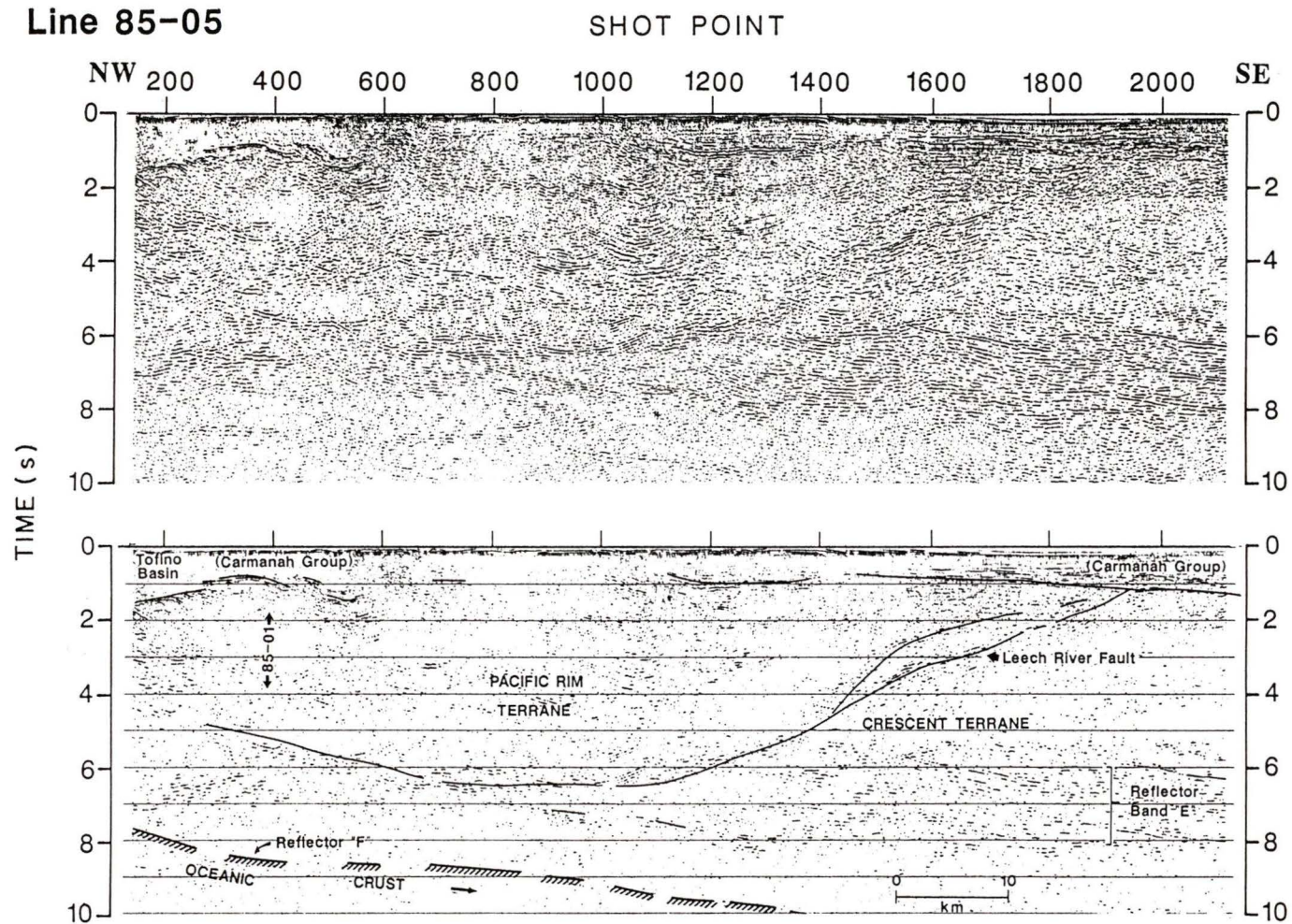


Figure 23: Multichannel seismic reflection data (migrated) and interpretation - Line 85-05
 (after Hyndman *et al* 1990).

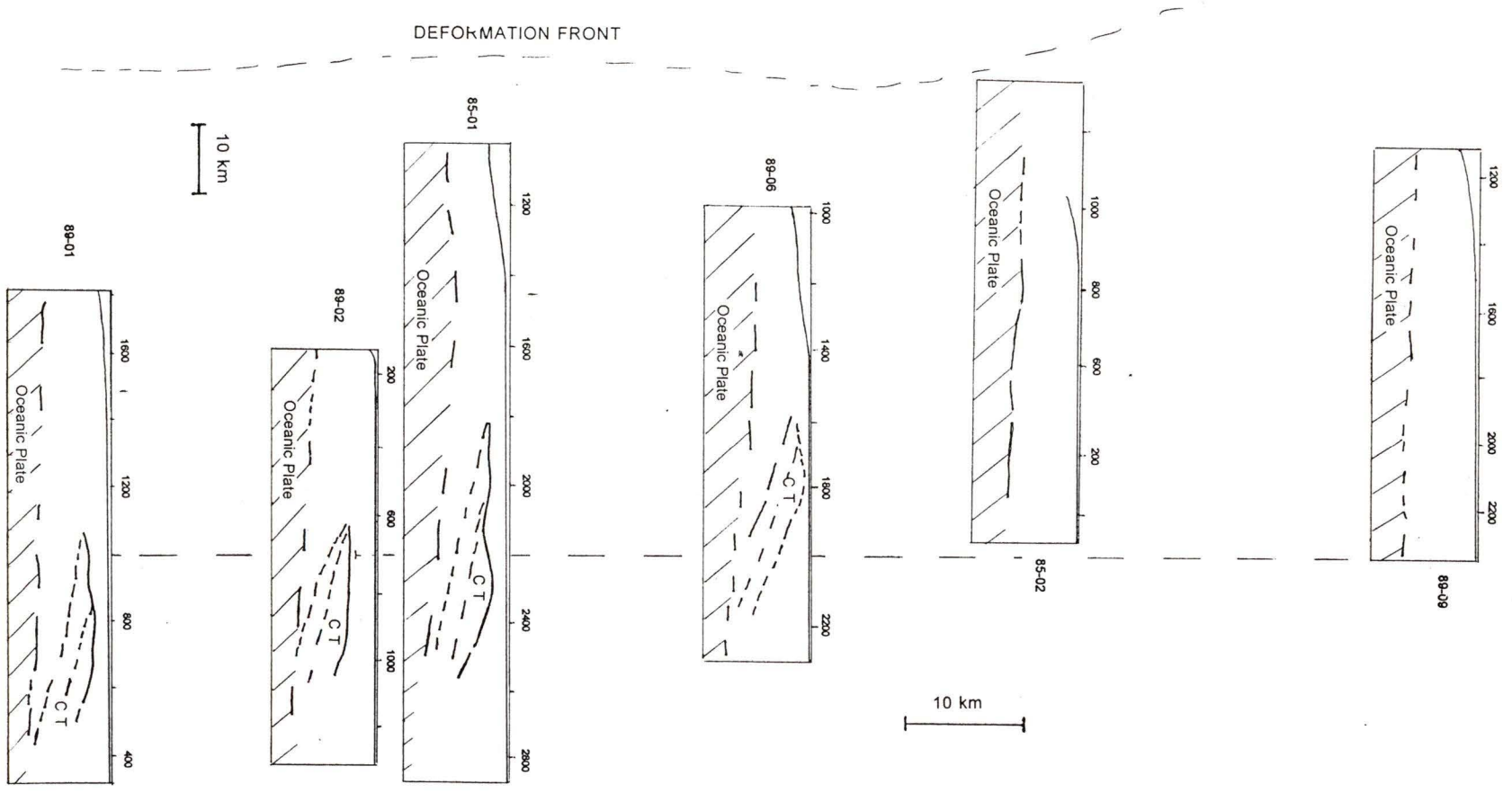


Figure 24: Interpretation of Crescent Terrane and Oceanic Plate. Reference line is roughly parallel to deformation front. Vertical separation of seismic lines is scaled to distance between lines (Fig. 6) . Vertical scale on profiles as in figure 17 to 23 (2-way time - 0s to 10 s) CT = Crescent Terrane.

4.1.1 Oceanic Plate

West of the deformation front, the top of the oceanic crust is imaged on the 1985 and 1989 seismic data as a high amplitude, relatively smooth reflector, which dips at a low angle to the east, and lies beneath 2-4 km of pelagic and hemipelagic sediments (Hyndman *et al.* 1990; Davis & Hyndman 1989; Spence *et al.* 1991). The oceanic crust can be correlated from the strong reflections in the Cascadia abyssal plain and deformation front region, through reflections under the continental shelf and down-dip beneath Vancouver Island to a reflector observed on the 1984 Lithoprobe data (reflector F: Clowes *et al.* 1987; Hyndman *et al.* 1990). Under Vancouver Island, earthquake data constrain the location of the subducting plate (Davis and Hyndman 1989) (Fig. 3), which is estimated to be at depths greater than 30 km. Refraction data (Spence *et al.* 1985; Drew and Clowes 1989) are also consistent with a model which includes subducting oceanic crust to depths of 35 km or more beneath Vancouver Island. The interpretation of the location of the top of the oceanic plate is shown with the seismic data in Figures 17-23. The 6 seismic profiles are displayed with the interpretations of the Crescent Terrane and oceanic plate in Figure 24. Each line was located horizontally on the display to align along a line roughly parallel to the shelf break and deformation front. The vertical position is scaled to the distance between each line. Reflection times to the top of the oceanic plate were used to calculate the dip of the oceanic plate (Table 2). The depths are calculated by multiplying one way time to the oceanic crust by the stacking velocity value at the two-way time. The stacking velocity is used as an estimate of average velocity at each location. The dip calculated from the seismic data is relatively low, but agrees with data from Benioff-Wadati earthquakes farther landward (Hyndman *et al.* 1990). Spence *et al.* (1991) propose that reflections beneath the continental shelf on Line 89-06 cannot result from lithological contrast between the oceanic crust and accreted sediments, but are due to fluids trapped in a shear zone between the oceanic crust and the overlying accretionary prism or backstop. Thus the values shown in table 2 may represent the dip of a shear zone and thus a lower limit for the actual dip of the oceanic plate.

LINE	SP	Time (s) 2-way	Vel. (m/s)	Depth (m)	Dip (deg)
89-01	850	7.0	3590	12500	8.5
	650	7.7	3640	14000	
89-02	100	6.3	3400	10700	3
	550	6.7	3500	11750	
89-02	780	7.2	3650	13150	7
	900	7.5	3700	13880	
85-01	1800	5.8	4650	13500	13
	2500	7.5	5800	21750	
89-06	1400	5.8	3500	10150	6
	1700	6.0	3940	11820	
89-06	1800	6.25	3900	12200	13
	2000	7.5	3900	14600	
85-02	950	5.4	3800	10300	15
	500	6.4	5100	16300	
89-09	1300	5.75	3150	9050	9
	1550	6.5	3400	11050	

Table 2: Dip of the oceanic crust beneath the continental shelf.

Reflections from the oceanic plate are interpreted on Line 89-01 (Fig. 17) as intermittent reflectors between SP 1000 and SP 600 at 7.0-7.5 s. This represents a depth

of greater than 12 km. The horizon is flat lying from SP 1000-850, and changes to an average dip of approximately 8.5° between SP 850 and SP 650. Pullup of the seismic reflections due to velocity effects from thinning Tofino Basin sediments and high velocity Crescent Terrane may account for some of the change in dip. The location of the strongest reflections from the top of the oceanic crust is directly beneath the interpreted position of the Crescent Terrane (see below). The amplitude of the reflections may be enhanced due to increased fluid pressures within the accreted oceanic sediments beneath the backstop provided by the Crescent and Pacific Rim terranes.

Oceanic plate reflections are observed on line 89-02 (Fig. 18) from SP 100 at 6.3 s to SP 550 at 6.7 s with dip of 3° . There are few strong reflectors eastward as far as SP 780 where another strong reflector is observed at 7.2 s continuing to SP 900 (7.5 s) at a slightly steeper dip of 7° . Although the accuracy of dip values at specific locations is restricted by lateral velocity variations, the trend in dips is consistent with other models as previously detailed. Lithoprobe Line 1 extends beneath Vancouver Island northeast of the landward end of Line 89-02. A zone of reflectors representing the top of the oceanic plate dips at approximately 10° to 12° (Yorath *et al.* 1985, Figure 13 Yorath 1987) from the western end of that line, which is also consistent with the interpretation of Line 89-02.

On Line 85-01 (Fig. 19) the reflection from the oceanic crust is clearly imaged seaward of the deformation front (SP 100-1000). The reflections are seen intermittently northeast of the deformation front with poor continuity under the continental slope (the rise of the interpreted horizon on the time section, immediately east of the deformation front from SP 1000 to SP 1500, is due to change in water depth). Greater continuity is observed on the horizon dipping to the east under the shelf, where the dip from SP 1800 to SP 2500 is calculated to be 13° . Hyndman *et al.* (1990) extrapolated beyond the end of line 85-01 to correlate with a deep reflector on land data (line 84-01 Reflector "F", Fig. 3 - Hyndman *et al.* 1990).

The horizontal continuity of the reflections beneath the continental shelf is greater

on Line 89-06. From SP 1400 to SP 1700, a 0.5 s package of reflectors at approximately 6 s (Fig. 20) contains strong continuous reflections which dip at approximately 6° northeast of SP 1740 reflector continuity decreases, but the dip increases to over 13° between SP 1800 and SP 2000. Oceanic crust cannot be identified beyond SP 2000.

Line 85-02 (Fig. 21) images the oceanic crust from the Cascadia Basin to the landward edge of the continental shelf. As interpreted by Hyndman *et al.* (1990), the top of the oceanic crust occurs at the base of reflections representing the accretionary wedge, and has near zero dip from the deformation front at SP 2000 across the shelf slope to SP 1050. From SP 950 to SP 500 reflections are identified on the seismic data from which an average dip is calculated to be 15°.

On the migrated data of line 89-09 (Figure 22) identification of the oceanic crust cannot be made with any certainty beneath the shelf since few reflectors are seen northeast of SP 1730. Weak reflections at SP 1950-2050 at 7.0 s may represent the oceanic crust, as may the overmigrated reflections between SP 2200 and the end of the line, below 6.5 s. The dip of the oceanic crust between SP 1300 and SP 1550 was calculated to be 9°.

Several of the seismic sections display an anomalous low amplitude reflection between 1.5 s and 2.0 s below the top of the oceanic crust. An example of this can be seen on Line 89-06 between SP 1450 and SP 1700. The reflection is not continuous over the same region as the top of the oceanic crust and the depth of the reflection below the oceanic crust varies between lines. On Line 85-02, Calvert and Clowes (1991, Fig.3) have interpreted these events as the base of the oceanic crust.

Depth to the oceanic plate was calculated along each seismic profile from a straight line through the reflections from the oceanic plate of Figure 24. A contour map of these values is shown in Figure 25. This map is in general agreement with a regional map of depth to the oceanic plate shown in Hyndman *et al.*(1990)

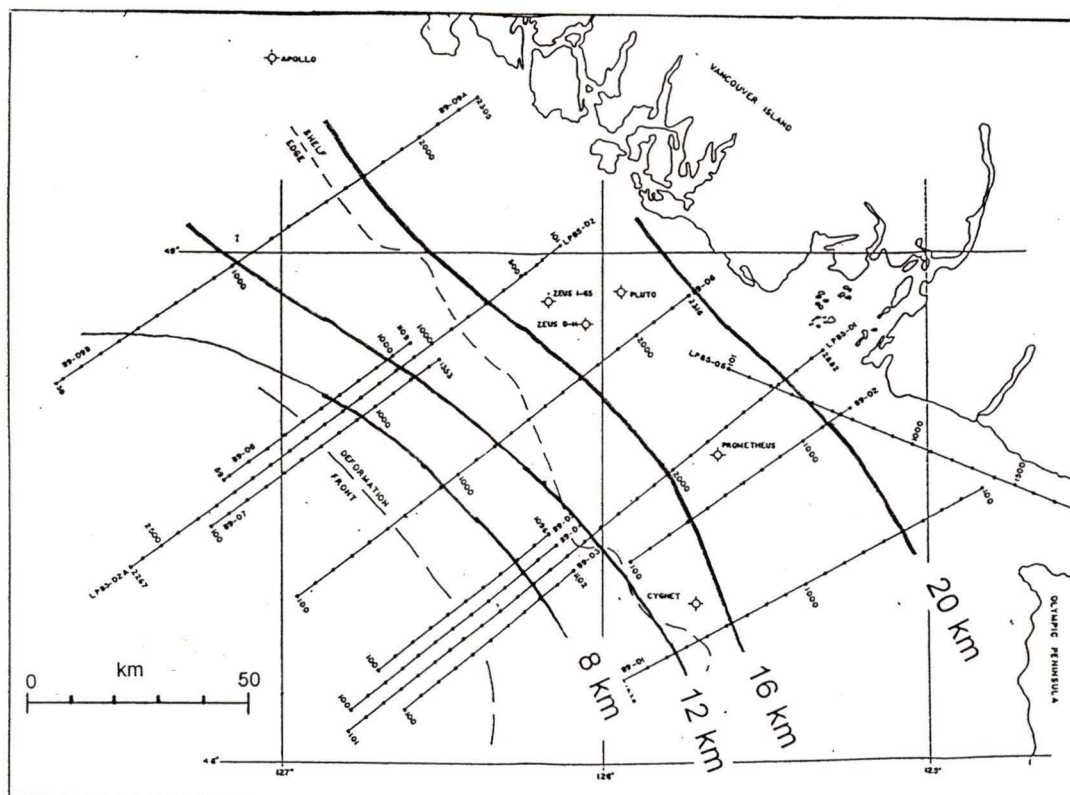


Figure 25: Depths in kilometres to the top of the downgoing oceanic plate.

4.1.2 Pacific Rim Terrane

The eastern limit of the Pacific Rim Terrane is not imaged on the seismic data used for this thesis. This limit is defined by the magnetic field data and in a few locations by outcrop of the Pacific Rim Terrane on land. The western boundary of the Pacific Rim Terrane is in contact with the Crescent Terrane at depth, but is separated from the upper portion of the Crescent Terrane by Tofino Basin sediments emplaced in the Eocene sedimentary trough (Fig 19, Line 85-01: SP 2400-2500) (Hyndman *et al.* 1990).

Line 89-01 lies to the south of the Prometheus Magnetic High (PMH), with the northeast end of the line (SP 101-600) extending over the magnetic low anomaly expressing the Pacific Rim Terrane. Northeast of SP 400 the top of the Pacific Rim Terrane is interpreted at 1.5 s, below the shallow layered reflections corresponding to Tofino Basin sediments. Reflections in the section below 6 s may be associated with the base of the Pacific Rim Terrane overlying the Crescent Terrane and the subducting

oceanic plate.

On Line 89-02 the Pacific Rim Terrane cannot be identified with any degree of confidence. West dipping reflections of Tofino Basin sediments at SP 1050 and the reflection from the top of the Crescent Terrane at SP 950 (at 2.8 sec) mark the maximum western limit of the Pacific Rim Terrane, but the remaining eastern end of the line has no coherent reflections below 1 s.

Line 85-01 (Fig. 19) has been interpreted by Hyndman et al. (1990) with the Pacific Rim Terrane east of SP 2500 below 1.0 s. It is separated from the Crescent Terrane by Tofino Basin sediments in the fossil trench above 3.5 s and by the Tofino Fault below. Strong reflections from SP 2600 to SP 2900, from 5.5 s to 7.0 s have been interpreted by Calvert and Clowes (1990) correspond to the "E" reflections interpreted on seismic profiles under and to the east of Vancouver Island. On Line 85-01 these reflections are located beneath the Pacific Rim Terrane, near the eastward limit of the Crescent Terrane, and above the oceanic crust. Calvert and Clowes (1990) have suggested that these reflections are due to the presence of sheared rocks, similar to reflections from the subduction decollement beneath the Crescent Terrane, where the decollement zone is approximately 0.5 s thick and interpreted as a zone of distributed shear.

On Line 89-06 the top of the Pacific Rim Terrane is interpreted east of SP 2100 near 2.0 s, overlain by a clearly imaged section of reflective Tofino Basin sediments. The lower boundary of the Pacific Rim Terrane can only be inferred from the extension of the Crescent Terrane (see below). The lines north of Line 89-06 do not extend landward past the Prometheus Magnetic High into the Pacific Rim Terrane.

4.1.3 Crescent Terrane

The location of the Crescent Terrane, beneath Tofino Basin sediments, to the west of the Pacific Rim Terrane is best constrained by the location of the Prometheus Magnetic High (Fig. 8a). This magnetic high is indicated on the magnetic field anomaly profile above each seismic section (Fig. 17-23). The seismic interpretation of the Crescent Terrane on Lines 89-01,02,06 and 85-01 has the terrane seaward of the limits of the Prometheus Magnetic High. One explanation is that material at the seaward edge of the Crescent Terrane has low susceptibility. This could have resulted if sedimentary material were deposited or accreted to the Crescent Terrane before the accretion of the complete unit to North America. A more likely possibility is that a reversal in the earth's magnetic field occurred during creation of the Crescent Terrane. The accepted date for formation of the Crescent Terrane is 52-57 Ma (see summary: Hyndman *et al.* 1990). The Crescent Terrane has a minimum width measured from the seismic data of over 30 km. If the rate of crustal formation was similar to that at the present Juan de Fuca Ridge (approx. 30 mm/a) then the minimum period for formation would be greater than 1 Ma. Between 52 Ma and 57 Ma there are 5 reversals of the earth's magnetic field (Harland *et al.* 1990). Formation of the Crescent Terrane could have occurred during a time span which overlapped one of these reversals, resulting in a magnetic field with large variation. The measured field would then show a decrease, even though the lithology was identical. There is evidence from outcrop of the Metchosin Igneous Complex on Vancouver Island of both normal and reverse polarities (Irving and Massey, 1990). The interpretation of the Crescent Terrane from the seismic data is displayed in its relative position in Figure 24.

The top of Crescent Terrane is more irregular and less well defined on the seismic data than the base of Crescent Terrane. On Line 89-01 the top of the Crescent Terrane is a rough surface extending from SP 1050 to a structurally high position at SP 800 and continues to SP 600 where the seismic reflection terminates. The Crescent Terrane is then assumed to dip steeply through broken reflectors to intersect the Pacific Rim Terrane near SP 400. A thick section of chaotic, low frequency reflections below 3.0 s at SP 500 is

of uncertain origin, but is interpreted as Tofino Basin sediments equivalent to the fossil trench on Lines 85-01 and 89-06. On a number of seismic sections the interpreted base of the Crescent Terrane is a simple planar reflection. This is in agreement with the sharp boundary observed in outcrop on the Olympic Peninsula. The dip of the base of the Crescent Terrane was calculated as shown in Table 3.

LINE	SP	Time (s)	Vel. (m/s)	Depth (m)	Dip (deg)
89-01	850	4.0	3200	6400	20
	550	6.5	3650	11850	
89-02	700	5.0	2250	2800	26
	1000	7.5	4500	16900	
85-01	2000	2.5	2800	3500	20
	2700	5.5	5800	16000	
89-06	1550	1.5	1950	1450	28
	1950	6.5	3800	12350	

Table 3: Estimate of Average Dip of the base of Crescent Terrane (Crescent Thrust)

On Line 89-01, southeast of the Prometheus Magnetic High (Fig. 8a), the base of Crescent Terrane is interpreted from SP 850 at 4.0 s to SP 550 at 6.5 s resulting in a 20° apparent dip. East of SP 650 the interpretation can be extended to a depth coincident with the reflections from the top of oceanic crust. Curvature and deflection of these seismic reflections (SP 600 to SP 400, 6.0 s to 8.0 s) may indicate interaction between the Crescent Terrane and the oceanic crust. The base of the Crescent Terrane can be extrapolated upward to the base of Tofino Basin sediments at SP 1050-1100. This location coincides with a horizontal change in the seismic character at the base of Tofino Basin sediments, interpreted to represent the boundary between the Crescent Terrane and sediments of the accretionary prism.

The surface of the Crescent Terrane on Line 89-02 extends from SP 600 at the Crescent Fault to SP 1000 against the Pacific Rim Terrane. The boundary between the Crescent and Pacific Rim terranes cannot be determined, since the interpretation of Pacific Rim Terrane on Line 89-02 was uncertain. Two alternatives are identified for the Crescent Thrust at the base of Crescent Terrane. The first is defined by extrapolating upward along seismic reflections from the oceanic crust at SP 1000 (7.5 s) to the base of Tofino Basin sediments at SP 600. Reflections from SP 700 to SP 1000 indicate a relatively constant dip calculated to be 26° . From SP 700 to the top of the Crescent Terrane at SP 600 this interpretation of the Crescent Thrust has very steep dip. The alternate interpretation is a more uniformly dipping horizon (26°), located approximately 1.5 seconds higher in the section at SP 900, which also terminates against Tofino Basin sediments near SP 600.

The Crescent Thrust (base of Crescent Terrane) is identified on Line 85-01 by Hyndman et al. (1990 - Fig. 3) at SP 2000 dipping steeply to the east. The Prometheus well penetrated volcanics at 5850' (1780 m)(approximately 1.5 s). The top of the Crescent Terrane on Line 85-01 (Fig. 19) is structurally high near the Prometheus location and dips steeply to the east to SP 2500 along the Tofino Fault. The fossil trench interpreted by Hyndman et al. (1990) is observed on the section to 3.0 s between SP 2300 and SP 2500.

The base of the Crescent Terrane, the Crescent Thrust, has been interpreted on Line 89-06 (Fig. 20) by Spence et al. (1991) as a reflector dipping relatively steeply to the east from SP 1550 at 1.5 s to SP 1950 at 6.5 s. Uplift of the seaward portion of the Crescent Terrane has separated the Tofino Basin into two sub-basins with the Crescent Terrane near the surface at SP 1800 and penetrated in the nearby Zeus D-14 well. On Line 89-06 the top of the Crescent Terrane dips at a steep angle to the east from SP 1800 to the boundary with the Pacific Rim Terrane at SP 2050. The stratigraphic thickness of the Crescent Terrane on this part of Line 89-06 is nearly 9000 m. East of SP 2050 the Crescent and Pacific Rim terranes cannot be resolved.

Although the Prometheus Magnetic anomaly continues north to the location of Lines 85-02 and 89-09, no clear identification of Crescent Terrane could be made on those lines. However, Calvert and Clowes (1991) interpret Crescent Terrane on Line 89-02 in the shallow crust east of SP 620, based on a corresponding increase in magnetic values and interval velocities. At the eastern limit of Line 85-02, where the magnetic anomaly (+160 nT) is consistent with the interpretation of Crescent Terrane on profiles to the south, Dehler and Clowes (1995) interpret reflections as possibly Crescent Terrane. At the location of Line 89-09 the Prometheus Magnetic anomaly is small (maximum value +50 nT) and no Crescent Terrane is interpreted, while further north at the Nootka Fault zone magnetic and gravity data indicate that the Crescent Terrane is either absent or deeply buried. (Dehler and Clowes 1995).

Values of depth to the top of the Crescent Terrane were calculated from the time to the reflections in Figure 24 and the values contoured in Figure 26. This map shows a general increase in depth to the north with several local highs including the Zeus anomaly. This agrees with the interpretation of Dehler and Clowes (1995). A map of thickness of Crescent Terrane obtained from time values from Figure 24 converted to depth, using an interval velocity of 6000 m/s, is shown in Figure 27. The thickness of Crescent Terrane was determined from the lower of the two possible horizons interpreted as the base of Crescent Terrane. This map therefore represents a maximum thickness of Crescent Terrane under Tofino Basin.

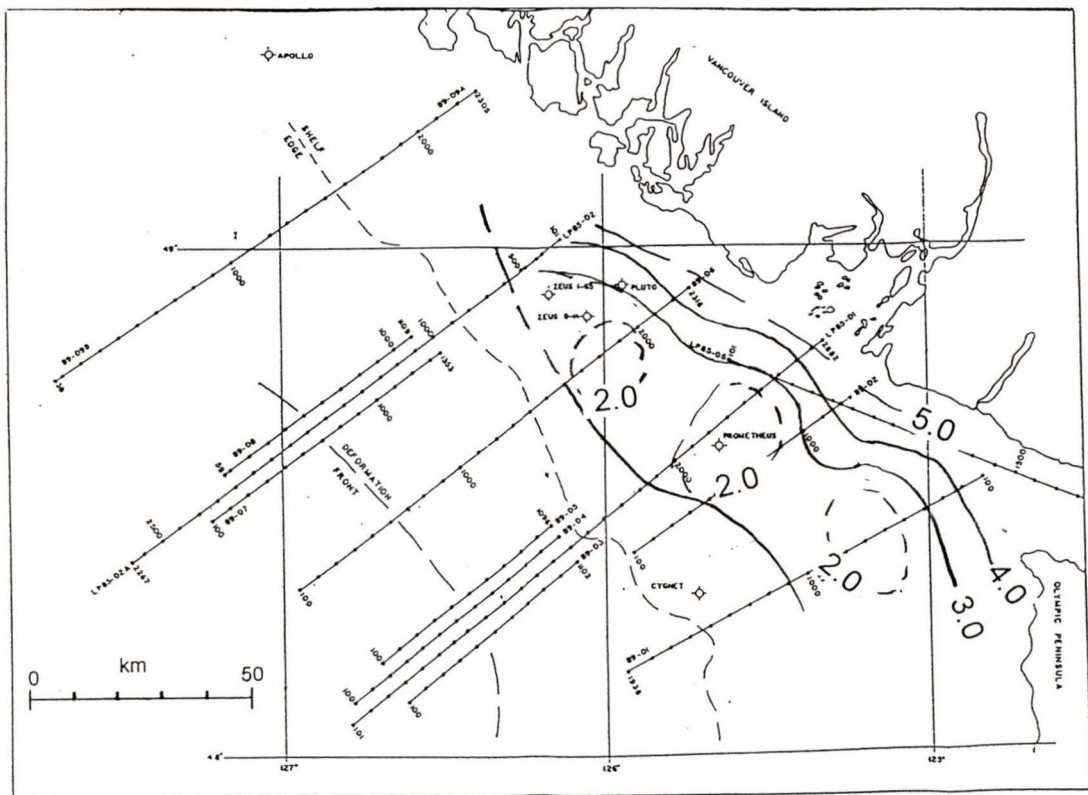


Figure 26: Depth in kilometres to the top of Crescent Terrane.

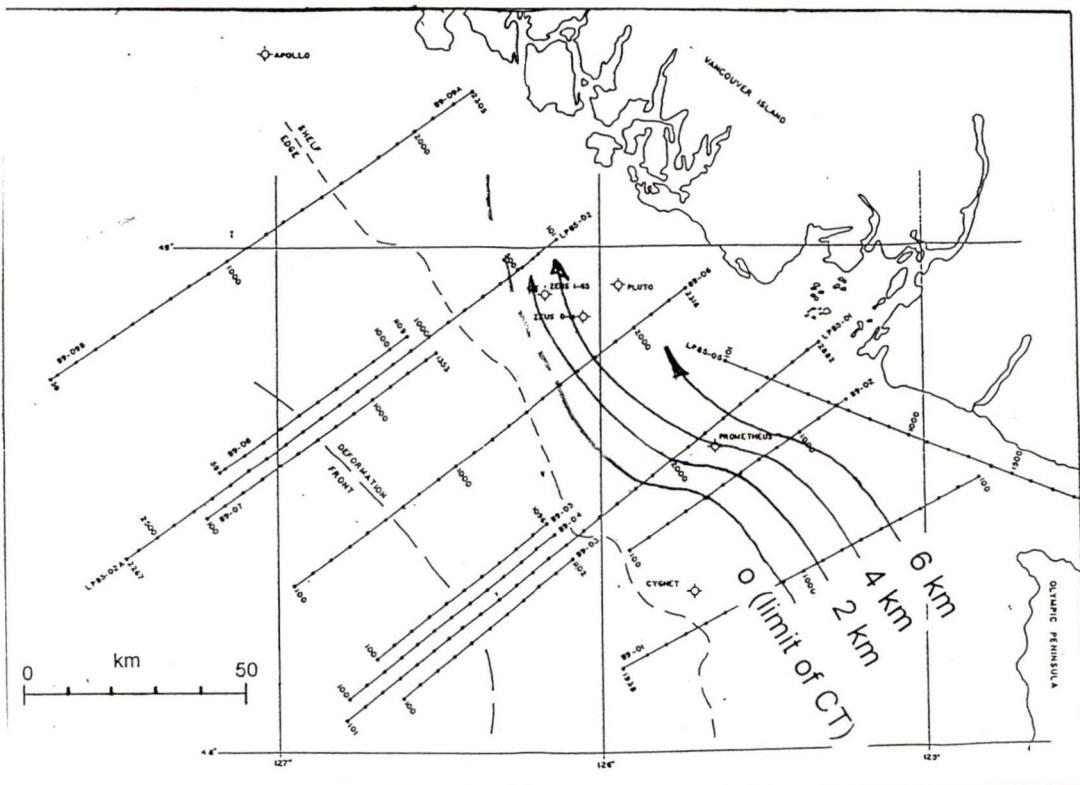


Figure 27: Thickness in kilometres of Crescent Terrane.

4.1.4 Accretionary Prism

The Crescent Terrane formed a backstop for sediment accumulation of the accretionary prism (Spence *et al.* 1991). The progressive formation of the accretionary prism can be seen especially well on Line 85-01 (Fig. 19). West of SP 600 sediments of the Cascadia Basin rest undisturbed on the oceanic plate. From SP 600-1000, in the region of the deformation front, thrust faulting and folding provide evidence that the oceanic plate is continuing to move eastward, while the overlying sediments are restricted in horizontal motion by the backstop to the existing accretionary prism. Motion is taken up by folding and thrust faulting of the sediments and associated vertical displacement. This indicates that shortening continues beneath the basin. East of SP 1000 the seismic character of the accretionary prism is chaotic, indicating a change to more intense penetrative deformation. Dipping reflectors observed within the accretionary prism may be associated with thrust faults along planes which originated at the deformation front. Subsequently these faults may have been rotated, uplifted, and extended as the sediments were relocated into the older section of the accretionary wedge.

The interpretation of Crescent Terrane on Lines 85-01 and 89-06 indicates that the seaward end of the Crescent Terrane may have been elevated as sediments of the accretionary prism were forced beneath it. The Zeus structure (discussed later in this thesis) was formed from the structurally high Crescent Terrane observed on Line 85-01 near SP 2300 and on Line 89-06 near SP 1800. The Crescent Terrane may, on Line 89-06, be at or near the water bottom. Dehler and Clowes note that the anticline at SP 1800 on Line 89-06 is not Crescent Terrane due to the relatively low magnetic anomaly and the 2200 m depth of the Crescent Terrane volcanics in the nearby well. The cross section through the wells (Figure 5) illustrates the locally elevated position of the volcanics penetrated by the Zeus well. If the Crescent terrane is dipping to the north from Line 89-06, in the direction of the 20 km distant well (Figure 6), then the reflection from the top of Crescent Terrane could be higher in the section on Line 89-06.

Beneath the continental shelf on Lines 89-01 and 89-06, Calvert (1995) interpreted two units within the accretionary prism which were shortened by duplex formation. In this thesis, these reflections are interpreted to be from within the Crescent Terrane or at its base. At the eastern end of several lines steeply dipping reflectors that intersect the oceanic plate (Line 89-01 SP 400-600) may be similar to the "E" reflectors of interpretations beneath Vancouver Island. In both cases, the reflections may originate from rocks close to the subduction decollement that have been intensely sheared (Calvert & Clowes 1990). According to this interpretation these reflectors represent a maximum depth for the base of the accretionary prism, or the base of the Crescent and Pacific Rim terranes.

On the seismic data across Tofino Basin (Figs. 17-23) the top of the accretionary prism is identified on the geological interpretations below each seismic section. To the east it is bounded by the Crescent Terrane, the base of which corresponds to the Crescent Thrust at depth. To the west the accretionary wedge outcrops on the seafloor at the continental shelf edge and along the continental slope. In some locations along the continental slope there is local, post accretion sedimentary ponding.

4.1.5 Tofino Basin Sediments

Sediments of Tofino Basin overlie the Pacific Rim and Crescent terranes. Within the sedimentary section of Tofino Basin there is greater seismic detail than in the accretionary prism due to the intense deformation within the accretionary prism. The seismic data from Tofino Basin are characterized by clear stratigraphic layering disrupted by low amplitude folding and minor thrust faulting. Localized uplift expressed as either diapirism (Varsek and Cook, unpublished manuscript) or folding is also present over the Crescent Terrane and greater fold shortening is observed over the accretionary prism.

Confidence in the interpretation of the base of Tofino Basin sediments varies within the basin. In the southeast, where the Crescent Terrane is clearly imaged, an apparent

unconformity is interpreted as the top of Crescent Terrane and base of Tofino Basin sediments. Northward, in the area of Line 89-06 (Figure 6), there is less certainty in the depth of Crescent Terrane. The base of Tofino Basin sediments has been interpreted as a similar unconformity across which the seismic character changes from continuous parallel reflectors of Tofino Basin sediments to discontinuous reflectors representing Crescent Terrane. Seaward, toward the deformation front, the boundary between Tofino Basin sediments and the accretionary prism is increasingly difficult to determine. From the shelf break seaward there is very little change in the seismic character between near surface sediments and deeper sediments of the accretionary prism.

The Cygnet J-100 well was drilled on the anticlinal structure seen at SP 1400-1500 on Line 89-01. Two similar, but smaller, structures are located at SP 1650-1700 at 1.5-2.0 s on Line 89-01. The total thickness of Tofino Basin sediments decreases toward the structurally high Crescent Terrane (SP 800). Onlap of Tofino Basin sediments onto the Crescent Terrane indicates that the Crescent Terrane may have been exposed before the deposition of Tofino Basin sediments. From SP 600-400, above approximately 4.0 s, where the Crescent Terrane dips steeply to the east, the Tofino Basin sediments above the Crescent and Pacific Rim terranes are equivalent to sediments within the "fossil trench" of Line 85-01, but have a broader lateral extent. The near-surface anticlinal feature centred at SP 560 (above 2.0 s) may have resulted from small movement of the Crescent Terrane relative to the Pacific Rim Terrane during the Late Tertiary. East of SP 400 Tofino Basin sediments overlie the Pacific Rim Terrane to as deep as 1.5 s (approximately 2000 m). From SP 1000-1150, above the interpreted location of the Crescent Fault, Tofino Basin sediments are mildly disturbed; possible motion between the Crescent Terrane and the accretionary prism along the Crescent Fault may have been responsible. Above 1.0 s the character of the seismic data becomes more coherent.

The seismic character on Line 89-02 indicates less deformation of Tofino Basin sediments than on Line 89-01. The structure and stratigraphy of Tofino Basin sediments indicate that the Crescent Terrane may have been at or near the water bottom, in the early stages of basin formation. The seismic reflectors of Tofino Basin sediments truncate

against the Crescent Terrane at SP 740 and 2.5 s, and the section thins below 2.0 s from SP 750 to SP 950. Truncation of seismic horizons from SP 550 to SP 700, below 1.6 s, indicate either uplift of the accretionary prism west of SP 750 after deposition of Tofino Basin sediments or a period of renewed subduction of the Crescent Terrane east of SP 750. Steep dip of reflections from SP 950-1050 indicate an episode of late structural motion through the complete sedimentary section, involving either sediments of the "fossil trench" or Pacific Rim Terrane. The anticline centred at SP 325 is similar to the Cygnet structure on Line 89-01.

The cross section of Tofino Basin sediments on Line 85-01 is similar to Line 89-02 with folding seaward of the Crescent Terrane and horizontal strata to the east. An unconformity is clearly imaged, with numerous others evident in the section. Continuous deposition of the sediments appears within and above the "fossil trench". The Prometheus well encountered a thick section of monotonously fine grained sediments which may be represented by the seismic image of Tofino Basin sediments on Line 85-01, SP 2200-2300.

Tofino Basin sediments on Line 89-06 are separated into two sub-basins by the uplifted seaward end of the Crescent Terrane at SP 1800 (the Zeus structure). Eastward, the sediments form a thick parallel stratified section with the thickest section over the boundary between the Crescent and Pacific Rim terranes (SP 2000 to SP 2050). Major unconformities are imaged at very shallow depths. West of SP 1800 the section overlying the accretionary prism is relatively thin (less than 1.5 s - approximately 1300 m). Depositional downlap and prograding sedimentation can be observed west of SP 1550. There is no evidence of significant structural deformation on this part of the line. In contrast to data to the south, the continental slope on this line has a low gradient with sedimentation occurring in small ponds (west of SP 1200).

On Line 85-02 the deformation front is separated from Tofino Basin (limited by definition for this paper by the shelf break at SP 1050) by a 30 km wide, deep water (1300 m), plateau covered by a thin section of sediments. Resolution of Tofino Basin sediments on Line 85-02 is not as good as on other lines, possibly due to multiples from

a slightly deeper water bottom. The sediments are relatively undeformed with unconformities apparent above 1.0 s. A major anticlinal structure interpreted as a diapir by Hyndman *et al.* (1990) can be seen at the eastern end of the line. This feature may be similar to the Apollo Structure of Yorath (1980) .

A shallow continental slope gradient continues to the north, with the shelf break on Line 89-09 occurring at SP 1450-1500, over 50 km east of the deformation front. A section of Tofino Basin sediment less than 1000 m thick overlies the accretionary wedge east of SP 1800, and in some locations (SP 1830, SP 1900, SP 2050) accretionary prism sediments appear to outcrop on the sea floor. West of SP 1800 uniform deposition to over 2.0 s appears to have been uniform and continuous with wide structural folding centred at SP 1530 affecting the complete geological section. The section contains several local unconformities with truncation of reflection horizons west of SP 1450 below 1.0 s.

4.2 Mapping

Two-way times from the interpreted seismic sections and from the two wells which drilled into volcanics (Prometheus and Zeus D-14) were contoured to produce a map of the reflection time to the base of Tofino Basin sediments (Fig. 28). This base horizon is the top of accretionary prism, top of the Crescent Terrane or top of the Pacific Rim Terrane, depending on the location. In the region of the fossil trench (Lines 89-01, 85-01 and 89-06), the base of Tofino Basin sediments was chosen to correspond to a minimum depth. Values from the four wells which reached total depth while still within sedimentary sections (Apollo, Zeus I-65, Cygnet and Pluto) were used as control for minimum thickness. Stacking velocities determined from semblance analysis were interpolated at the seismic horizon time and a contoured velocity map was produced (Fig. 29). The horizon map and velocity map were cross contoured and two way times were converted to depth at each cross contour point. The water depth (from the seismic section header) was subtracted from each cross contour value and these values contoured for a Tofino Basin sediment thickness map (Fig. 30).

The 1985, 1989 and CSP data were used to construct a map of anticlinal features within Tofino Basin (Fig. 31). Although there is variation in depth of burial, the structures on the map are either folds or diapirs involving Tofino Basin sediments, or structural features of the underlying accreted sediments. Some of the features such as the Apollo structure (Yorath, 1980) outcrop on the sea-bed, while others are buried by Tofino Basin sediments. Since the map is a consolidation of features most of which are seen on only one seismic line, or at most a few lines, no correlation across the basin between structures is inferred.

4.2.1 Tofino Basin sediment thickness

A linear sediment filled trough representing the fossil trench (Fig. 30) trends parallel to Vancouver Island from the Juan de Fuca Channel in the south to the Zeus structure north of the end of Line 89-06. Sediment thicknesses greater than 3000 m occur at a local closure near the eastern limit of the basin, between Lines 89-01 and 89-02. Northwest of this location the trench shallows and is not apparent on Line 89-02. It reappears and deepens to over 3000 m on Line 89-06 before the trench terminates against the Zeus structure.

A large lobe of sediments with maximum thickness greater than 2500 m covers an area of approximately 500 km² at the southern limit of the basin. To the west and northwest along the seaward boundary of the basin the sediments thin to less than 1000 m. The basin width decreases north of Line 89-02 and the sediment thickness increases to approximately 3000 m in an elongate region parallel to Vancouver Island along the Apollo structure (Yorath 1987). A local uplift at SP 1800 on Line 89-06 is expressed as a thinning to less than 500 m on the Tofino Basin Sediment Thickness map (Fig. 30).

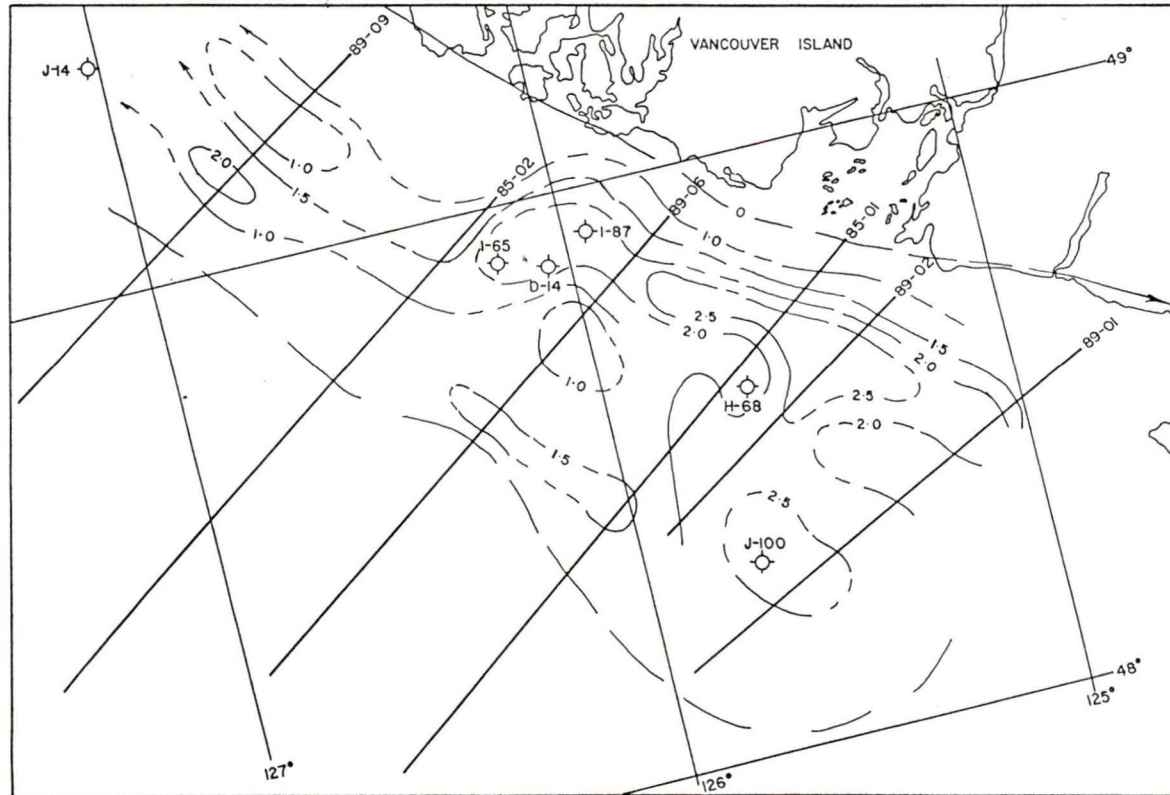


Figure 28: Time (from seismic data) to base of Tofino Basin sediments. Contour intervals in seconds.

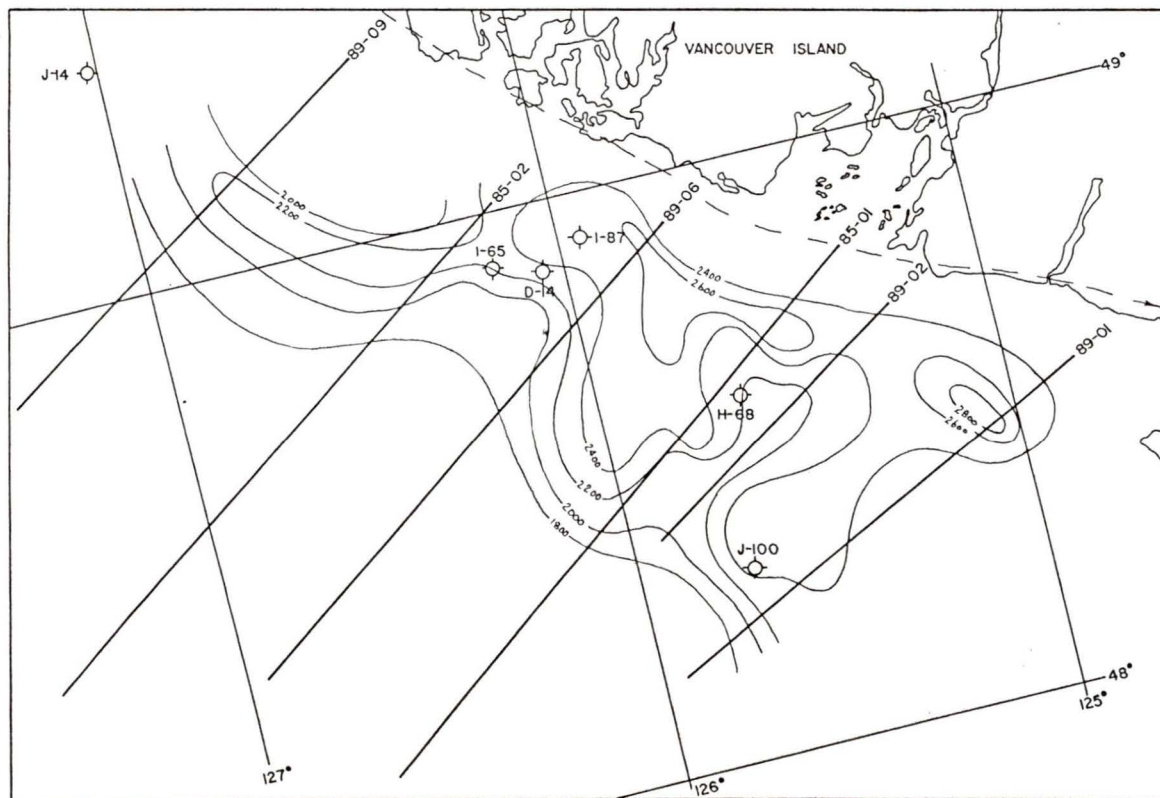


Figure 29: Interpolated stacking velocity (from seismic section headers) at base of Tofino Basin sediments. Contour intervals in m/s.

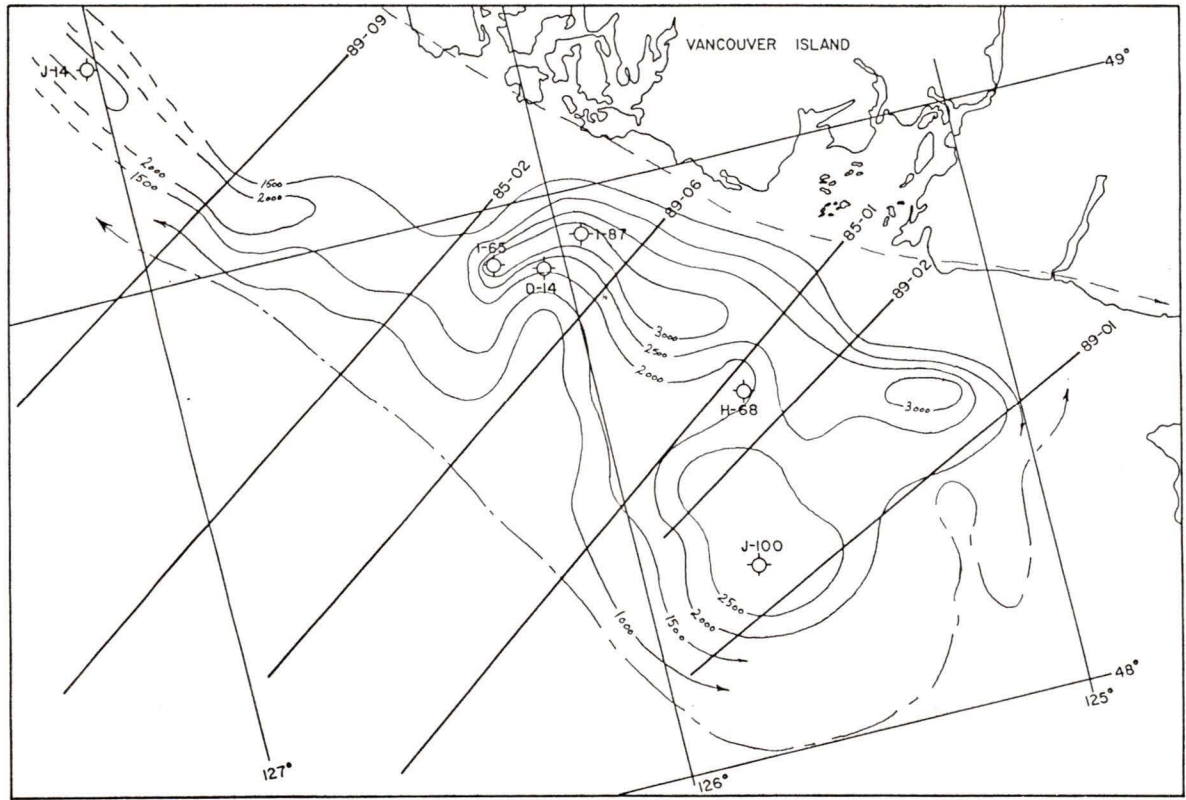


Figure 30: Thickness of Tofino Basin sediments. Contour intervals in metres.

4.2.2 Tofino Basin Structure

The northern portion of Tofino Basin is dominated by the Apollo structure. Several other features similar to the Apollo structure trend parallel to Vancouver Island and outcrop at the seafloor (eg. CSP Line 68-B-10 Fig. 32). The Apollo structure has been detailed by Yorath (1980) and is representative of the group. It is an anticlinal body 18 km long and 3 km wide which rises up to 20 m above the sea floor. It is interpreted as a Pleistocene disharmonic fold or diapiric structure localized above a detachment surface overlying Palaeogene rocks. The structure may have been induced by seaward sliding and creep of the Neogene sediments. Several local features above the accretionary wedge include the structure on Line 89-01 at SP 1450 penetrated by the Cygnet well. These features are anticlinal folds with possible faulting.

In the southern portion of Tofino Basin, the Zeus structure is an irregularly shaped feature which rises to near the sea floor at the northern limit of the fossil trench (Fig. 30). The Pluto and Zeus I-65 wells were drilled near the crest and the Zeus D-14 on the flank. The structure on Line 89-06 has been interpreted as the seaward uplift of the Crescent Terrane due to underthrusting of sediments of the accretionary wedge. The broadening of the Zeus structure northward from Line 89-06 to Line 89-02 is coincident with the termination of the fossil trench.

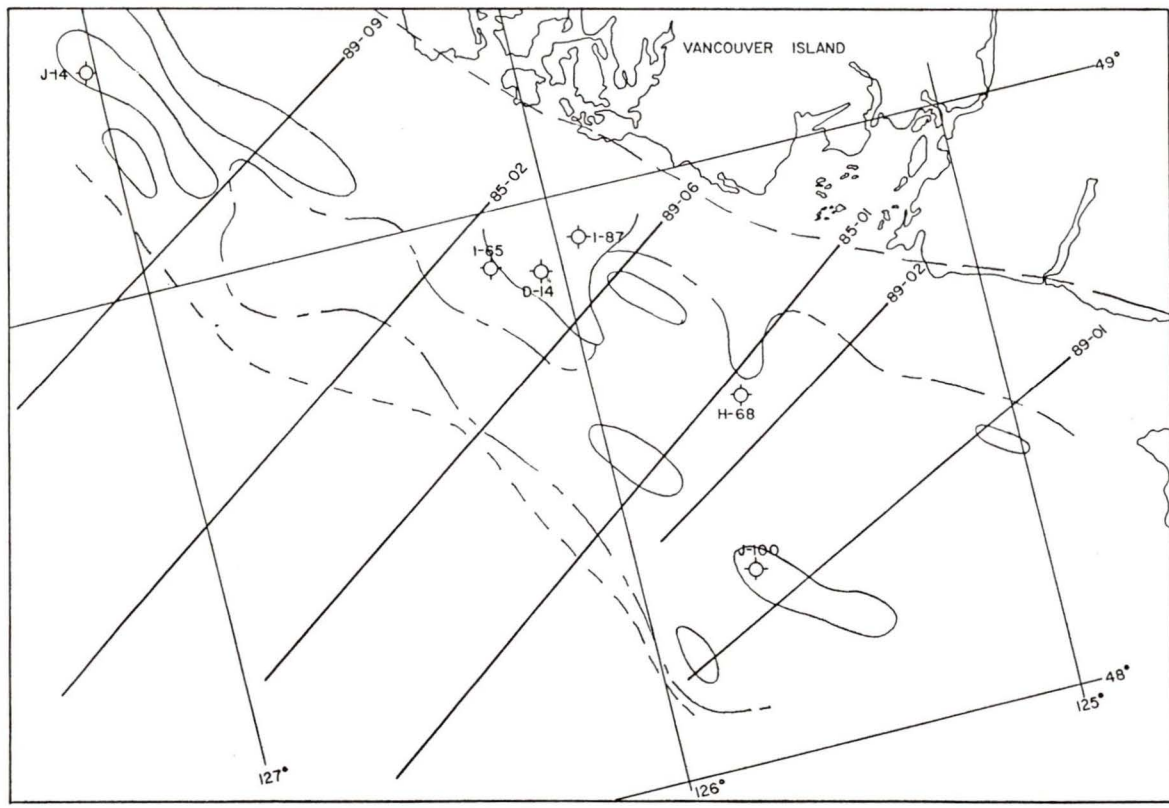


Figure 31: Structural features within Tofino Basin sediments.

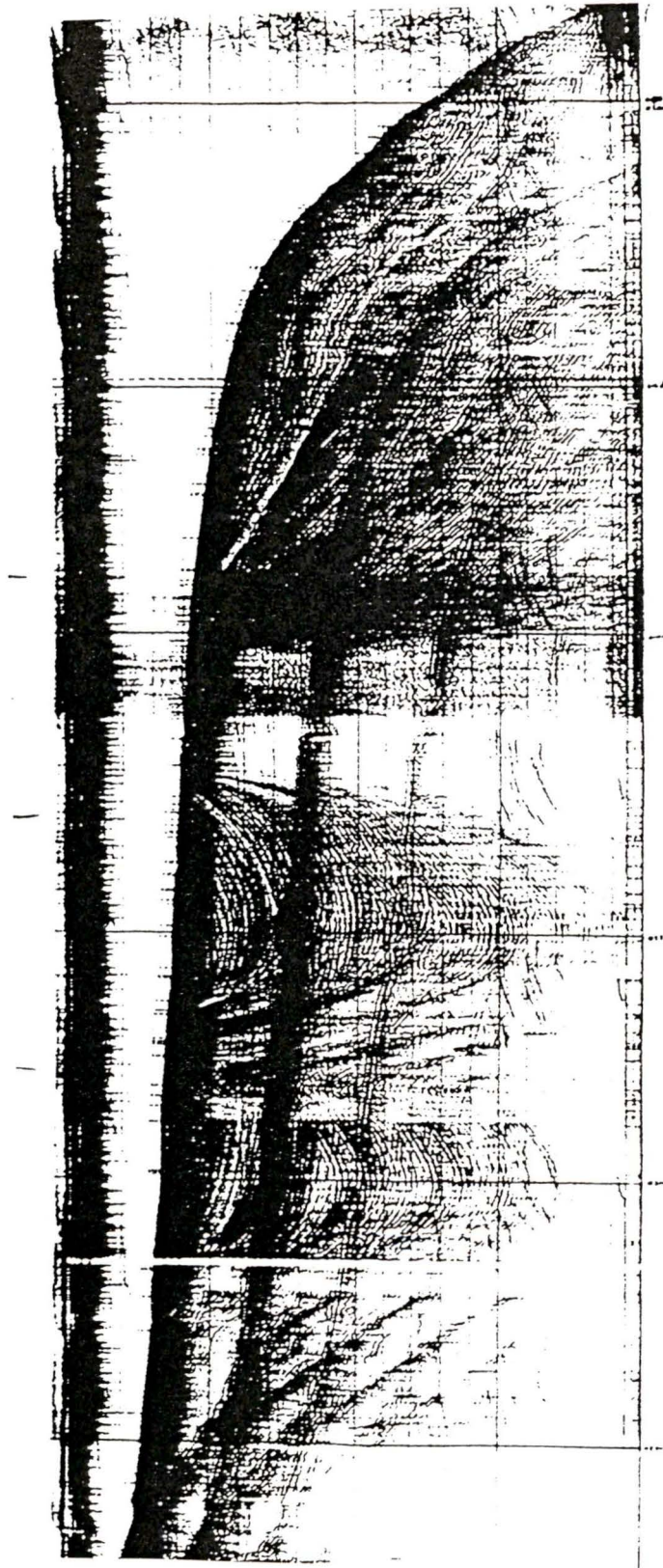


Figure 32: CSP Line 68-B-10

Chapter 5

DISCUSSION

Interpretation of seismic data from the 1989 and 1985 programmes constrained by magnetic field anomalies and well data has provided an improved 3-D description of the geological features within and beneath the Tertiary Tofino Basin. Several structural features from previous interpretations have been extended over a larger area of the basin.

Dip of subducting oceanic crust and growth of accretionary prism. Measurements of the dip from the downgoing oceanic crust agree with a model of critically tapered wedges which Davis and Hyndman (1989) have applied to explain the limited vertical growth of the accretionary wedge beneath Tofino Basin. With the exception of periods of low sea level during the Pleistocene, accretionary wedge sediments and depositional sediments of the Tofino Basin have been below sea level since initiation of the present phase of subduction at 42 Ma. In comparison, sediments on the Olympic Peninsula have been elevated to over 2000 m above sea level in the same period. At the western limits of Tofino Basin, the dip of the oceanic crust varies from about 3° to 9° (Table 2 - Lines 89-02, 89-06, 89-09), but landward of the shelf edge dips are greater than the critical angle of 11° (Table 2 - Lines 85-01, 89-06, 85-02), above which growth of the accretionary prism cannot occur. Growth of the accretionary prism is continuing at the deformation front and as Tofino Basin increased in size westward, the increasing load of accreted and deposited sediments depressed the oceanic crust, and the location of the critical plate dip angle advanced with the deformation front toward the west. Over the full width of the basin, slow subsidence and loading due to increasing thickness of Tofino Basin sediments occurred, but the rate of subsidence is uncertain.

Boundaries of Crescent Terrane. The location of the top of the Crescent Terrane has been determined on the seismic profiles to correspond to, but displaced seaward of, the area of the Prometheus Magnetic High. The Crescent Formation is observed in outcrop on the Olympic Peninsula and may correspond to the Siletz Terrane of the Oregon

coast. Thus, the Crescent Terrane continues southward beyond Tofino Basin. To the north, the PMH terminates near the location of Line 89-09 (Fig. 8a). The Crescent Terrane is not observed on Lines 89-09 or 85-02, although its presence cannot be excluded. However, the northern limit of the fossil trench appears to coincide with the Zeus structure of Figures 28 & 30. At the north-eastern limit of the seismic data, the interpreted presence of the Crescent Terrane on Lines 89-06 (Fig. 20), Line 89-01 (Fig. 17), and Line 89-02 (Fig. 18) is consistent with the interpretation of Line 85-01 by Hyndman *et al.* (1990). At those locations a thin section of Crescent Terrane has underthrust the Pacific Rim Terrane. The interpretation of Line 85-05 by Hyndman *et al.* (1990) includes a trough on the upper surface of the Crescent Terrane southeastward from Line 85-01 which accommodates the observations of the Crescent Terrane within Tofino Basin and the outcrop on Vancouver Island. Toward the southeastern end of Line 85-05 the upper boundary of the Crescent Terrane (the Leech River Fault) rises to the southeast, since the Leech River Fault and Metchosin Igneous Complex (Crescent Terrane) outcrop on Vancouver Island. The northeastern end of Line 89-01 (Fig. 17) is located near SP 1400 on Line 85-05, where the top of Crescent Terrane is near 5.0 s. Thus the Crescent Terrane along Line 89-01 may extend beneath the Pacific Rim Terrane, with zero apparent dip, from SP 400 on Line 89-01 (Fig. 17) eastward to SP 1400 on Line 85-05 (Fig. 23), such that the direction of maximum dip over this portion of the line is perpendicular to the line direction. This indicates a change in the trend of the Crescent Terrane in the region of Line 89-01.

The lower boundary of the Crescent Terrane is interpreted from clear, steeply dipping seismic reflections which can be extended downward to nearly intersect with reflections interpreted as the oceanic plate. On Line 89-06, SP 1950 (Fig. 20) and on Line 89-02, SP 1000 (Fig. 18), there appears to be direct contact between the Crescent Terrane and oceanic crust which may have resulted in a downwarping of the oceanic crust at the point of contact. This indicates that almost no sediments from the accretionary prism are being subducted and that there is little or no subduction erosion of the accretionary wedge (the transfer of accreted material from the accretionary prism to the lower plate (von Huene and Scholl 1991)). This is consistent with the interpretation of

the southeastern end of Line 85-05 by Hyndman *et al.* (1990) where the oceanic plate and the Leech River Fault are separated by approximately 6 km of Crescent Terrane at a depth of approximately 20 km. The continuation of Crescent Terrane to this depth, proposed by Hyndman *et al.* (1990), contrasts with earlier interpretations of land data on Vancouver Island (Yorath *et al.* 1985; Green *et al.* 1986; Clowes *et al.* 1987) in which the Crescent Terrane was truncated at 15 km and that significant amounts of material had been underplated beneath and to the west of Vancouver Island. The interpretation of the base of Crescent Terrane in this thesis has been interpreted by Calvert (1995) as imbrication and duplex formation within the accretionary prism, resulting in a very thin Crescent Terrane.

The Crescent Terrane is bounded to the east by the Pacific Rim Terrane along the landward dipping Tofino Fault. The Tofino Fault is not directly imaged on the seismic data, but the location is constrained by the location of the fossil trench, and by the location of the low magnetic anomaly between the Prometheus Magnetic High and Vancouver Island, as modelled by Dehler (1992). This boundary, which extends eastward beneath Vancouver Island, is consistent with the interpretation by Hyndman *et al.* (1990).

The reflections above and seaward of the steeply dipping reflectors representing the base of the Crescent Terrane intersect the base of Tofino Basin sediments at a location where a horizontal change occurs in the seismic character at the base of Tofino Basin sediments - e.g. Line 89-01 SP 1000 (Fig. 17). This has been interpreted as the boundary between the Crescent Terrane and the seaward part of the accretionary prism. The top of the Crescent Terrane is interpreted eastward beneath Tofino Basin sediments as far as the fossil trench where the Crescent Terrane dips steeply to the east. Onlapping sediments at the top of Crescent Terrane along Lines 89-01 (Fig. 17) and 89-02 (Fig. 18) indicate that, at the time of formation of Tofino Basin, the Crescent Terrane may have been exposed and eroded.

Hyndman *et al.* (1990) proposed two models for the mechanism of accreted Terrane emplacement: 1) the complete lithosphere was faulted and the present Juan de

Fuca plate is underthrusting the old lithospheric slab or 2) a thin sliver of oceanic crust was detached from the subducting oceanic plate. The interpretation of the 1989 data set tends to eliminate the first possibility. The thickness of Crescent Terrane on Line 6 is estimated to be 9.0 km. Dehler (1992) and Dehler and Clowes (1992) modelled Crescent Terrane as a 4 km thick slab. If the thickness of the lithosphere is estimated by $8.5 \sqrt{t}$ km (where t is the age in Ma), then if the Crescent Terrane was emplaced 12 Ma after formation, the thickness of the lithosphere would have been approximately 30 km. The Siletz Terrane, equivalent to Crescent Terrane offshore Oregon and Washington, has thicknesses varying from 17 km offshore Oregon, decreasing to approximately 9 km offshore northern Washington (Figure 2, Trehu *et al.* 1994). Thus the thickness of the Crescent Terrane beneath Tofino Basin is evidence which supports the second model.

Fossil Trench. A narrow sediment trough occurs parallel to Vancouver Island between the locations of the Crescent and Pacific Rim Terranes. Sediment thickness is over 3500 m thick at locations within the trench, the greatest thickness of Tertiary sediments observed within Tofino Basin (Fig. 30). The trough terminates to the north against the Zeus structure which, together with the uncertain interpretation of Crescent Terrane north of the Zeus structure, may indicate that it is associated with structural interaction between the Crescent and Pacific Rim terranes. It has been interpreted by Hyndman *et al.* (1990) as a fossil trench marking the locus of underthrusting of the Crescent Terrane beneath the Pacific Rim Terrane. There is no evidence from within the trough to indicate whether the Crescent and Pacific Rim terranes were accreted to North America simultaneously or at separate times. The interpretation of Line 89-02 indicates a trough that is broader and shallower than in the region to the north and south. When combined with the interpretation of exposed Crescent Terrane at the time of emplacement, and the termination of Crescent Terrane north of Line 89-06, it is possible to infer the following paleo-geographical environment at 42 Ma. From the location of Line 89-02 south to Line 89-01 a small area, the Zeus structure, was elevated relative to the surrounding Crescent Terrane to the north and south. The Crescent Terrane continued north, possibly as far as the Nootka Fault Zone and to the south the Crescent Terrane extended as far as Oregon. Water depths were shallow over and to the east of the Zeus

structure, rapidly deepening to the north and south within the fossil trench. As the accretionary wedge began to build to the west Tofino Basin sediments were deposited over the deeper portions of the Crescent Terrane and began to onlap the Crescent Terrane of the Zeus structure. As Tofino Basin developed, the Zeus structure was uplifted or subsidence occurred less rapidly than in the adjacent area over the accretionary prism. Thus the present topography of the top of the Crescent Terrane varies with areas of relative uplift.

Thickness and deformation of Tofino Basin sediments. There is significant structural variation within Tofino Basin north and south of the Zeus structure. To the south structural features are dominated by effects of the underlying Crescent Terrane and accretionary prism. The Zeus anticlinal structure formed due to elevation of the seaward portion of the Crescent Terrane. This uplift is greatest along Line 89-06 (Fig. 20, Fig. 24) as seen at SP 1500. The effect decreases to the south with the Crescent Terrane being covered by an increasing thickness of Tofino Basin sediments. Tofino Basin sediments overlying the Crescent Terrane and the adjacent portion of the accretionary prism have relatively little structural deformation.

The Crescent Terrane may act as a solid buttress which inhibits deformation of the overlying sediments. Nearer the outer shelf Tofino Basin sediments have been deformed as a result of interaction with the deforming accretionary prism. The Cygnet structure as seen on Lines 89-01 and 89-02 is formed by this mechanism. Tofino Basin is wider and thicker in the south with a steep continental slope to the deformation front, which along line 89-02 is within 30 km of the shelf edge. North of Line 89-06 the basin narrows to less than 40 km, but the continental slope is greater than 50 km wide and contains numerous sediments ponds. The Apollo structure is typical of the series of shallow elongate anticlinal structures parallel to Vancouver Island within northern Tofino Basin.

Deformation of Tofino Basin sediments appears greatest in two locations. Parallel to Vancouver Island above the fossil trench (e.g. Line 85-01 (Fig. 19)) sediments in the upper layers have been deformed. On Lines 89-02 and 85-01 west of the underlying Crescent Terrane (or for the full width of the basin in the north) the complete section of Tofino Basin sediments has been shortened by folding. The sediments overlying the Crescent Terrane appear to be undeformed. In the eastern area it is possible that a late episode of motion along the Tofino Fault (ie. late motion between the Crescent and Pacific Rim Terranes) resulted in the observed deformation of Tofino Basin sediments. Structural deformation in the west and north is more likely due to present and continuing accretion processes, with shortening that decreases landward from the deformation front.

The early history of Tofino Basin is dominated by effects due to the accretion of the Crescent and Pacific Rim Terranes. Sedimentation would have begun immediately within the fossil trench. As the accretionary wedge began to develop seaward, the distal portion of the Crescent Terrane was uplifted forming the Zeus structure. The width and thickness of Tofino Basin is limited by the restricted sediment supply and the relatively steep dip of the subducting oceanic plate. At the western limits of the basin the structural development is due to continuing growth of the accretionary prism, associated intense deformation within the accretionary prism and the consequent shortening transmitted to the overlying sediments of Tofino Basin.

Chapter 6

CONCLUSIONS

Interpretation of multichannel seismic reflection data, constrained by well and magnetic field data, has been carried out to determine the geometry of geological features of Tofino Basin. Reprocessing of a portion of Line 89-02 has shown that velocity analysis can be used to improve the quality of the seismic data and that the observed velocities are consistent with well information and geological interpretation.

The dip of the subducting oceanic plate increases smoothly eastward from less than 5° to a maximum of 15° at the west coast of Vancouver Island. This is consistent with critical wedge theory which predicts uplift of the accretionary wedge at angles less than 11° and subsidence at subduction angles greater than 11° .

The location of the Crescent Terrane beneath Tofino Basin is delineated by the seismic reflection and magnetic data. The Crescent Terrane is clearly observed only on seismic profiles to the south of the Zeus structure. Clear dipping seismic reflections which extend to the oceanic crust are interpreted as near the base of Crescent Terrane which therefore may be in contact with the oceanic crust. The Crescent Terrane thus acts as a backstop for the accretionary wedge and allows only restricted underplating of material beneath Vancouver Island. The present topography of the top of the Crescent Terrane and the onlap of Tofino Basin sediments against Crescent Terrane indicates an area of elevated Crescent Terrane at or after the time of formation and accretion.

Sediment thickness in Tofino Basin is maximum in an elongate region parallel to Vancouver Island coincident with the location of the sedimentary fossil trench, marking the axis of underthrusting of the Crescent Terrane beneath Pacific Rim Terrane. The trench terminates against the Zeus structure to the north and is separated into two segments by elevation of the Crescent Terrane. The depth of the fossil trench was controlled by the initial and subsequent structural development of the Crescent Terrane.

The thickness of Tofino Basin sediments is controlled by the geometry of the Crescent Terrane in the eastern portion of the Basin and by the underlying accretionary wedge to the west. Tofino Basin sediments are relatively undeformed where they directly overlie the Crescent Terrane. Greater, but localized, deformation is observed at the eastern boundary of the Basin overlying the fossil trench and Pacific Rim Terranes. It is possible that small continued motion of the Crescent Terrane with respect to Pacific Rim has contributed to deformation of the Tofino Basin sediments. Continuing prism accretion and shortening beneath the western limits of the basin have resulted in deformation of Tofino Basin sediments overlying the accretionary prism.

REFERENCES

- Adams, J., 1984. Active deformation of the Pacific Northwest continental margin. *Tectonics*, v3: 449-472.
- Atwater, T., 1970. Implications of plate tectonics for Cenozoic tectonic evolution of western North America. *Geological Society of America Bulletin*, 81: 3513-3536.
- Atwater, T., 1989. Plate tectonic history of the northeast Pacific and western North America. *In The Eastern Pacific Ocean and Hawaii. Edited by E.L Winterer, D.M. Hussong, and R.W. Decker. Geological Society of America, Boulder, CO pp 21-72.*
- Babcock, R.S., Burmester, R.F., Engebretson, D.C., and Warnock, A., 1992. A rifted margin origin for the Crescent basalts and related rocks in the Northern Coast Range volcanic province, Washington and British Columbia. *Journal of Geophysical Research*, 97: 6799-6821.
- Brandon, M.T., 1989. Origin of igneous rocks associated with melanges of the Pacific Rim Complex, western Vancouver Island, Canada. *Tectonics*, 8: 1115-1136.
- Calvert, A.J., and Clowes, R.M., 1990. Deep, high amplitude reflections from a major shear zone above the subducting Juan de Fuca plate. *Geology*, 18, 1091-1094.
- Calvert, A.J. and Clowes, R.M., 1991. Seismic evidence for the migration of fluids within the accretionary complex of western Canada. *Canadian Journal of Earth Sciences*, 28: 542-556.
- Calvert, A.J., 1995. Imbrication and underplating of the Cascadia accretionary wedge. *Canadian Journal of Earth Sciences* (in press).
- Cameron, B.E.B., 1980. Biostratigraphy and depositional environment of the Escalante and Hesquiatic Formation (early Tertiary) of the Nootka Sound area, Vancouver Island, British Columbia. *Geological Survey of Canada, Paper 78-9.*
- Coney, P.J., 1977. Mesozoic-Cenozoic Cordilleran plate tectonics. *In Cenozoic tectonic and regional geophysics of the Western Cordillera. Ed by R.B. Smith and F.P. Eaton, Geological Society of America Memoir, 1552: 33-50.*
- Coney, P.J., Jones, D.L., Monger, J.W.H., 1980. Cordillera suspect terranes. *Nature*, 288: 329-333.
- Crosson, R.S., and Owens, T.J., 1987. Slab geometry of the Cascadia subduction zone beneath Washington from earthquake hypocentres and teleseismic converted waves. *Geophysical Research Letters*, v14: 824-827.

- Currie, R.G., Cooper, R.V., Riddihough, R.P., and Seeman D.A., 1983. Multiparameter geophysical surveys off the west coast of Canada. *In* Current research, part A. Geological Survey of Canada, Paper 83-1A, pp. 207-212.
- Davis, D., Suppe, J., and Dahlen, F.A., 1983. Mechanic of fold-and-thrust belts and accretionary wedges. *Journal of Geophysical Res.*, 88:1153-1172.
- Davis, E.E., and Hyndman, R.D., 1989. Accretion and recent deformation of sediments along the northern Cascadia subduction zone. *Geological Society of America Bulletin*, 101: 1465-1480.
- Dehler, S.A., 1992. Integrated geophysical modelling of the Northern Cascadia subduction zone. Ph.D. Thesis, University of British Columbia, Vancouver, 144 pp.
- Dehler, S.A., and Clowes, R.M., 1992. Integrated geophysical modelling of terranes and other structural features along the western Canadian margin. *Canadian Journal of Earth Sciences*, 29: 1492-1508.
- Dehler, S.A., and Clowes, R.M., 1995. Structure of the northern Cascadia subduction zone derived from integrated geophysical modelling. *Canadian Journal of Earth Sciences*, in press.
- Drew, J.J., and Clowes, R.M., 1989. A re-interpretation of the seismic structure across the active subduction zone of western Canada. *In* Studies of laterally heterogeneous structures using seismic refraction and reflection data (Proceedings of the 1987 Commission on Controlled Source Seismology Workshop), edited by A.G. Green, Geological Survey of Canada Paper 89-13.
- Engebretson, D.C., Gordon, R.G., and Cox, A., 1985. Relative motions between oceanic and continental plates in the Pacific basin. *Geological Society of America, Special Paper* 206.
- Garland, G.D., 1979. Introduction to Geophysics - mantle, core and crust. W.B. Saunders, Toronto.
- Grow, J.A., and Atwater, T., 1970. Mid-Tertiary tectonic transition in the Aleutian Arc. *Geological Society of America Bulletin*, 81: 3715-3722.
- Hajnal, Z., and Sereda, I.T., 1981. Maximum uncertainty of interval velocity estimates. *Geophysics*, V6 #11:1543-1547.
- Hyndman, R.D., and Hamilton T.S., 1991. Cenozoic relative plate motions along the northeastern Pacific margin and their association with Queen Charlotte area tectonics and volcanism. *In* Evolution and Hydrocarbon Potential of the Queen Charlotte Basin. Geological Survey of Canada paper 90-10.

- Hyndman, R.D., Yorath, C.J., Clowes, R.M., and Davis, E.E., 1990. The northern Cascadia subduction zone at Vancouver Island: seismic structure and tectonic history. *Canadian Journal of Earth Sciences*, 27: 313-329.
- Hyndman, R.D., Riddihough, R.P., and Herzer, R. 1979. The Nootka fault zone - a new plate boundary off western Canada. *Geophysical Journal of the Royal Astronomical Society*, 58: 667-683.
- Irving, E., and Wynne, P.J., 1991. Paleomagnetism: review and tectonic implications. *In Geology of the Cordilleran Orogen in Canada*, H. Gabrielse and C.J. Yorath (ed.); Geological Survey of Canada, Geology of Canada, no. 4: 61-86.
- Irving, E., and Massey, N.W., 1990. Paleomagnetism of ocean layers 2 and 3: evidence from the Metchosin Complex, Vancouver Island. *Physics of the Earth and Planetary Interiors*, 64: 247-260.
- Johnson, S.Y., 1984. Evidence for margin truncating transcurrent fault (pre-late Eocene) in western Washington. *Geology*, 12: 538-541.
- Jones, D.L., Silberling N.J., and Hillhouse J., 1977. Wrangellia - a displaced terrane in northwestern North America. *Canadian Journal of Earth Sciences*, 14: 2565-2577.
- Macleod, N.S., Tiffin, D.L., Snively, P.D., and Currie, R.G., 1977. Geological interpretation of magnetic and gravity anomalies in the Strait of Juan de Fuca, U.S. - Canada. *Canadian Journal of Earth Sciences*, 14: 223-238.
- Massey, N.W.D., 1986. Metchosin Igneous Complex, southern Vancouver Island: ophiolite stratigraphy developed in an emergent island setting. *Geology*, 14: pp. 602-605.
- McKenzie, D.P., and Morgan, W.J., 1969. Evolution of triple junctions. *Nature*, 224: 125-133.
- Muller, J.E., 1977. Evolution of the Pacific margin, Vancouver Island and adjacent regions. *Canadian Journal of Earth Sciences*, 14: 2062-2085.
- Muller, J.E., Snively, P.D., and Tabor, R.W., 1983. The Tertiary terrane, southwest Vancouver Island and northwest Washington. Geological Association of Canada Meeting, Victoria, B.C., Guidebook, Field Trip 12.
- Riddihough, R.P., 1982. One hundred million years of plate tectonics in Western Canada. *Geoscience Canada*, 9: 28-34.
- Shell Canada Limited, 1968-1971. Well History Reports.

- Shouldice, D.H., 1971. Geology of the western Canadian continental shelf. Canadian Society of Petroleum Geologists, Bulletin 19; pp. 405-424.
- Shouldice, D.H., 1973. Western Canadian continental shelf. Canadian Society of Petroleum Geologists, Memoir 1, 7-35.
- Snively, P.D. 1987. Tertiary geologic framework, neotectonics, and petroleum potential of the Oregon-Washington continental margin. *In* Geology and resource potential of the continental margins of western North America and adjacent basins - Beaufort Sea to Baja California. *Edited by* D.W. Scholl, A. Grantz, and J. Vedder. Circum Pacific Council for Energy and Mineral Resources, Earth Sciences Series, v6, United States Geological Survey, Menlo Park, CA, pp. 305-335.
- Spence, G.D., Clowes, R.M., and Ellis, R.M., 1985. Seismic structure across the active subduction zone of western Canada. *Journal of Geophysical Research*, 90: 6754-6772.
- Spence, G.D., Hyndman, R.D., Langton, S.G., Yorath, C.J., and Davis, E.E., 1991. Multichannel seismic Reflection profiles across the Vancouver Island continental shelf and slope. Geological Survey of Canada, Open File 2391.
- Spence, G.D., Hyndman, R.D., Davis, E.E., and Yorath, C.J., 1991. Seismic structure of the northern Cascadia accretionary prism: evidence from new multichannel seismic reflection data. *Geodynamics* 22: 257-263.
- Stock, J.M. and Molner, P. 1988. Uncertainties and implications of the Late Cretaceous and Tertiary positions of North America relative to the Farallon, Kula and Pacific plates. *Tectonics*, 6: 1339-1384.
- Taber, J.J., and Smith, S.W., 1984. Seismicity and focal mechanisms associated with the subduction of the Juan de Fuca plate beneath the Olympic Peninsula, Washington. *Seismological Society of America Bulletin*, v75: 237-249.
- Trehu, A.M., Asudeh, I., Brocher, T.M., Luetgert, J.H., Mooney, W.D., Nabelek, J.L., and Nakamura, Y., 1994. Crustal architecture of the Cascadia forearc. *Science*, 265: 237-243.
- Von Huene, R., and Scholl, D.W., 1991. Observations at convergent margins concerning sediment subduction, subduction erosion, and the growth of continental crust. *Reviews of Geophysics*, 29: 279-316.
- Wang, X., and Clowes, R.M. 1995. Seismic structure across the Cascadia subduction zone off Vancouver island: New evidence from seismic refraction and wide-angle reflection data. Geological Association of Canada, Program and Abstracts, v.20: p.A109.

- Wells, R.E., Engebretson, D.C., Snavely, P.D., and Coe, R.S., 1984. Cenozoic plate motions and the volcanic-tectonic evolution of western Oregon and Washington. *Tectonics*, 3: 275-294.
- Yilma, O. 1987. *Seismic Data Processing*. Edited by S.M. Doherty. Society of Exploration Geophysicists, Tulsa.
- Yole, R.W., and Irving E., 1980. Displacement of Vancouver Island, palaeomagnetic evidence from the Karmutsen Formation, *Canadian Journal of Earth Sciences*, 17: 1210-1228.
- Yorath, C.J., 1980. The Apollo structure in Tofino Basin, Canadian Pacific continental margin. *Canadian Journal of Earth Sciences*, 17: 758-775.
- Yorath, C.J., 1987. Petroleum geology of the Canadian Pacific continental margin. *In* *Geology and resource potential of the continental margins of western North America and adjacent basins - Beaufort Sea to Baja California*. Edited by D.W. Scholl, A. Grantz, and J. Vedder. Circum Pacific Council for Energy and Mineral Resources, Earth Sciences Series, Vol. 6, United States Geological Survey, Menlo Park, CA, pp. 283-304.
- Yorath, C.J., 1995. Tectonic synthesis of the Alberni region. Geological Survey of Canada, in press.
- Yorath, C.J., Clowes, R.M., MacDonald, R.D., Spencer, C., Davis, E.E., Hyndman, R.D., Rohr, K., Sweeney, J.F., Currie, R.G., Halpenny, J.F., and Seeman, D.A., 1987. Marine multichannel seismic reflection, gravity and magnetic profiles - Vancouver Island continental margin and Juan de Fuca Ridge. Geological survey of Canada, Open File 1661.12
- Yorath, C.J., Green A.G, Clowes R.M., Sutherland-Brown A., Brandon M.T., Kanasewich E.R., Hyndman R.D., and Spencer, C. 1985. LITHOPROBE, southern Vancouver Island: seismic reflection sees through Wrangellia to the Juan de Fuca plate. *Geology*, 13: 759-762.
- Yuan T., Spence, G.D., and Hyndman, R.D., 1994. Seismic velocities and inferred porosities in the accretionary wedge sediments at the Cascadia margin. *Journal of Geophysical Research*, 99: 4413-4427.

APPENDIX 1 - Processing Parameters, 1989 seismic data.

1. First Break Mute
2. True Amplitude recovery - compensation for spherical divergence and exponential gain recovery.
3. Velocity (F-K) Filtering of coherent linear noise in common shot domain:
 -7ms/trace to 15ms/trace at water depths of less than 1000m.
 -7ms/trace to 14ms/trace at water depths of greater than 1000m.
4. Designature - Zero phase source filter applied to shot gathers.
5. Output to 9 track tape.
6. Velocity Analysis - for demultiple.
7. F-K Demultiple - Laterally varying velocities used for elimination of water bottom multiples and peglegs.
8. Velocity Analysis for NMO - Nominally spaced at 3 Km.
9. Deconvolution - offset and time variant from water bottom
10. Trace equalization - 9000 ms design gate
11. Statics - Correction for shot and receiver depths.
12. Trace Mute
13. Normal Moveout -
14. Trace Mute
15. Deconvolution - Water bottom multiple attenuation
 Filter length - .3 times water depth (in time)
 Gap - .9 times water depth (in time)
 Autocorrelation start/end - 50/9000 ms
16. Time variant filter - 8,12/36,44 @ 0 to 1750 ms
 3,6 /26,34 @ 1750 - 14000 ms
17. Time Variant Scaling - water bottom datum
18. Output at 20 tr/cm. and 3 cm/sec

19. Migration - F-K dip limited to 45 degrees. migration velocities = 90% stacking velocities.
-followed by steps 16, 17, and 18.

APPENDIX 2 - Well sonic logs

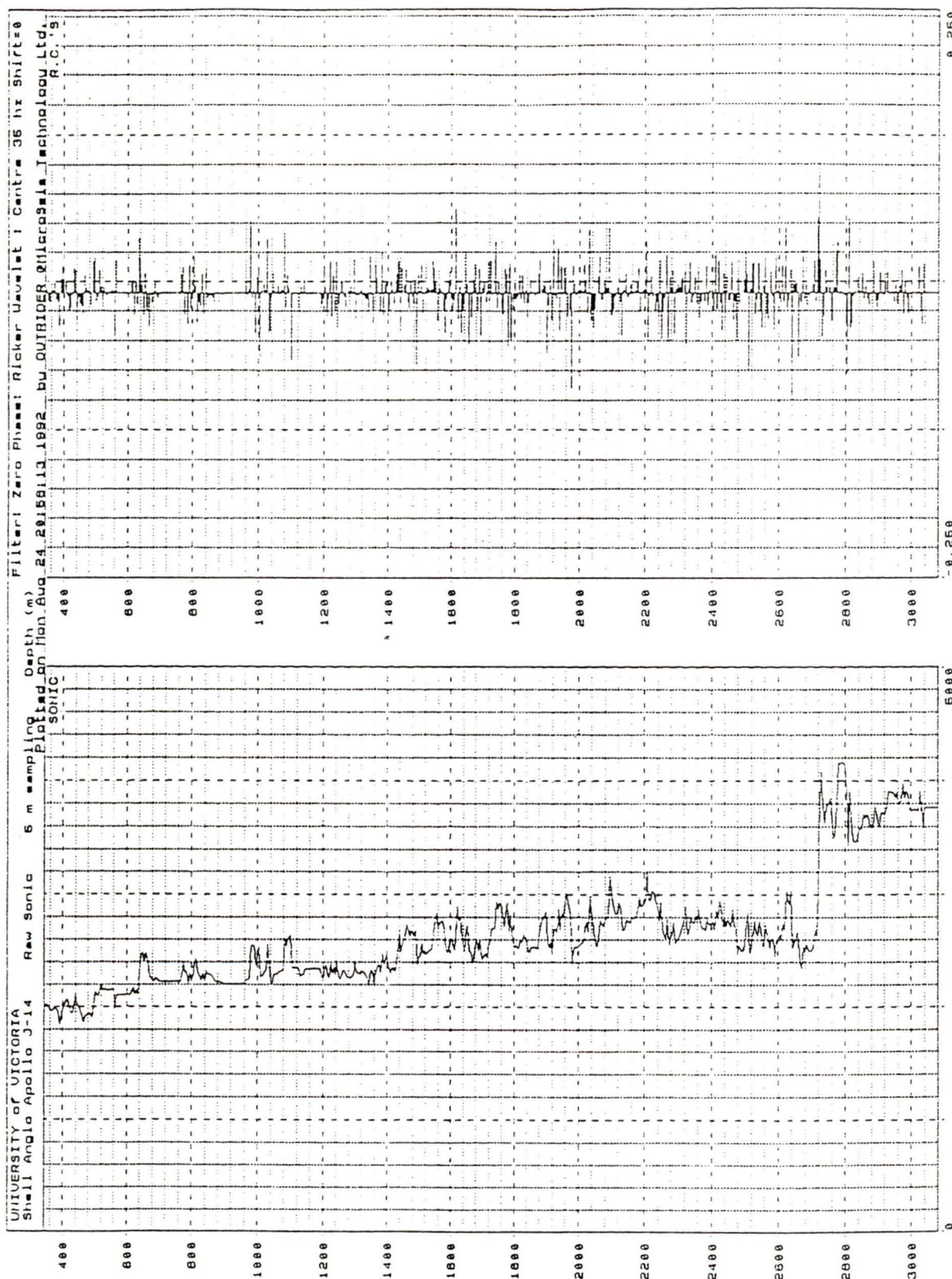
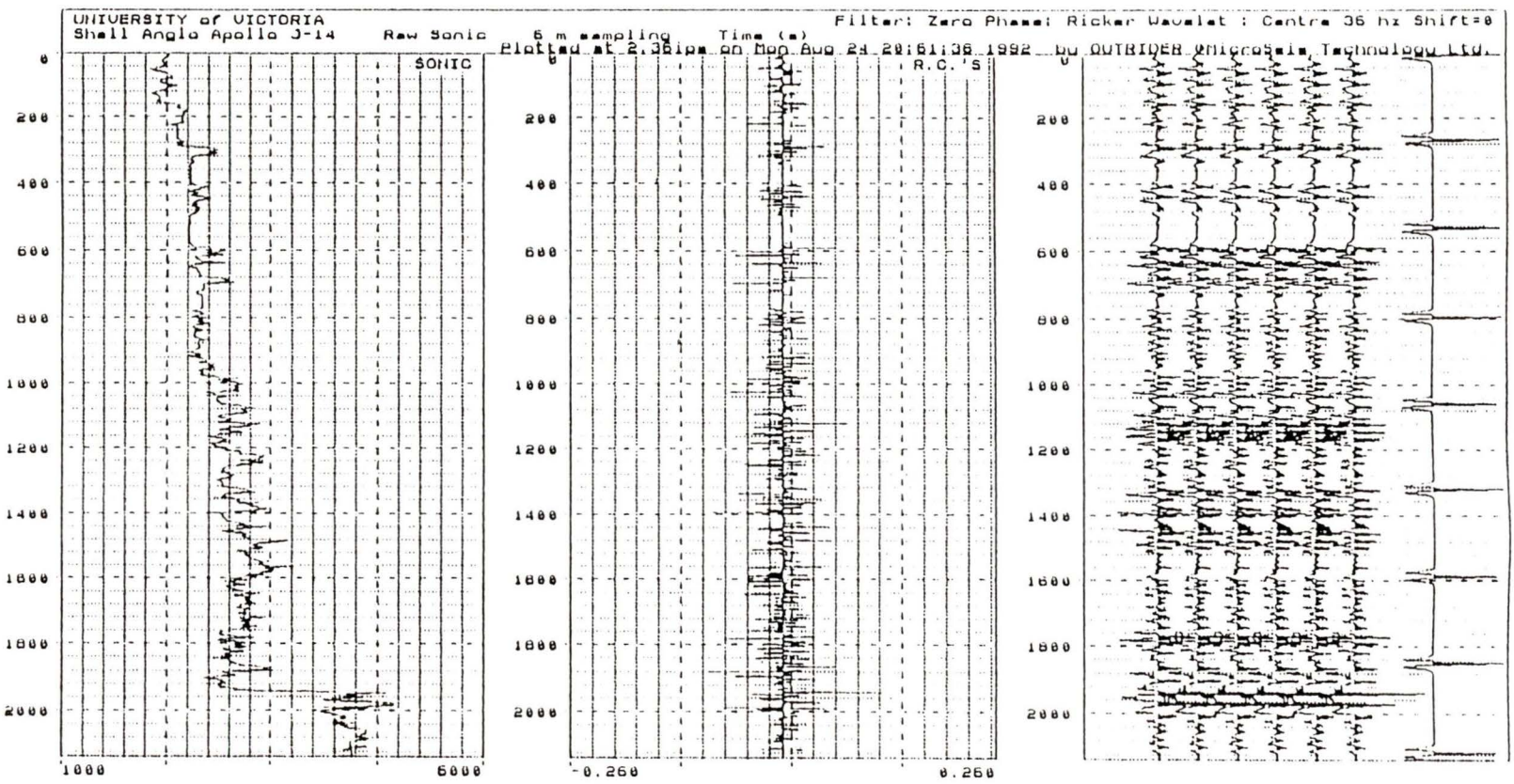


Figure 33: Shell Anglo Apollo J-14. Log and reflectivity in depth.

Figure 34: Shell Anglo Apollo J-14. Log, reflectivity and synthetic seismogram in time.



UNIVERSITY of VICTORIA
 Shell Anglo Zeus D-14 Raw Sonic 6 m sampling Depth (m) Filter: Zero Phase; Ricker Wavelet; Centre 36 Hz Shift=0
 Plotted on Mon Aug 23 21:42:55 1992 by OVIIRIEN MicroSeis Technology Ltd.
 SONIC R.C.'S

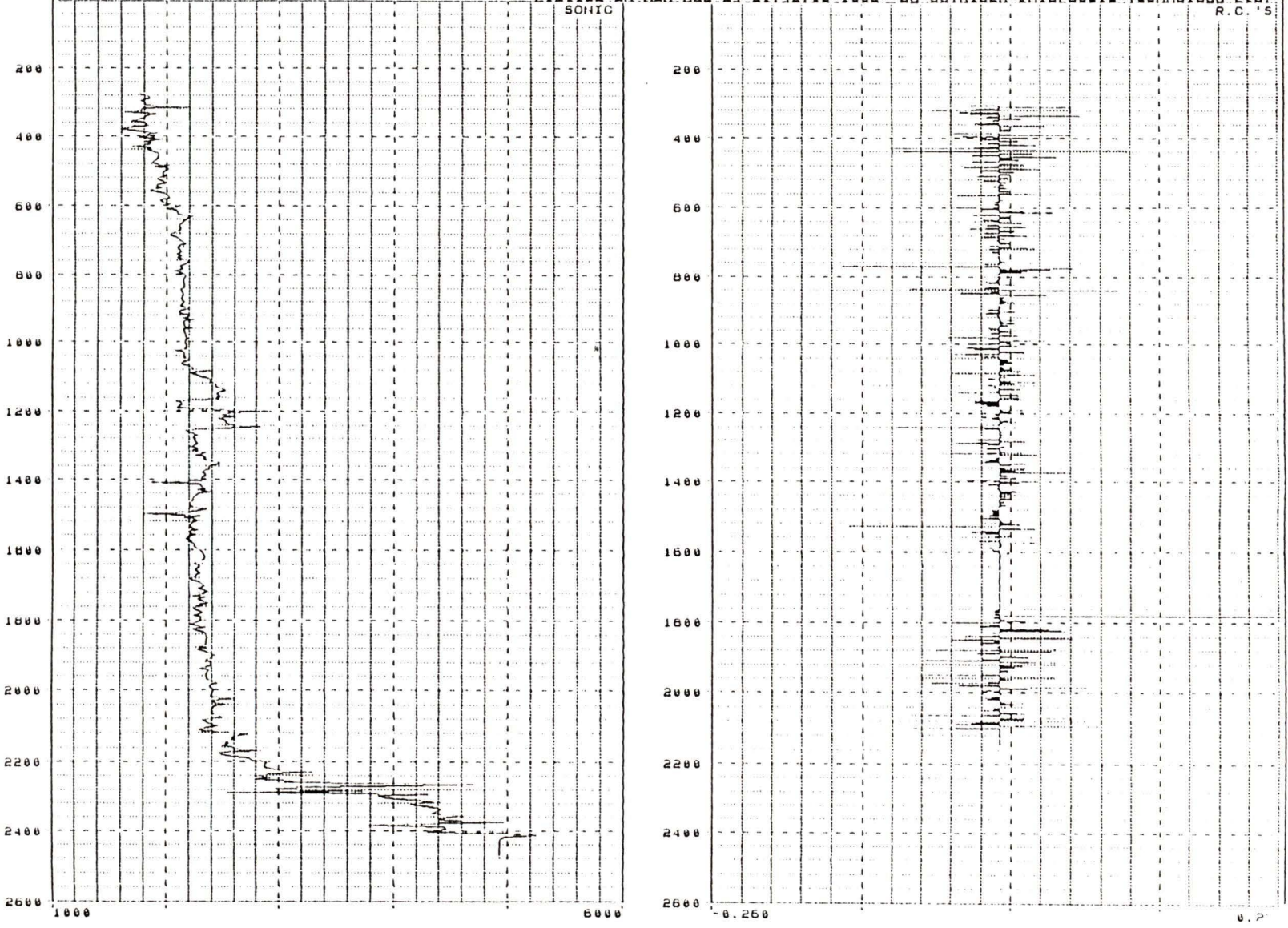
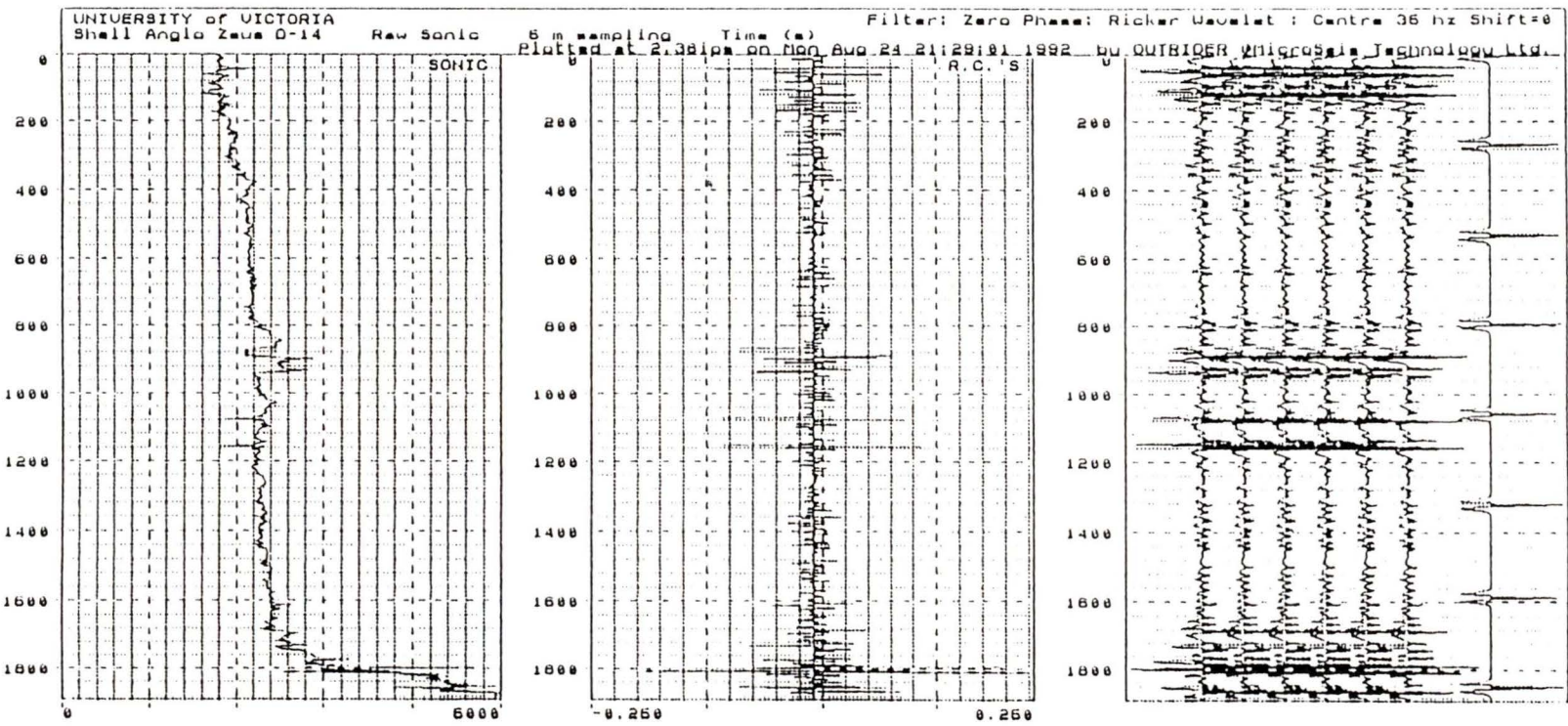


Figure 35: Shell Anglo Zeus D-14. Log and reflectivity in depth.

Figure 36: Shell Anglo Zeus D-14. Log, reflectivity and synthetic seismogram in time.



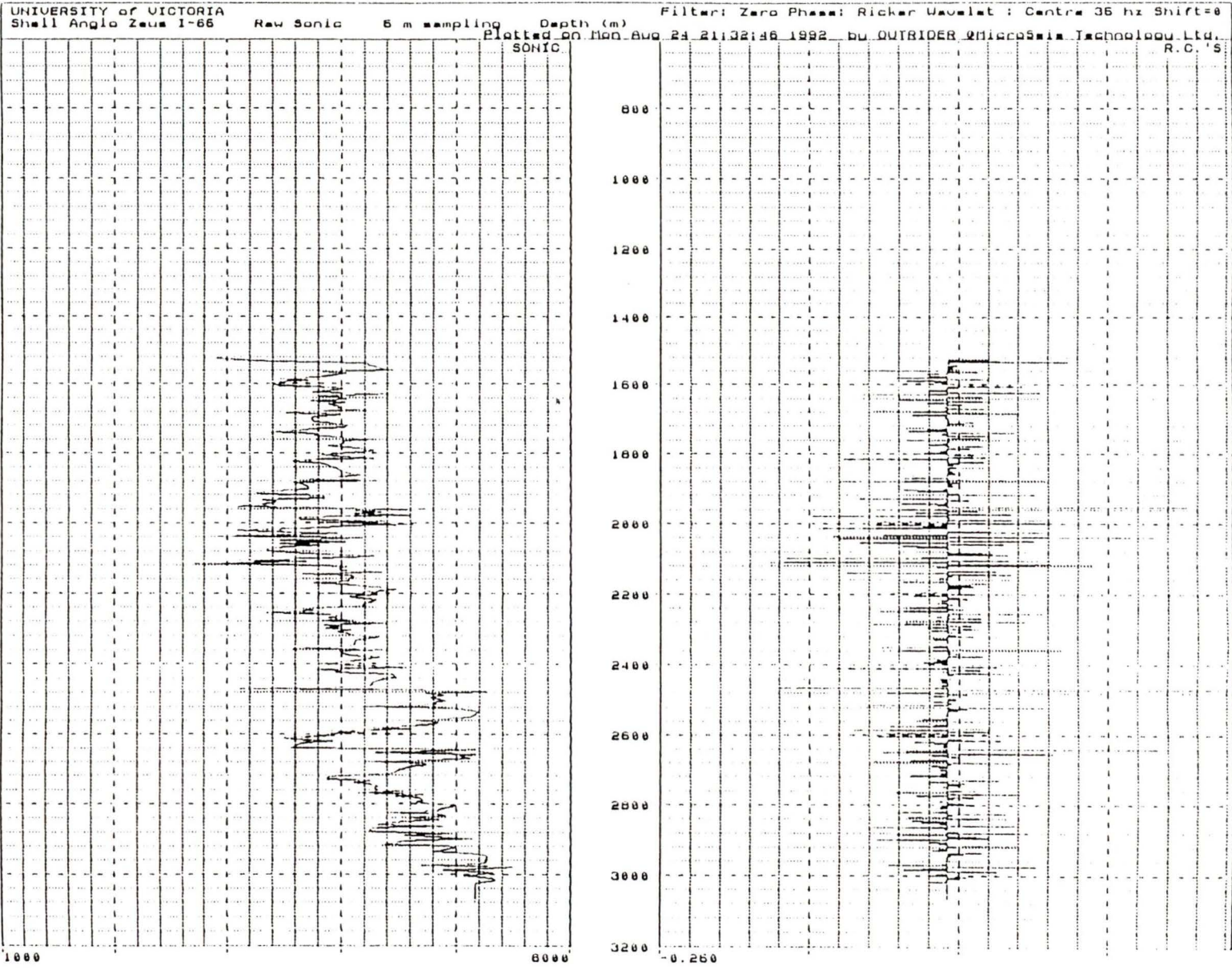


Figure 37: Shell Anglo Zeus I-65. Log and reflectivity in depth.

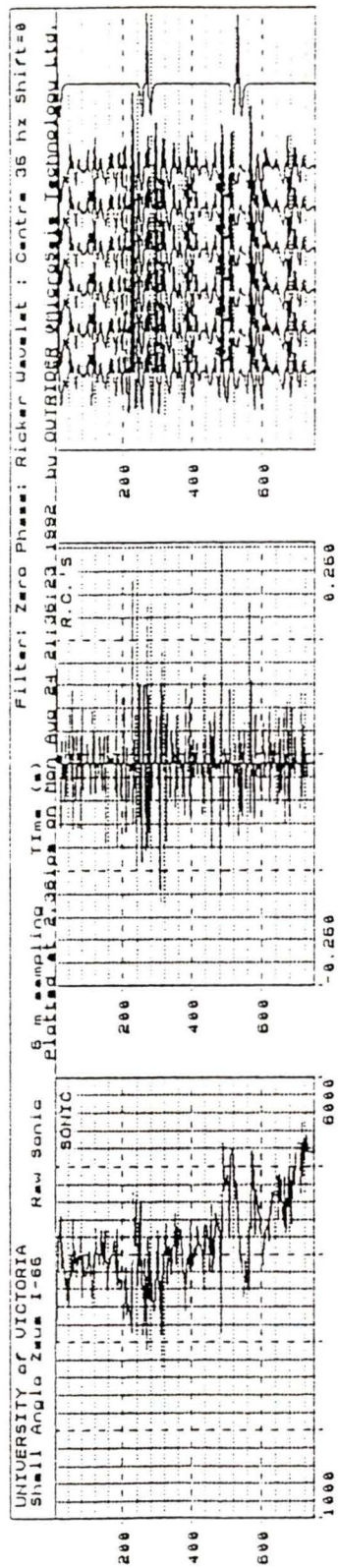


Figure 38: Shell Anglo Zeus I-65. Log, reflectivity and synthetic seismogram in time.

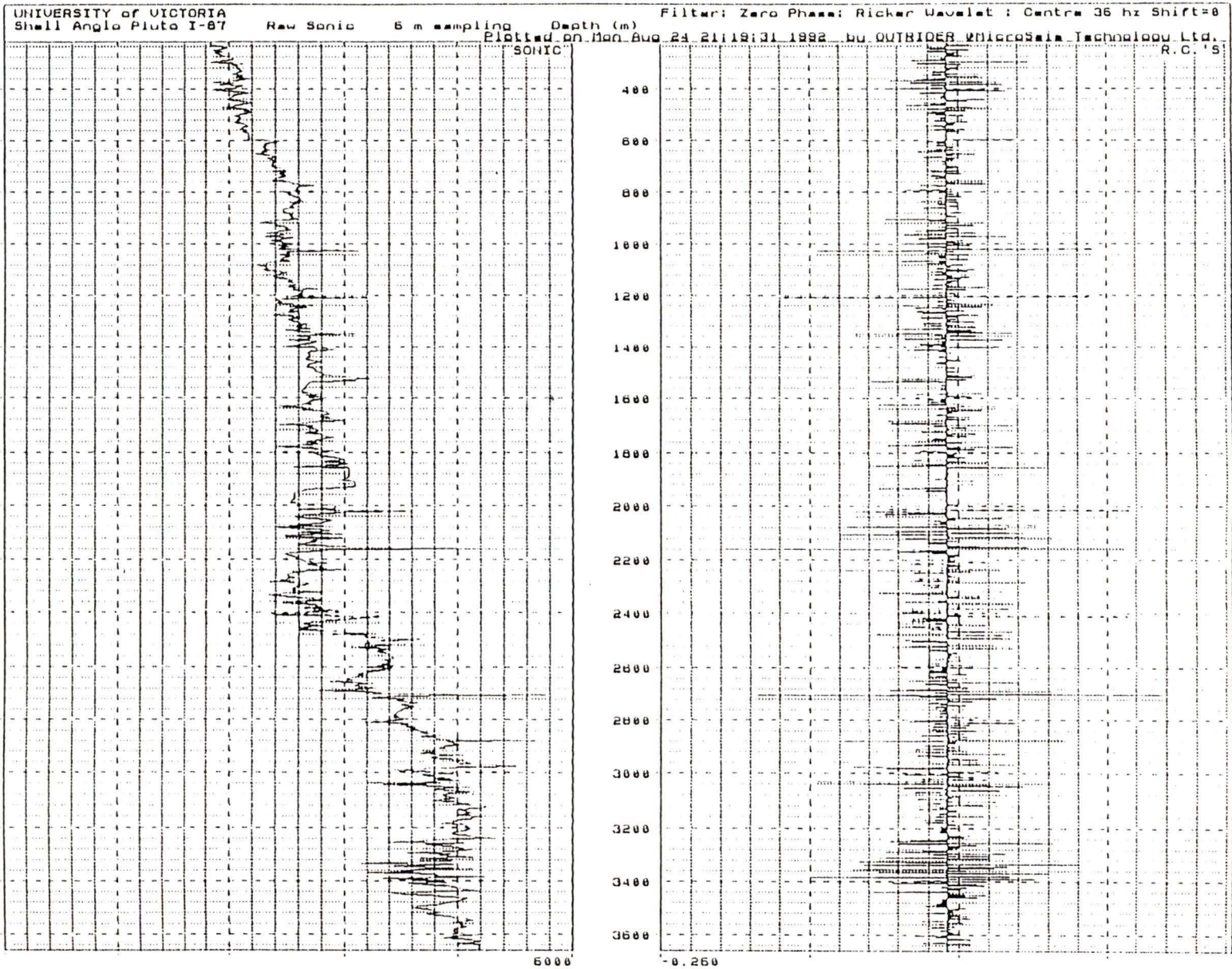


Figure 39: Shell Anglo Pluto I-87. Log and reflectivity in depth.

Figure 40: Shell Anglo Pluto I-87. Log, reflectivity and synthetic seismogram in time.

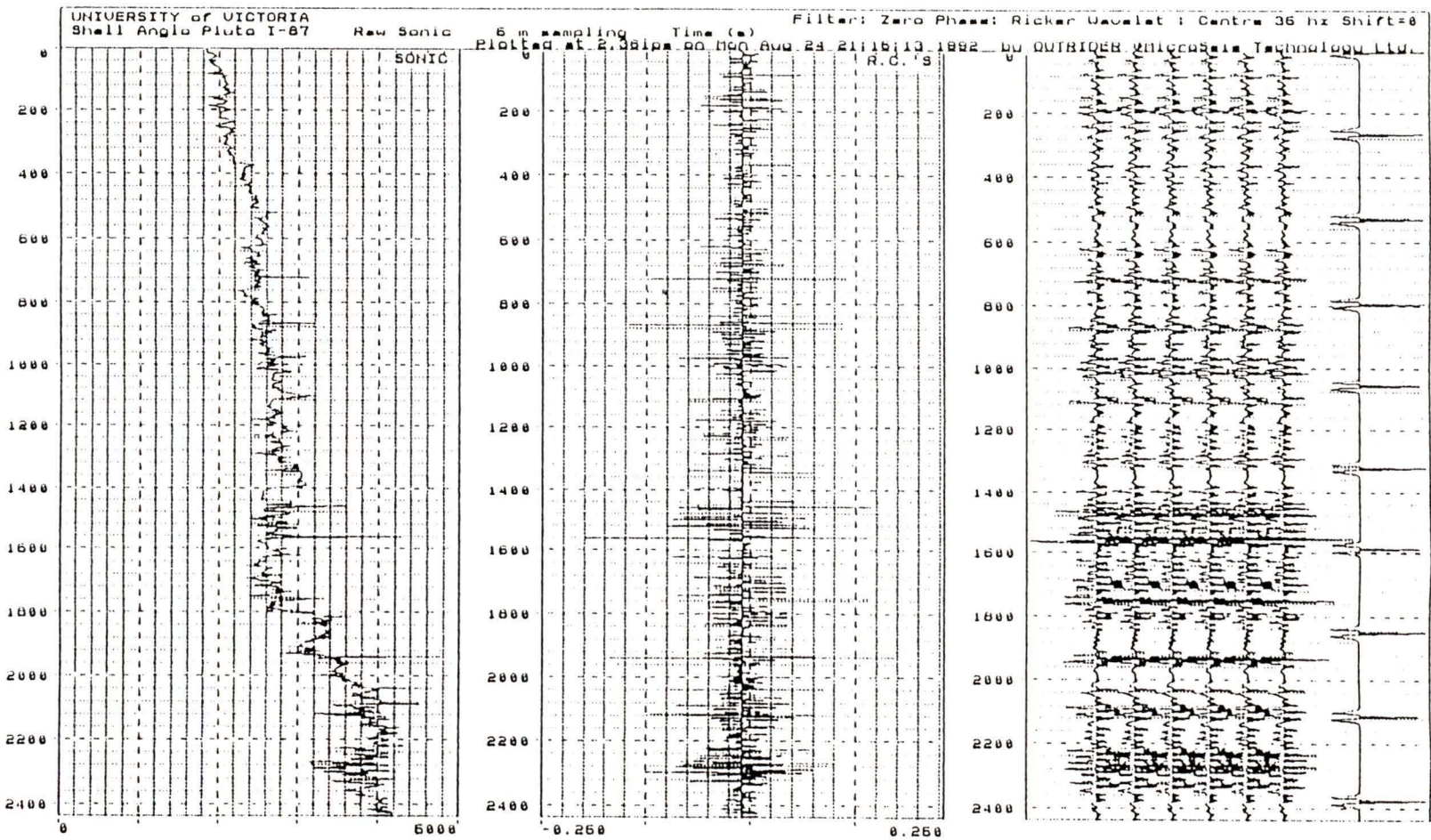
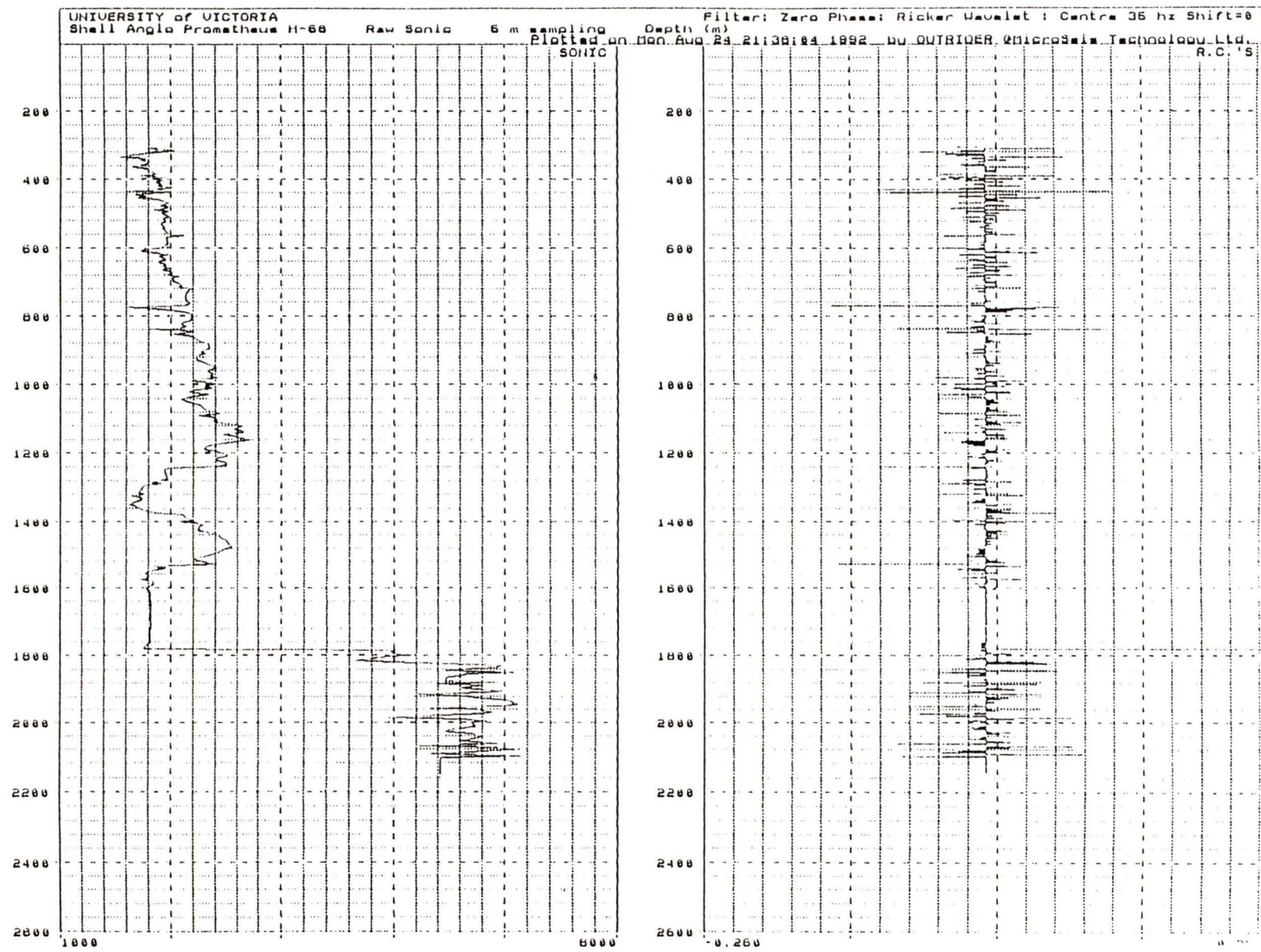


Figure 41: Shell Anglo Prometheus H-68. Log and reflectivity in depth.



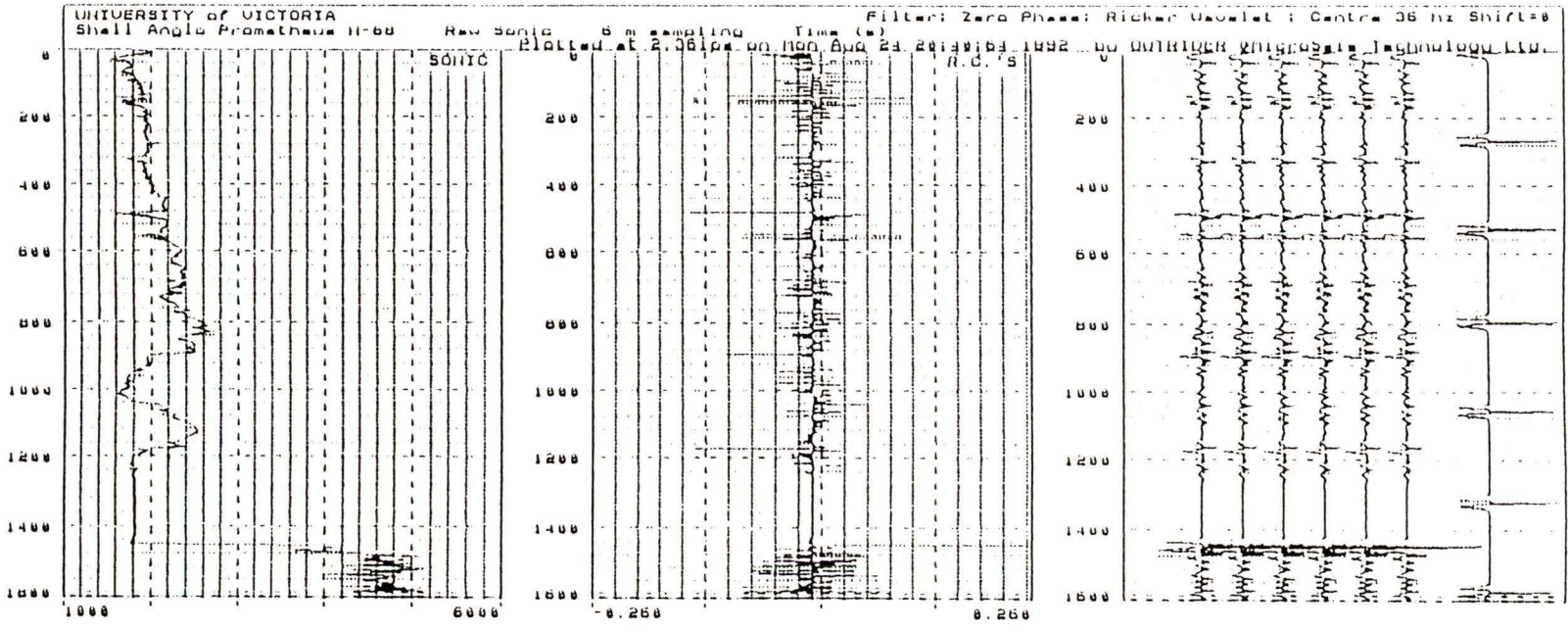


Figure 42: Shell Anglo Promethus H-68. Log, reflectivity and synthetic seismogram in time.

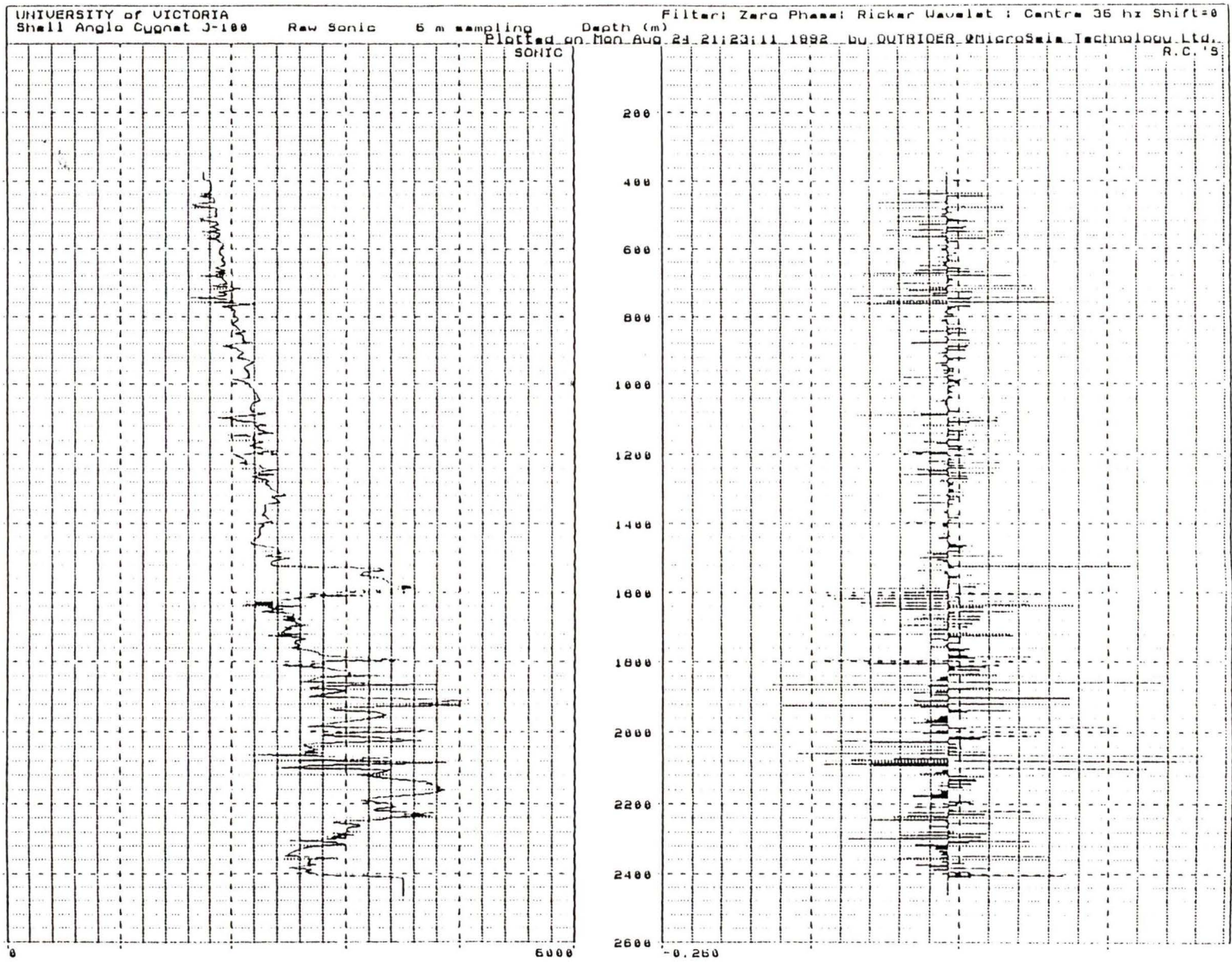


Figure 43: Shell Anglo Cygnat J-100. Log and reflectivity in depth.

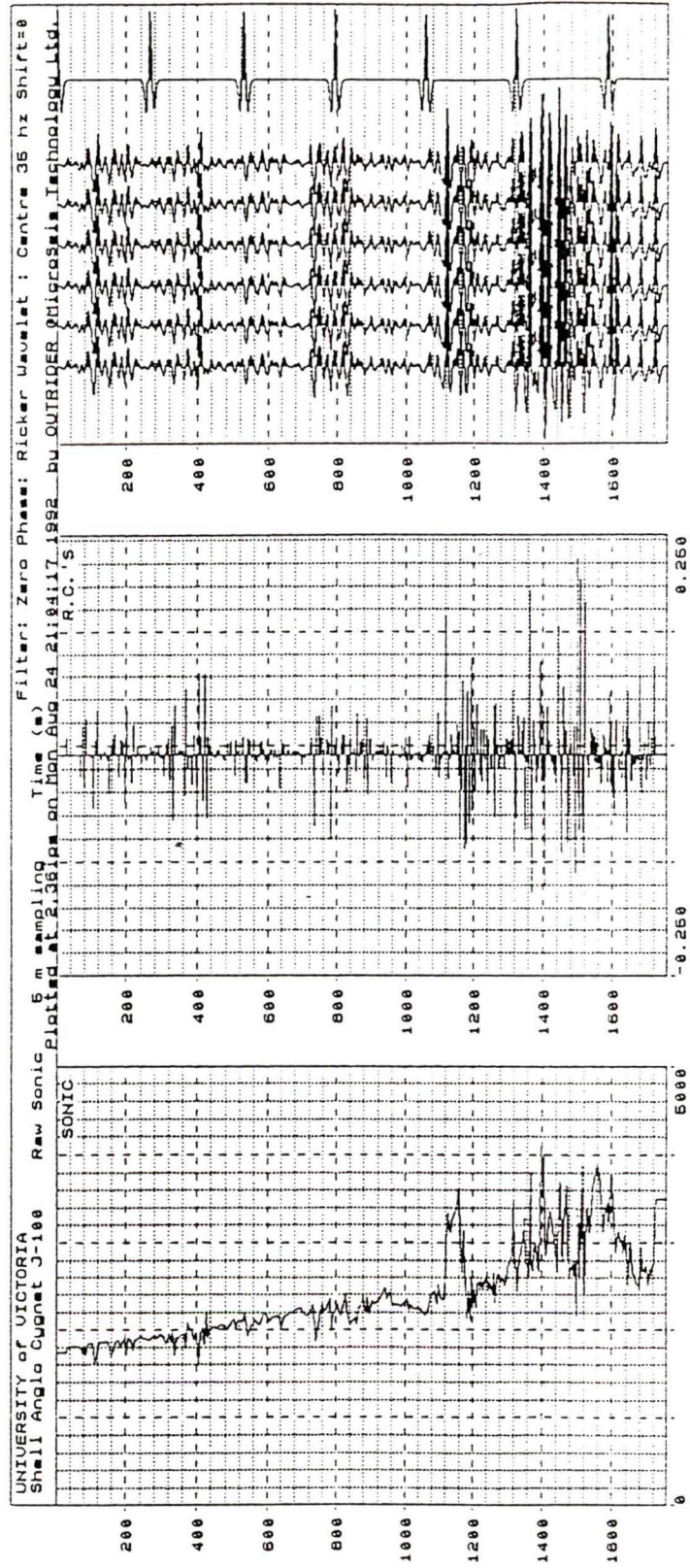


Figure 44: Shell Anglo Cygnet J-100. Log, reflectivity and synthetic seismogram in time.

VITA

Surname: Langton
Given Names: Stewart Gordon
Place of Birth: Victoria, British Columbia, Canada
Date of Birth: May 15, 1952.

Educational Institutes Attended:

University of Victoria	1970-1971, 1978-1981, 1989-1995
British Columbia Institute of Technology	1971-1973

Degrees Awarded:

B. Sc.	University of Victoria	1981
Diploma in Electronic Technology	B.C. Institute of Technology	1973

PARTIAL COPYRIGHT LICENCE

I hereby grant the right to lend my thesis to users of the University of Victoria Library, and to make single copies only for such users or in response to a request from the Library of any other university, or similar institution, on its behalf or for one of its users. I further agree that permission for extensive copying of this thesis for scholarly purposes may be granted by me or a member of the University designated by me. It is understood that copying or publication of this thesis for financial gain shall not be allowed without my written permission.

Title of Thesis: The Seismic Structure of Tofino Basin and Underlying Accreted Terranes.

Author:

Stewart Gordon Langton

September 29, 1995.